CSCS
Swiss National Supercomputing Centre

Scientific Report
Scientific Report
Scientific Report
Scientific Report
Scientific Report
Scientific Report
Scientific Report
Scientific

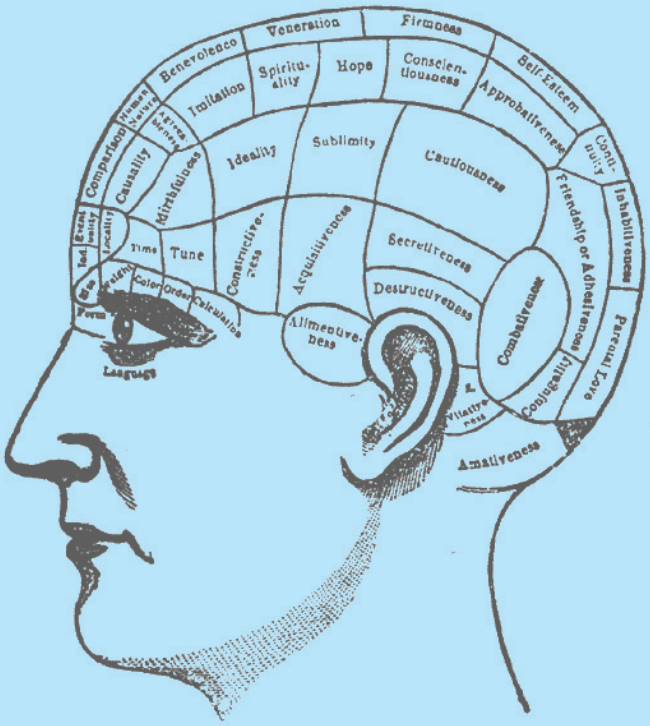

Scientific Report 2004/2005

CSCS
Swiss National Supercomputing Centre

Scientific Report 2004/2005

Content

Editorial by Dr. Hans Peter Lüthi, Chairman Scientific Review Committee of CSCS

Dr. Hans Peter Lüthi

Over the past two decades, Computational Science and Engineering (CSE), the investigation of physical processes through computer-modelling and simulation, has established itself as the third pillar of science, next to theory and experiment. Initially focused on solving problems of science and technology, new areas of application where computation becomes important are developing. One such example is the modelling of risk in the financial industry. At the same time, we observe that the scope of modelling and simulation moves to larger and more complex scales of phenomena. Modelling is no longer focused on single physical processes, but rather on ensembles of interacting processes. The simulations of the biological cell or the change in climate represent multidisciplinary ventures that require new forms and cultures of collaboration.

For Switzerland, as for most other industrialized countries, the economic growth certainly will be coupled more and more closely to the successful inclusion of computation in the innovation process: the knowledge society depends on the capability of CSE to generate, process and/or visualize complex data and information. Fortunately, with all the investments made and being made, Swiss CSE takes a leading position in quite a number of areas. We are proud to know that some of the researchers setting the research agendas of science and technology work at Swiss research institutions; some are also users of the infrastructure of the Swiss National Scientific Computing Centre (CSCS).

The Swiss National Scientific Computing Centre in this respect has a very important mandate. It is the most important provider of state-of-the-art computing capacity for Swiss academia. Its role, however, is not restricted to the one of a cycle-provider. The timely introduction of new technologies and the transfer of the corresponding knowledge to the users are another important task of the centre. In this context, CSCS has made a major effort in the past two years to create new opportunities for its users in scientific vizualization and in Grid Computing.

CSCS with its staff and its machines is a precious resource to research in science and engineering in this country. Clearly, shared computational resources are rarely big enough, so that decisions regarding their use have to be made. The efficient use of these resources is a primary task of the Scientific Review Committee (SRC). One way of achieving this is to create transparency with respect to the research conducted using CSCS resources. In this first edition of the CSCS Scientific Report, we present the reports on the Large User Projects. We are inviting you to browse through this report, and we are hoping that the science presented will inspire new interactions between the readers and the authors of the accounts.

Hydrogenation reactions in heterogeneous enantioselective catalysis and homogeneous catalysis in supercritical CO_2

Prof. Alfons Baiker

with A. Vargas and A. Urakawa
Department of Chemistry and Applied Biosciences
ETH Zürich, Switzerland

A. Heterogeneous enantioselective catalysis

The demand for enantiopure compounds has steadily increased in the past decades and the ready availability of single enantiomers is one of the frontiers of contemporary synthetic chemistry. Furthermore environmental concerns are increasingly conditioning the development of new synthetic routes. Asymmetric heterogeneous catalysis can combine high enantioselectivities with "clean" techniques (green chemistry), and is therefore a highly interesting field of research. In heterogeneous catalysis most promising results have been obtained by chiral modification of a metal surface, through adsorption of a chiral modifier[1]. The most prominent example is the cinchona alkaloid modified platinum system, originally discovered for the enantioselective hydrogenation of α-ketoesters, and later extended to the enantioselective hydrogenation of α-ketolactones, α-diketones, α-ketoacetals, α,α,α-trifluoroketones, and linear and cyclic α-ketoamides[2-4]. Knowledge of the molecular interaction of reactants with the chiral modifier and of the adsorption of these species on the metal surface is at the origin of a mechanistic understanding of these catalytic systems. This aim is pursuit in our laboratory by a combined theoretical and experimental approach.

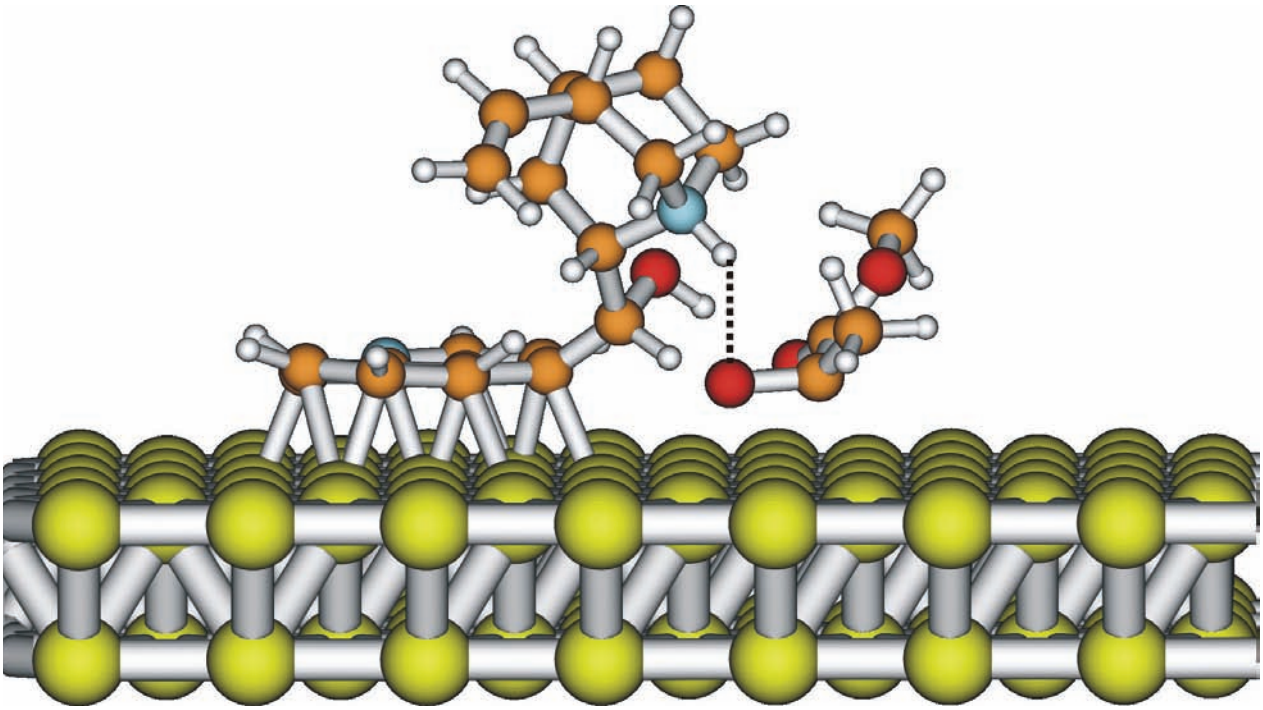

Figure 1: Interaction between surface modifier and adsorbed substrate

Using in situ ATR-IR spectroscopy[5] and STM[6] considerable knowledge could be gained about important features of the adsorption of the reactants and modifier as well as on the structure of the enantio-discriminating diastereomeric complexes formed between modifier and reactant. Neverthe-less several steps of the surface processes could so far only be predicted by theoretical calculations which are extremely important because they allow to fill gaps in the knowledge of the surface processes which are inaccessible by experimental techniques.

The theoretical adsorption studies that have been carried out until now[7-9] have greatly improved our knowledge on the nature of the adsorbed substrates and modifier and on their interactions.

Figure 1 shows an example of surface interaction between chiral modifier and adsorbate that can lead to enantioselectivity[8]. Figure 2 shows the protonation of the surface modifier by adsorbed hydrogen which is considered one of the crucial steps for the activation of 1:1 interaction complexes between substrate and modifier when the reaction is performed in non-acidic solvents[9] (Figure 2).

The major aim of our investigations in this field is a comprehensive understanding of the reactivity of metal surfaces in presence of co-adsorbed chiral molecules (chiral surface modifiers) acting as enantioselectors. It has been shown[10] that in the hydrogenation of activated ketones the effect of such surface modifiers is both the generation of chiral surface sites, and lowering of the activation barrier for the reaction path leading to only one of the two possible enantiomers. The ongoing experimental research in this field has shown that the same chemical technology can be extended to the generation of heterogeneous enantio-switches[11],

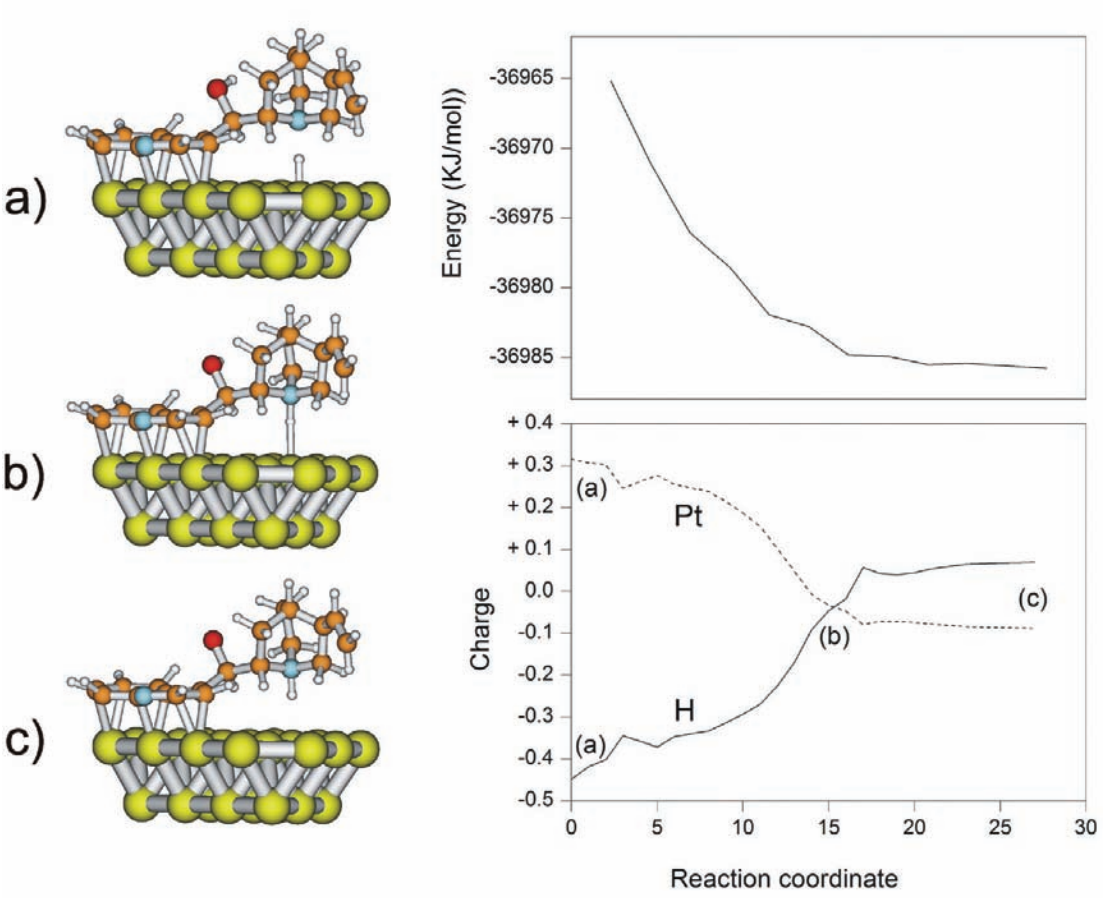

Figure 2: Protonation of surface modifier by means of adsorbed hydrogen. The process is energetically favored and leads to charge transfer from hydrogen to the metal

chemical devices that operate with the principles of heterogeneous catalysis and that are able to change their enantioselective properties when competition between modifiers having different chemisorption potential is possible. When competition for surface sites is followed by an opposite shape-discrimination towards a substrate, switching between (*R*) and (*S*) configuration of the final product is possible within the same batch reaction. An important contribution to this already partially known phenomenon was the discovery of cases where the change in selectivity occurred without changing the absolute configuration of the surface modifier, which on the one hand simplifies the system and on the other emphasizes the importance of functionalization to selectivity[11]. The interest for a computational study lays in the possibility to calculate from first principles both the chemisorption potential and the shape discrimination, in order to both rationalize known results, and tailor new systems. The critical issue is the determination of substituent effects and functionalization on known systems, such as the cinchona alkaloids and some of its synthetic analogs such as (R)-2-(1-pyrrolidinyl)-1-(1-naphthyl)ethanol[12] in order to pass from a phenomenological to a mechanistic comprehension of the chemistry involved.

The model proposed for the rationalization of the enantioselectivity of cinchona alkaloid-modified platinum towards the hydrogenation of activated ketones is based on both experimental and computational efforts, and delivers a coherent view of the interactions involved in the phenomena that lead to chemical selectivity. A limit of the current view is that it is necessarily a static one, since calculations have aimed to determine the chiral sites, and not their dynamic behaviour. Since it emerges that the dynamic behaviour of the highly flexible surface modifiers is one of the key factors for understanding the selectivity of modified surfaces, part of our current research is addressed to the investigation of surface dynamics of reactants and modifiers on a metal surface by means of ab-initio molecular dynamics. The extension of the comprehension of this reaction system can, in our opinion, lead to interesting developments of the control of metal interface phenomena, possibly leading to tailored catalysts and engineered nano-devices.

B. Homogeneous catalysis in supercritical CO_2

Fixation and utilisation of CO_2 have gained considerable attention, triggered by environmental concerns and its abundant availability at low costs. Supercritical CO_2 can be used as an environmentally benign solvent, which has several distinct advantages over conventional liquid solvents (e.g. tunable density, easy separation, relatively high solubility of gases and improved mass- and heat-transfer properties). Particularly challenging is the use of supercritical CO_2 in synthesis where it acts simultaneously as a reactant as well as a solvent. Among the successful applications, the synthesis of formic acid (Scheme 1) and its derivatives using homogenous Ru complexes has attracted considerable attention[13-14].

Scheme 1

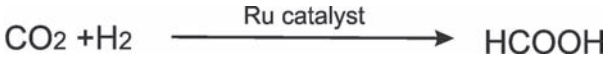

Despite the attractive reaction, the outstanding reactivity of the catalysts, and a number of related issues badly need clarification, since understanding of the nature of the active site and of the reaction mechanism are hardly studied and are lagging behind. Theoretical study by computational means with the help of in situ spectroscopy (e.g. NMR and IR at high pressure) is of great help to understand the nature of the reaction system and to design more efficient catalysts. The target of the present project is the investigation of the properties of CO_2 in supercritical phase, the CO_2 insertion mechanism, and the effects of ligands.

B1. Properties of supercritical CO_2: Current status

IR spectra from ab initio calculations can be considered as a severe test for modelling due to its high sensitivity to atomic positions, interactions, and potential energy surface[18]. Furthermore, the unique properties of supercritical CO_2 as solvent, i.e. 'green' solvent, for various organic molecules are also the target of our investigation. Experimentally, the measurement of supercritical CO_2 is not an easy task. Recently, we have developed a state-of-the-art high pressure IR setup applying both transmission and ATR (attenuated total reflection) techniques with a possibility of looking at phase behaviour through a window[19]. The CO_2 IR spectra at different conditions are now measured and ready for comparison with the theoretical results obtained by the ab initio MD (CPMD). The simulations of supercritical CO_2 ranging from gas to supercritical phase have now been obtained. Currently, the analysis of the simulated data and property comparisons between experiments and theory, such as IR spectra, diffusion, rotational movement, and dynamic dipole strength, are underway.

B2. Mechanism of formic acid formation: Current status

In the past years we have reported highly active Ru catalysts for the synthesis of formic acid derivatives from CO_2[15,16]. Especially $RuCl_2(dppe)_2$ (dppe: $Ph_2P(CH_2)_2PPh_2$) is an extremely active catalyst in the synthesis of both formic acid and its derivatives[15-17]. However, the mechanisms of the reaction system are not yet clear. In order to understand the mechanism both experimentally and theoretically, we have decided to simplify the catalyst complexity by choosing a smaller ligand, dmpe (dmpe: $Me_2P(CH_2)_2PMe_2$). Now the catalyst, $RuH_2(dmpe)_2$ has been synthesized and the reaction has been studied spectroscopically by IR and NMR. The stable intermediates during the CO_2 insertion into the catalyst and formic acid formation have been identified. Theoretically, the rate-limiting step during the hydrogenation reaction has been determined by DFT (Gaussian 03, B3PW91 hybrid functional, Ru (LanL2DZ), other atoms (6-311G(d,p)), however, the degree of freedom of the catalytic system retards the confident understanding of the reaction pathway. Currently, the insertion mechanism is investigated by the meta-dynamics implemented in CPMD[20].

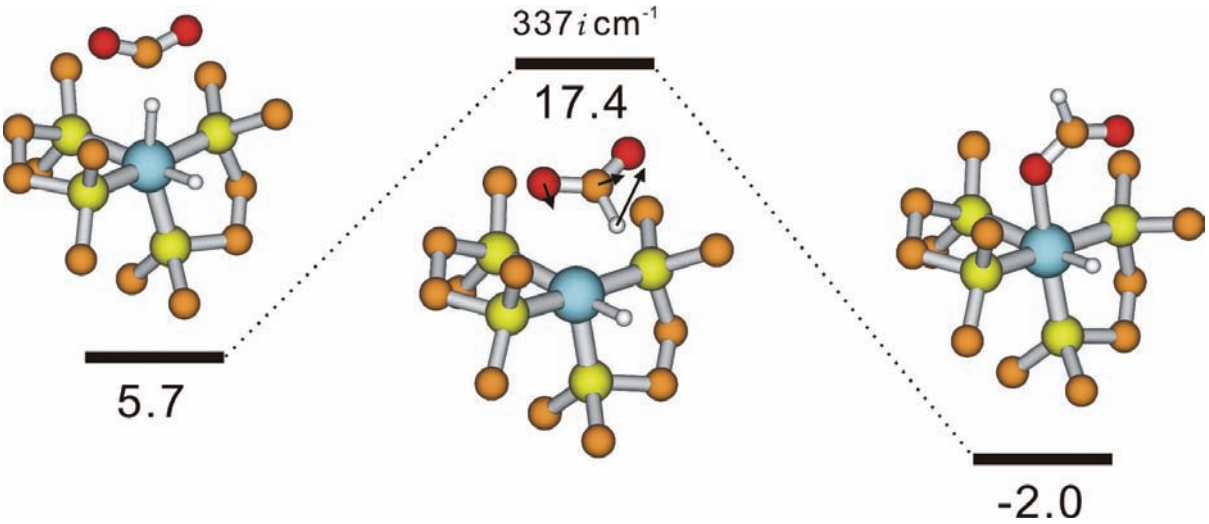

Figure 3: Concerted CO_2 insertion mechanism elucidated by the static DFT. Energy values are shown relative to the sum of $RuH_2(dmpe)_2$ and H_2 in kcal/mol.

References

[1] A. Baiker, Catal. Today 100 (2005) 159.

[2] M. Studer, H.U. Blaser, C. Exner, Adv. Synth. Catal. 45 (2003) 345.

[3] T. Bürgi, A. Baiker, Acc. Chem. Res. 37 (2004) 909.

[4] D. Y. Murzin, P.M. Mäki-Arvela, E. Toukoniitty, T. Salmi, Catal. Rev. 47 (2005) 175.

[5] N. Bonalumi, T. Bürgi, A. Baiker, J. Am. Chem. Soc. 125 (2003) 13342.

[6] M. vonArx, M. Wahl. T.A. Jung, A. Baiker, Phys. Chem. Chem. Phys. 7 (2005) 273.

[7] A. Vargas, T. Bürgi, A. Baiker, J.Catal. 222 (2004) 439.

[8] A. Vargas, T. Bürgi, A. Baiker, J. Catal. 226 (2004) 69.

[9] A. Vargas, D. Ferri, A. Baiker, J. Catal. 236 (2005) 1.

[10] R. Hess, A. Vargas, T. Mallat, T. Bürgi, A. Baiker, J. Catal. 222 (2004) 117.

[11] N. Bonalumi, A Vargas, D. Ferri, T. Bürgi, T. Mallat, A. Baiker, J. Am. Chem. Soc. 127 (2005) 8467.

[12] M. Schürch, T. Heinz, R. Aeschimann, T. Mallat, A. Pfaltz, A. Baiker, J. Catal. 173 (1998) 187.

[13] P.G. Jessop, Y. Hsiao, T. Ikariya, R. Noyori, J. Am. Chem. Soc. 118 (1996) 344.

[14] P.G. Jessop, T. Ikariya, R. Noyori, Science 269 (1995) 1065.

[15] O. Kröcher, R.A. Köppel, A. Baiker, Chem. Commun. (1996) 1497.

[16] L. Schmid, M.S. Schneider, D. Engel, A. Baiker, Catal. Lett. 88 (2003) 105.

[17] C.C. Tai, J. Pitts, J.C. Linehan, A.D. Main, P. Munshi, P.G. Jessop, Inorg. Chem. 41 (2002) 1606.

[18] M.P. Gaigeot, M. Sprik, J. Phys. Chem. B 107 (2003) 10344.

[19] M.S. Schneider, J.D. Grunwaldt, T. Bürgi, A. Baiker, Rev. Sci. Instrum. 74 (2003) 4121.

[20] M. Iannuzzi, A. Laio, M. Parrinello, Phys. Rev. Lett. 90 (2003) art. no.-238302.

Atomization energies from *ab initio* calculations without empirical corrections

Dr. Dirk Bakowies

Laboratorium für Phyikalische Chemie
ETH Zürich, Switzerland

Scientific Abstract

Accurate thermochemistry has turned out to be a major challenge for standard *ab initio* quantum chemistry. High levels of electron correlation combined with very large basis sets are required to adequately treat the formation of a molecule from its constituent atoms. The application of current approaches is thus limited to very small molecules unless empirical corrections are permitted to account for the average effects of basis set incompleteness and higher order electron correlation. Here we test economical compound methods based entirely on *ab initio* electronic structure theory and void of empirical corrections, taking advantage of the observations that (a) higher-order electron correlation corrections are much less basis-set dependent than low-order (MP2) correlation energies, and (b) basis set incompleteness errors can largely be eliminated through extrapolation techniques. These compound methods should be accurate enough even for larger molecules so that they provide useful references for the parametrization of more approximate methods, particularly in semiempirical quantum chemistry.

Motivation

The calibration of semiempirical quantum-chemical methods requires highly accurate reference data, including energies, geometries, and electronic properties. For parametrizations geared towards biomolecular applications it appears mandatory to provide these data for reasonably sized models of typical biomolecules. Atomization and relative (conformational, complexation, activation) energies are usually not available from experiment and need to be obtained from high-level *ab initio* theory.

Model compounds of interest to biomolecular simulation include hydrogen-bonded complexes, nucleic acid base pairs, as well as conformations of small peptides, sugars, lipids, and transition states of typical chemical reactions. Most of these molecules are too large to be studied at reliable levels of standard *ab initio* theory. Here we explore the accuracy of less expensive, yet fully *ab initio* compound methods, taking advantage of the observation that higher-order electron correlation corrections are much less basis set dependent than low-order (MP2) correlation energies.

Related Work in the Literature

Atomization energies – also referred to as dissociation energies – are available from experiment only for very few small molecules since they require the precise knowledge of anharmonic zero-point energies which are typically not known experimentally. They can be calculated by *ab initio* electronic structure theory, but high levels of electron correlation and basis set saturation are usually required to achieve chemical accuracy.

A number of research groups have demonstrated that accurate atomization energies can be obtained from compound methods, combining the results from less expensive electron correlation

methods extrapolated to the full basis set limit with higher order correlation corrections obtained with medium-sized basis sets.

The success of these methods relies on the observation that the complete correlation energy is much more sensitive to basis set saturation than correlation corrections beyond the MP2 or CCSD levels of theory. The focal point analysis introduced by Allen and coworkers[1] and the W-1 (Weizmann 1) theory of Martin[2] are based on such combinations of various levels of theory.

However, these methods are still limited to fairly small molecules with just a few heavy atoms as they still involve CCSD(T) calculations with sizeable basis sets. On the other hand, a number of approaches introduced by the groups of Pople (G1, G2, G3,...),[3] Petersson (CBS-Q, CBS-q, ...),[4] and Truhlar (MCCM/3, SAC/3)[5] follow similar ideas, but are less computationally demanding and applicable to medium-sized organic molecules with 10 and more heavy atoms. The caveat is that they require additional empirical corrections for acceptable accuracy and that these corrections have been determined by calibration with experimental heats of formation for large sets of mostly organic molecules. Zero-point energies and thermal corrections are obtained from scaled frequencies computed typically at the Hartree-Fock level to convert calculated atomization energies to heats of formation.

These approaches predict heats of formation of many molecules – also outside the initial training sets – very well, but are not necessarily well suited to calculate atomization energies for which accurate reference data are very limited. It is quite likely – and a recent study by Feller supports this point of view[6] – that the empirical corrections also absorb non-negligible deficiencies in the calculated zero-point energies, rendering predicted atomization energies significantly less reliable than calculated heats of formation.

Project

We test economical compound methods to calculate atomization energies which are based on *ab initio* electronic structure theory but do not contain any empirical corrections. Their accuracy is assessed with respect to available experimental atomization energies for various small molecules, with respect to very high-level calculations for an extended set of reference molecules, and with respect to experimentally available heats of formation for an even larger set of reference molecules.

The latter comparison is certainly only of approximate nature as it requires the theoretical evaluation of zero-point energies and thermal corrections and thus introduces additional uncertainties. However, we are using a higher level of theory than typically applied in, e.g., the Gaussian (Gx) series of theories,[3] to calculate equilibrium geometries and harmonic frequencies. This level of theory, MP2/cc-pVTZ, requires much smaller scaling factors (around 0.98 instead of 0.90) for frequencies to reproduce experimental zero-point energies of small molecules and thus suggests a higher level of accuracy for larger molecules.

A hierarchy of various levels of compound methods will be analyzed and suggested, balancing computational expense with desired accuracy. These approaches should be able to provide reference data of known accuracy for the calibration of semiempirical methods. Relative energies, i.e. differences in atomization energies between various conformations, between a hydrogen-bonded complex and its constituent molecules, or between transition states, reactants and products of a chemical reaction should be significantly more accurate than the atomization energies themselves, as remaining deficiencies in the electron correlation treatment will largely cancel. This certainly plausible hypothesis will be tested in detail and quantified by comparing various compound methods with each other and by studying convergence of basis-set saturation and electron correlation

treatment. In the end, we shall be able to choose a particular compound method based on the size of a molecule and available computational resources and estimate the expected level of accuracy for atomization, activation, and relative conformational energies.

Preliminary Results

It may appear too ambitious to design accurate compound methods that are significantly more economical than e.g. the focal point analysis of Allen[1] and yet do not require empirical corrections like other popular approaches as e.g. G2 theory.[3] But a preliminary study for 14 small molecules[7] with accurately known atomization energies (see Figure 1) shows that we can achieve results of very useful accuracy (< 1 - 2 kcal/mol error) defining compound methods of type

$$\Delta E(X) = E(MP2/cc\text{-}pV(TQ)Z) + \Delta E_X(CCSD(T) - MP2) + \Delta E(core)$$

where

$$\Delta E_X\,(CCSD(T) - MP2) = E(CCSD(T)/cc\text{-}pVXZ) - E(MP2/cc\text{-}pVXZ)$$

$$\Delta E(core) = E(MP2(full)/cc\text{-}pCVTZ) - E(MP2/cc\text{-}pVTZ)$$

X defines the type of Dunning's correlation consistent valence polarized basis sets used (D, T, Q) for higher order correlation corrections, and MP2/cc-pV(TQ)Z refers to the MP2 energy at the basis set limit obtained from calculations with triple- and quadruple-zeta basis sets following the extrapolation protocol suggested by Halkier *et al*[8]. Note that all compound methods shown are significantly more accurate (X=D:1.5, T:0.6, Q:0.4 kcal/mol) than HF (102.8 kcal/mol), MP2 (5.9), CCSD(T) (4.6) and even CCSD(T)(full) (3.5) using basis sets of quad-

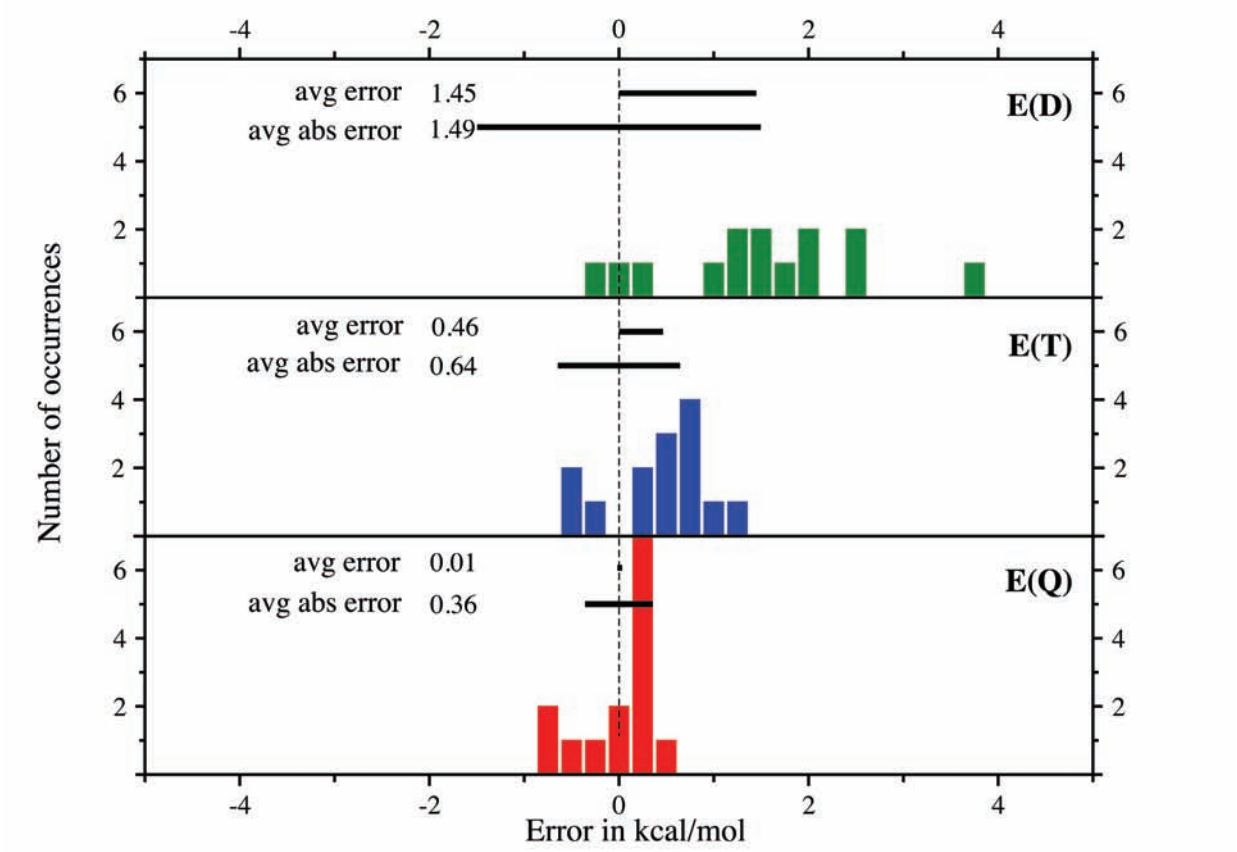

Figure 1: Distribution of errors in calculated atomization energies for 14 molecules with accurately known experimental data. E(D), E(T), E(Q) refer to the level of theory as defined above. All values are in kcal/mol.

ruple-zeta quality and that extrapolation to the basis set limit is just as essential as consideration of higher-order electron correlation and core-electron correlation. Using scaled MP2/cc-pVTZ frequencies, we have also calculated heats of formation for a subset of 53 molecules out of the G2/97[9] and G3[10] reference sets which cover a large number of types of organic and inorganic molecules containing H, C, N, and O atoms. The average errors are somewhat larger (X=D:2.3, T:1.3, Q:0.8 kcal/mol) than before, reflecting both the larger size of the molecules and the additional uncertainty in the calculated vibrational frequencies, but again significantly smaller than those of HF (200.6 kcal/mol), MP2 (6.7) and CCSD(T) (9.0) at the cc-pVQZ basis set level.

In summary, we are quite confident to be able to calculate reliable atomization energies with average errors not exceeding 1 – 2 kcal/mol, using computationally feasible compound methods. With state-of-the-art personal computers we can treat molecules with up to about 13 heavy atoms (C,N,O) using the E(D) level of theory, and up to about 8 heavy atoms using the E(T) level of theory.

Current Activities

We are extending our preliminary set of reference calculations to include highly accurate CCSD(T)/cc-pV(T,Q)Z and CCSD(T)(full)/cc-pCV(T,Q)Z calculations for a larger subset of molecules taken from the G2/97 and G3 reference sets. This will enable us to gauge less expensive compound methods like E(D) and E(T) against a larger set of reliable data for atomization energies. Furthermore we quantify how accurately atomization energies and relative energies (conformational, complexation, activation, see above) are predicted by any of the proposed compound methods. Production calculations at the E(D) and E(T) levels of theory are planned for larger molecules of biochemical interest to provide accurate reference data also for molecules that are too large for treatments of benchmark quality.

References

[1] East, A. L. L.; Allen, W. D. J. Chem. Phys. 1993, 99, 4638-4650.

[2] Martin, J. M. L.; de Olivera, G. J. Chem. Phys. 1999, 111, 1843-1856.

[3] Curtiss, L. A.; Redfern, P. C.; Frurip, D. J. Rev. Comp. Chem. 2000, 15, 147-210.

[4] Ochterski, J. W.; Petersson, G. A.; Montgomery Jr., J. A. J. Chem. Phys. 1996, 104, 2598-2619.

[5] Lynch, B. J.; Truhlar, D. G. J. Phys. Chem. A 2003, 107, 3898-3906.

[6] Feller, D.; Peterson, K. A. J. Chem. Phys. 1998, 108, 154-176.

[7] Bak, K. L.; Jørgensen, P.; Olsen, J.; Helgaker, T.; Klopper, W. J. Chem. Phys. 2000, 112, 9229-9242.

[8] Halkier, A.; Klopper, W.; Helgaker, T.; Jørgensen, P.; Taylor, P. R. J. Chem. Phys. 1999, 111, 9157-9167.

[9] Curtiss, L. A.; Raghavachari, K.; Redfern, P. C.; Pople, J. A. J. Chem. Phys. 1997, 106, 1063-1079.

[10] Curtiss, L. A.; Raghavachari, K.; Redfern, P. C.; Pople, J. A. J. Chem. Phys. 2000, 112, 7374-7383.

Structure and enantiospecificity of chiral nanoparticles and interfaces

Prof. Thomas Bürgi

Institut de Chimie, Université de Neuchâtel, Switzerland

Our group uses a combined experimental and theoretical approach to gain insight into enantiodifferentiation at chiral interfaces. We furthermore seek to clarify how chirality can be bestowed to metals and nanoparticles. Attenuated total reflection (ATR) infrared, vibrational circular dichroism (VCD) and electronic CD spectroscopy are used to investigate interfaces and size-selected metal nanoparticles protected with a chiral adsorbate layer. Vibrational, VCD and CD spectra are also calculated using quantum chemical methods. It is the comparison between experimental and calculated spectra that yields detailed molecular level structural information on chiral surfaces and nanoparticles.

Enantiodifferentiation at chiral interfaces

Chiral interfaces are ubiquitous in nature and play an important role in technology, for example in separation processes. The interest in chiral interfaces emerges from the importance to selectively produce, separate and detect enantiomers of a chiral compound, which is a consequence of the fact that enantiomers interact differently with a chiral environment, such as a metabolism. Chiral surfaces were furthermore proposed to be at the origin of homochirality on earth. Using a dedicated experimental technique chiral recognition processes at solid-liquid interfaces are investigated by vibrational spectroscopy. The experiments reveal the nature of the intermolecular interactions responsible for enantiodifferentiation. This information sets constraints for subsequent theoretical studies of the same interaction complex between chiral surface (selector) and chiral probe molecule (selectand). This combined strategy results in a structure of the relevant interaction complex.

The experimental technique that we have developed to study enantiodifferentiation at chiral interfaces relies on modulation excitation spectroscopy (MES), i.e. the phase-sensitive detection of periodically varying signals. In this application of MES the absolute configuration of the probe molecule that is admitted to the chiral interface is the stimulus, i.e. the parameter that is periodically varied (absolute configuration modulation). The resulting spectra selectively highlight the spectral differences arising due to the different diastereomeric interactions between the chiral interface and the two enantiomers of the probe molecule. The signals in the spectra reveal, which functional groups are involved in the relevant interaction. This information sets constraints for structure calculations of the interaction complex. Density Functional Theory (DFT) is used to refine the structure of the interaction complex. In addition, a normal mode analysis yields vibrational spectra and highlights frequency shifts induced by the relevant intermolecular interactions. By comparison with experiment the latter procedure represents a double check for the proposed structure.

The method was applied to reveal the mechanism of enantiodifferentiation of chiral stationary phases used in chromatography [1, 2] and to chiral self-assembled monolayers [3]. Figure 1 shows the relevant interaction complex between N-3,5-dinitroben-

zoyl-(S)-leucine (DNB-(S)-Leu, selectand) and tert-butylcarbamyl quinine (tBuCQN, selector). Among the different types of intermolecular interactions in this system the ionic one turns out to be the strongest, as expected. The main force causing the enantiodifferentiation is however the specific H-bonding of the DNB-(S)-Leu with the carbamate branch of the immobilized tBuCQN. The ATR-IR experiments lead to the conclusion that the (R)-enantiomer does not form such H-bond interactions and therefore is not adsorbed as strongly as the (S)-enantiomer. This finding is in agreement with HPLC experiments, where the t-BuCQN showed a preferential binding of the (S)-enantiomer [4].

The experimental indications for the formation of this H-bonding interaction are in particular the amide III (selectand) shift from 1266 up to 1282 cm^{-1}, the amide II shift from around 1500-1550 cm^{-1} up to 1585 cm^{-1} (selectand) and the shift of the amide I from 1727 cm^{-1} down to 1717 cm^{-1} (selector). These shifts were reproduced by a normal mode analysis for the interaction complex using Density Functional Theory (BLYP, 6-31G(d,p)), thus confirming the proposed model [2].

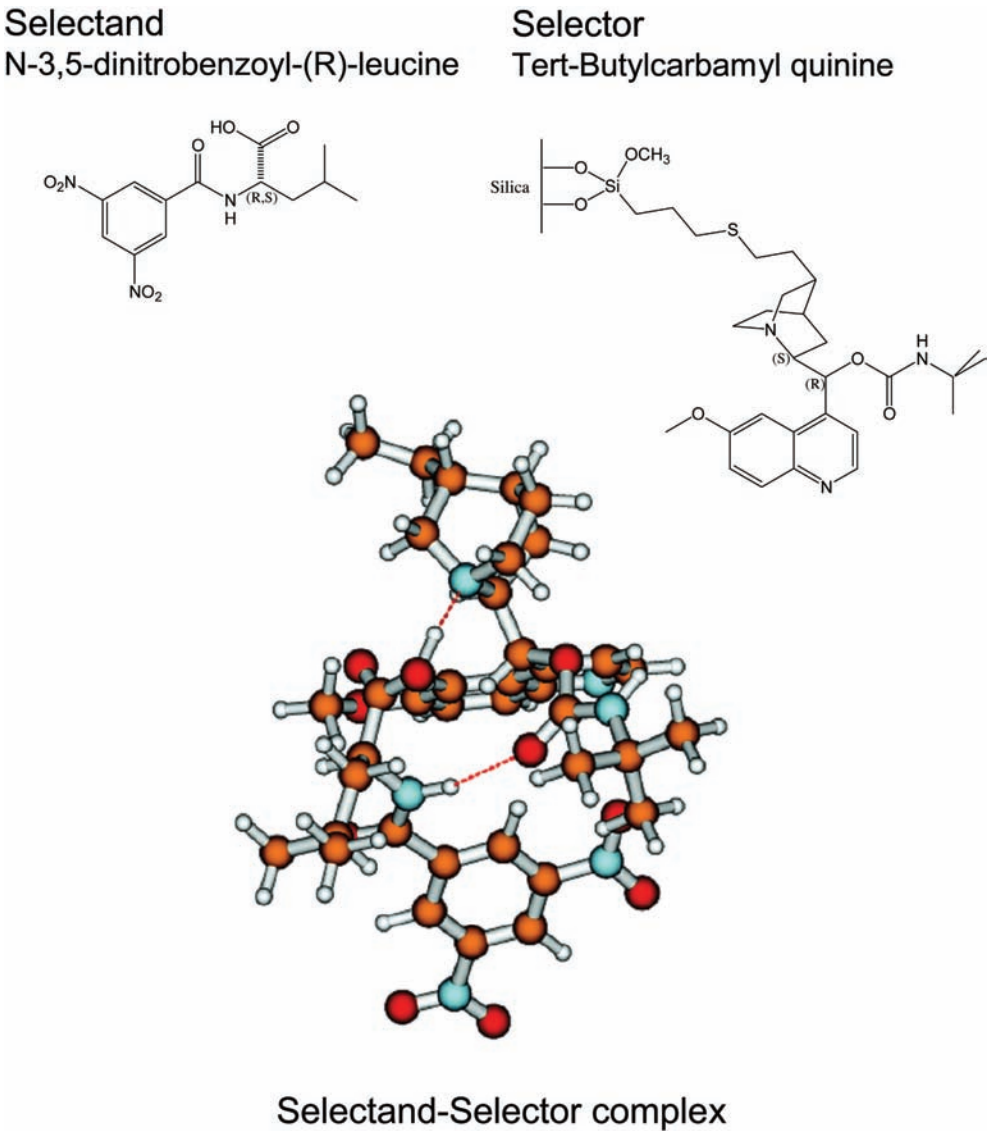

Figure 1: Structure of N-3,5-dinitrobenzoyl-leucine (DNB-Leu) and tert-butylcarbamoyl quinine (tBuCQN) and calculated interaction complex between the two.

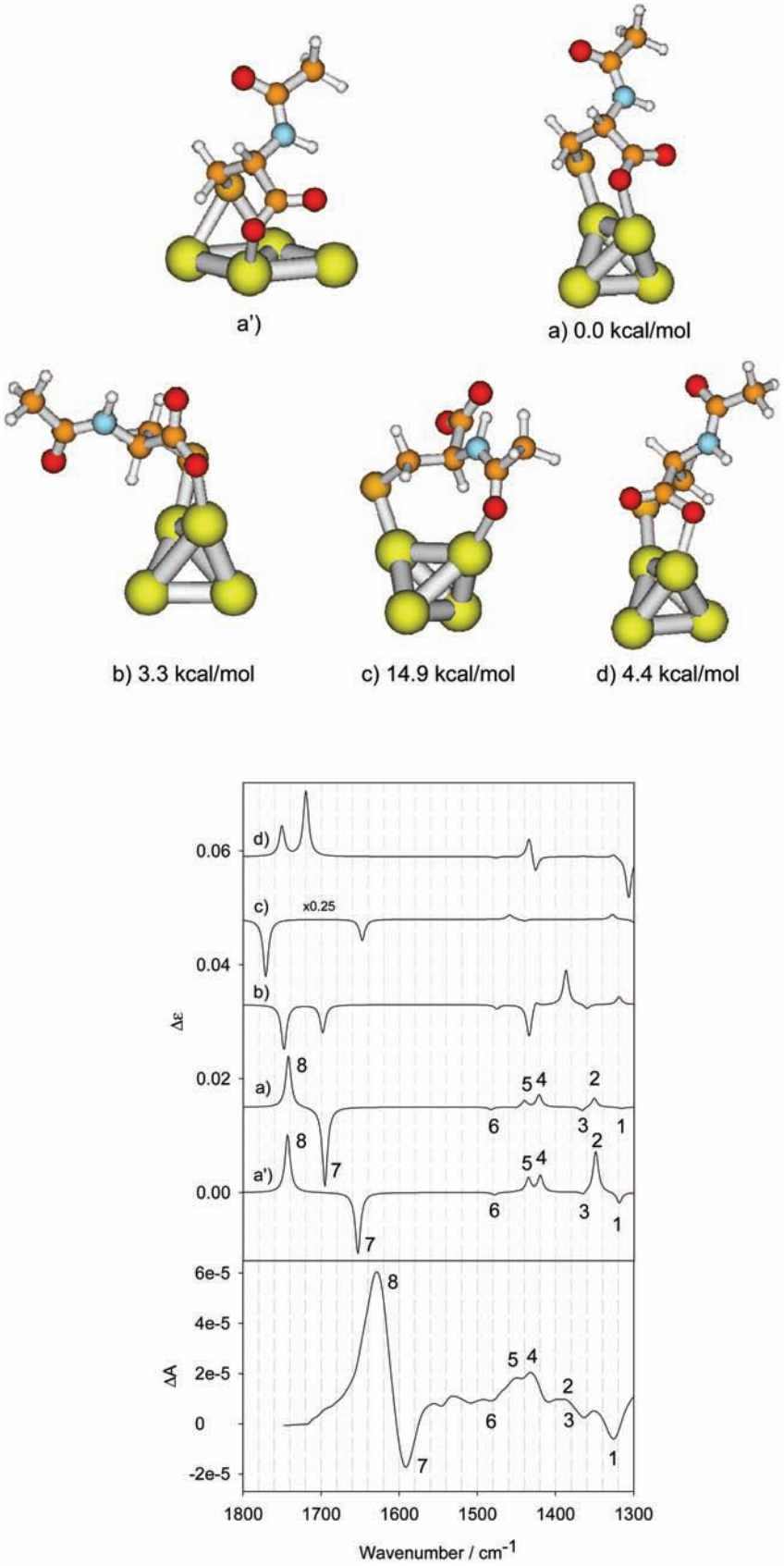

Figure 2: Top: Calculated conformers of deprotonated N-acetyl-L-cysteine on a Au_4 cluster. The structures were optimized using Gaussian03 [15]. For structure a') the Au_4 cluster was fixed planar. For the other structures all degrees of freedom were relaxed during optimization. The numbers indicate the relative stability with respect to the most stable conformation a). Bottom: Calculated and experimental VCD spectra. Calculations were performed for the different conformers a)-d). Labels indicate corresponding bands.

Vibrational circular dichroism (VCD) spectroscopy of chiral nanoparticles

Monolayer protected metal nanoparticles are of considerable interest due to their potential application in various fields such as bio-sensing, catalysis, electronics and nanotechnology [5]. Whereas the physical properties of monolayer protected nanoparticles (MPNs) are largely associated with the metal core, their chemical behaviour such as solubility, molecular recognition and organization, is determined by the protection layer. The engineering of the latter is currently making tremendous progress [6]. The conformation of the molecules adsorbed on the metal particles directly affects the chemical properties. Structure determination would therefore greatly help the rational design of functionalized particles.

Vibrational circular dichroism (VCD) spectroscopy, i.e. the differential absorption of left and right circular polarized infrared light, yields detailed information on the conformation of a chiral molecule in solution.[7] VCD is more sensitive towards conformation than infrared (IR) spectroscopy and its power for structure determination of dissolved molecules, by the comparison between experimental and theoretical spectra, has impressively been demonstrated in the past [8-13].

We recently observed that very small (< 2 nm) gold nanoparticles chirally modified with N-acetyl-L-cysteine exhibit VCD activity associated with the molecules in the protection layer. Comparison with calculated VCD spectra of N-acetyl-L-cysteine adsorbed on small gold clusters allowed getting rather detailed information on the conformation of the adsorbed molecule.

To extract the structural information from the experiment, the VCD spectra for the adsorbed molecule have to be calculated. To explore the potential energy surface for N-acetyl-L-cysteine adsorbed on gold, cluster calculations were performed using the ADF [14] and Gaussian [15] suite of programs with Au clusters of different size containing up to 19 Au atoms.

Figure 2 shows some conformations of N-acetyl-L-cysteine on Au_4 clusters calculated at the B3PW91 level using a 6-31G(d,p) basis set (LanL2DZ for Au). For the calculations of structure a') the positions of the gold atoms were fixed. Complete relaxation of all degrees of freedom, including the Au atoms, lead to structure a), where the four gold atoms adopt a tetrahedron. The conformation of the adsorbed N-acetyl-L-cysteine on the other hand hardly changed with respect to structure a'). The VCD spectra of structures a') and a) are very similar, indicating that the nature of the gold cluster has only minor influence on the vibrations located within the molecule. Figure 2 shows other conformers that were calculated. All of these were found to be less stable than conformer a). Conformers b) and d) also interact via the carboxylate group with the Au_4 cluster, whereas conformer c) interacts via the amide group. The difference between the most stable conformer a) and conformer d) is at the level of the CH_2 and COO^- groups. Figure 2 shows that the VCD spectra strongly depend on the conformation of the adsorbed N-acetyl-L-cysteine. This is most evident from the signals associated with the amide I (at 1627 cm^{-1}) and $\nu_{as}(COO^-)$ vibrations (at 1595 cm^{-1}). Both bands are negative for conformations b) and c), whereas both are positive for conformation d). Only conformer a) (and a')) has the correct sign for both bands. However, conformer a (a') yields the best fit between calculated and experimental spectra also for the rest of the spectrum, in particular bands 4 and 5 and also the C-H bending mode (band 1), which is clearly negative in the experimental spectrum. Our results indicate that VCD spectroscopy, combining experiment and theory, may greatly help elucidating the structure of chiral molecules adsorbed on metal particles.

References

[1] R. Wirz, T. Bürgi, A. Baiker, Langmuir 19 (2003) 785.

[2] R. Wirz, T. Bürgi, W. Lindner, A. Baiker, Anal. Chem. 76 (2004) 5319.

[3] M. Bieri, T. Bürgi, J. Phys. Chem. B 109 (2005) 10243.

[4] M. Lammerhofer, W. Lindner, J. Chromatography A 741 (1996) 33.

[5] M.-C. Daniel, D. Astruc, Chem. Rev. 104 (2004) 293.

[6] E. Katz, I. Willner, Angew. Chem., Int. Ed. 43 (2004) 6042.

[7] L. A. Nafie, Annu. Rev. Phys. Chem. 48 (1997) 357.

[8] P. L. Polavarapu, J. He, Anal. Chem. 76 (2004) 61.

[9] T. B. Freedman, X. Cao, R. K. Dukor, L. A. Nafie, Chirality 15 (2003) 743.

[10] P. J. Stephens, F. J. Devline, A. Aamouche, ACS Symp. Ser. 810 (2002) 18.

[11] T. Bürgi, A. Vargas, A. Baiker, J. Chem. Soc. Perkin Trans. 2 (2002) 1596.

[12] C. Herse, D. Bas, F. C. Krebs, T. Bürgi, J. Weber, T. Wesolowski, B. W. Laursen, J. Lacour, Angew. Chem, Int. Ed. 42 (2003) 3162.

[13] T. Bürgi, A. Urakawa, B. Behzadi, K.-H. Ernst, A. Baiker, New. J. Chem. 28 (2004) 332.

[14] E. J. Baerends, J. Autschbach, Bérces, A., B. C., P. M. Boerrigter, L. Cavallo, D. P. Chong, L. Deng, R. M. Dickson, D. E. Ellis, L. Fan, T. H. Fischer, C. Fonseca Guerra, S. J. A. van Gisbergen, J. A. Groeneveld, O. V. Gritsenko, M. Grüning, F. E. Harris, P. van den Hoek, H. Jacobsen, G. van Kessel, F. Kootstra, E. van Lenthe, D. A. McCormack, V. P. Osinga, S. Patchkovskii, P. H. T. Philipsen, D. Post, C. C. Pye, W. Ravenek, P. Ros, P. R. T. Schipper, G. Schreckenbach, J. G. Snijders, M. Sola, M. Swart, D. Swerhone, G. te Velde, P. Vernooijs, L. Versluis, O. Visser, E. van Wezenbeek, G. Wiesenekker, S. K. Wolff, T. K. Woo, T. Ziegler, 2004.01 ed., SCM, Amsterdam, 2004.

[15] M. J. Frisch, G. W. Trucks, H. B. Schlegel, G. E. Scuseria, M. A. Robb, J. R. Cheeseman, J. A. Montgomery, T. Vreven, K. N. Kudin, J. C. Burant, J. M. Millam, S. S. Iyengar, J. Tomasi, V. Barone, B. Mennucci, M. Cossi, G. Scalmani, N. Rega, G. A. Petersson, H. Nakatsuji, M. Hada, M. Ehara, K. Toyota, R. Fukuda, J. Hasegawa, M. Ishida, T. Nakajima, Y. Honda, O. Kitao, H. Nakai, M. Klene, X. Li, J. E. Knox, H. P. Hratchian, J. B. Cross, C. Adamo, J. Jaramillo, R. Gomperts, R. E. Stratmann, O. Yazyev, A. J. Austin, R. Cammi, C. Pomelli, J. W. Ochterski, P. Y. Ayala, K. Morokuma, G. A. Voth, P. Salvador, J. J. Dannenberg, V. G. Zakrzewski, S. Dapprich, A. D. Daniels, M. C. Strain, O. Farkas, D. K. Malick, A. D. Rabuck, K. Raghavachari, J. B. Foresman, J. V. Ortiz, Q. Cui, A. G. Baboul, S. Clifford, J. Cioslowski, B. B. Stefanov, G. Liu, A. Liashenko, P. Piskorz, I. Komaromi, R. L. Martin, D. J. Fox, T. Keith, M. A. Al-Laham, C. Y. Peng, A. Nanayakkara, M. Challacombe, P. M. W. Gill, B. Johnson, W. Chen, M. W. Wong, C. Gonzalez, J. A. Pople, Rev. C.01 ed., Gaussian, Inc., Wallingford CT, 2003.

Computation of Stellarator Coils, Equilibrium and Stability

Dr. W. Anthony Cooper (a)

with S. Ferrando i Margalet (a), N. Mellet (a), P. Popovich (a), M. Drevlak (b), M. Yu. Isaev (c), M. Mikhailov (c),A. Subbotin (c) and A. Martynov (d)

Institutions:
(a) EPF Lausanne, Centre de Recherches en Physique des Plasmas,Association Euratom-Confédération Suisse, Switzerland
(b) Max-Planck Institut für Plasmaphysik, IPP-Euratom Association, Greifswald, Germany
(c) Nuclear Reasearch Institute, Russian Research Centre 'Kurchatov Institute', Moscow, Russian Federation
(d) Keldysh Institute of Applied Mathematics, Russian Academy of Sciences, Moscow, Russian Federation

Description:

Electrical power stations based on the fusion reactor concept constitute an attractive long-term solution for the energy needs of the world population in the future. The recent agreement to build the ITER experimental reactor facility in Cadarache, France is an important step for the understanding of the physics properties of burning plasmas and the impact that high neutronic yields can have on the plasma facing material components of the device. Stellarator systems represent an alternative magnetic confinement concept that allows more flexibility with respect to the conflicting physics and engineering criteria that must be satisfied at the expense of a more complicated geometrical structure. Typically, physics properties that must be optimised are the volume average of the plasma $<\beta>$ (the ratio of the kinetic pressure to the magnetic pressure of the confining fields) imposed by local and global ideal magnetohydrodynamic (MHD) instabilities [1], the robustness of the magnetic field structure to changes in pressure and current, the confinement of α-particles long enough that they deposit the bulk of their birth energies in the background plasma [2], the confinement of the plasma thermal energy to guarantee sustainability of the burn conditions, etc. Engineering criteria include modularity of the coil system, constraints on coil curvature radii, accessibility of heating and diagnostic systems to the plasma, blanket design conditions to capture and shield the energetic neutrons resulting from the fusion reactions, etc.

The optimisation of the plasma boundary to satisfy the diverse physics criteria like MHD stability at high $<\beta>$, robustness of the magnetic field structure with respect to changes in $<\beta>$, vacuum magnetic well, satisfactory confinement of α-particles, poloidal pseudosymmetry of the magnetic field spectrum and poloidal closure of contours of the second adiabatic invariant have yielded $J_{\parallel}$-optimised stellarator configurations. Configurations with 3, 6, 9 and 12 field periods have been investigated such that the field period number divided by the aspect ratio remains roughly constant. The distribution of constant values of the magnetic field strength on a surface near the plasma edge is shown Figure 1 for a 6-field period $J_{\parallel}$-optimised stellarator system. To understand the confinement properties, the correlation between the conservation of the second adiabatic invariant and the α-particle confinement has been explored in various types of advanced stellarator systems. In a Helias

reactor configuration, a small yet still significant bootstrap current due to the effect of viscous and frictional forces on different classes of particles can develop. The bootstrap current can modify the equilibrium and stability properties which have to be evaluated under free boundary conditions to assess the full impact. Additional heating is required in a fusion reactor to ignite the plasma, after which the burn should be self sustained. The three-dimensional global wave propagation code (LEMan; Low frequency ElectroMagnetic code) [3] which includes finite parallel electric field effects (hence electron inertia) has been applied in the Alfvén frequency range in 2D and 3D geometry, but has been limited so far to 2D tokamak and simple mirror systems in the ion cyclotron range of frequencies. Furthermore, the auxiliary heating can distort the particle distribution functions and drive a pressure anisotropy. The effect of this anisotropy on the MHD equilibrium and stability properties warrants detailed evaluation.

Achievements:

α-particle confinement and conservation of the second adiabatic invariant.

Satisfactory long-time collisionless α-particle confinement can be achieved in reactor-scaled versions of quasi-axisymmetric (QA), quasi-helically symmetric (QH) and quasi-isodynamic (QI) stellarators. At constant plasma volume and magnetic field strength, the smallest α-particle banana widths are observed in QI systems while the largest occur in QA configurations. The principal reason is related to the distance between the trapped particle reflection points which is smallest in QI and largest in QA devices. For small banana size, the correlation between closed $J_{\parallel}$ contour behaviour and particle confinement is better. Therefore, the optimisation of $J_{\parallel}$ contours constitutes a useful method for the realisation of particle confinement improvement.

Free boundary equilibrium and stability properties of a Helias reactor with finite bootstrap current

Converged selfconsistent bootstrap current profiles computed in the collisionless 1/v regime in a 4-period Helias reactor cause a slight outward shift and elongation of the plasma column as $\langle\beta\rangle$ is raised from 0 to 4.5%. The most significant impact of the BC is on the rotational transform profiles which becomes flat and approaches unity in the outer 20% of the plasma volume at $\langle\beta\rangle \cong$ 2.5% and extends to the outer 40% at $\langle\beta\rangle \cong$ 4.5%. This destabilises the Mercier criterion and global external m/n = 1/1kink modes and underscores the relevance of rotational transform profile control. Adding a compensating current of 345kA, the edge rotational transform is decreased from unity to about 0.93 at $\langle\beta\rangle \cong$ 4.5% to stabilise the external

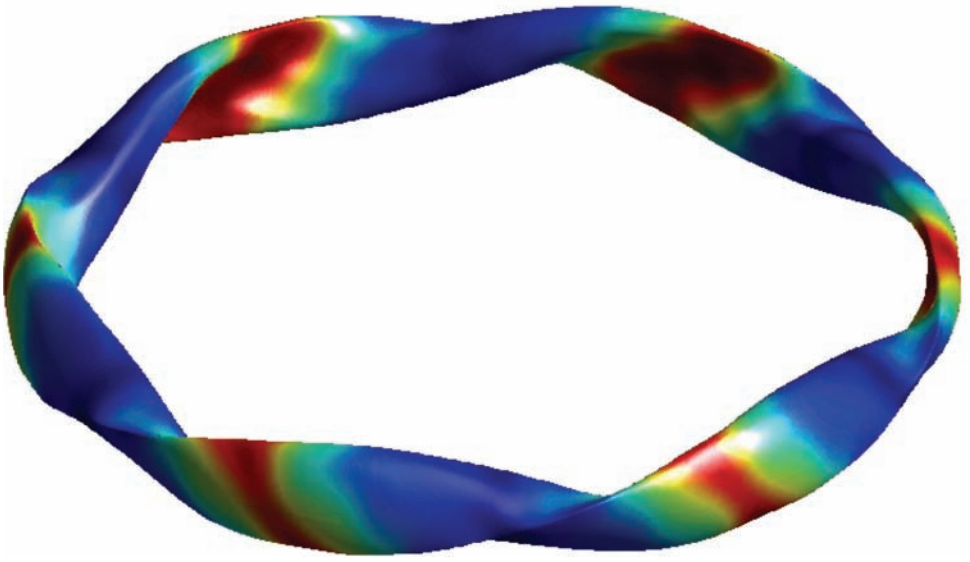

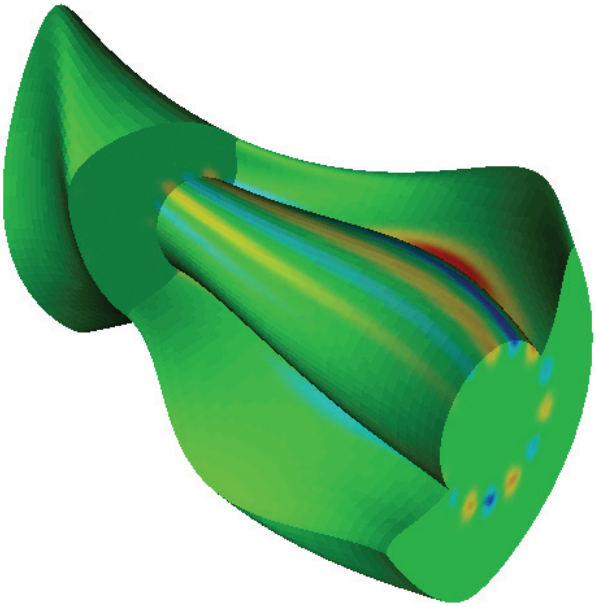

kink mode. The analysis of the various contributions to the energy principle reveals that 1) the parallel current density dominates the m/n = 1/1 energy perturbation, 2) the direct effects of the BC on the ballooning/interchange perturbed energy are weak and 3) the BC alteration of the Pfirsch-Schlüter current constitutes the dominant driving mechanism.

Electromagnetic Wave Propagation and Absorption in 3D Plasmas

The new code for the global solution of the Maxwell's equations in 3D plasmas (LEMan) [3] has been further developed and applied. The spectral representation of the wavefields along the magnetic surfaces implemented in the code is particularly efficient for the Alfvén frequency range. This made it possible to perform a full-wave analysis of the Alfvén spectrum in a realistic 3D geometry of the LHD stellarator with a very good convergence and high accuracy of the energy conservation. Figure 2 displays a distribution of the binormal component of the electric field at a frequency of 0.269MHz. At higher frequencies, the ion cyclotron (IC) resonance crosses the magnetic surfaces which broadens the Fourier spectrum of the solution and significantly increases the required computational resources. Several 2D configurations have been analysed in the IC frequency range. In a tokamak geometry, scenarios with different directions of the wave launching have been compared. The results reveal different character of the wave propagation and absorption for the high-field and the low-field side antenna in a two-species plasma. These results confirm previous analysis made with a 2D code called LION. As a first step towards the application in a 3D stellarator geometry at IC frequen-cies, we have analysed the spectrum of a mirror configuration. Similar to the tokamak case, patterns of the high- and low-field side propagation have been found. Also, absorption at the IC resonance in a single-ion species plasma has been shown which is an effect that cannot be obtained in tokamak geometry with the plasma model implemented.

Three-dimensional anisotropic pressure equilibria with balanced tangential neutral beam injection

Experimental discharges in the LHD heliotron in Japan using a high power neutral beam injection systen reveal a significant level of pressure anisotropy particularly at low plasma densities. The fixed boundary version of the VMEC equilibrium code [4] has been adapted to treat a family of distribution functions that can model tangential neutral beam injection to obtain equilibria with nested magnetic flux surfaces. Investigating a currentless 2-field period quasi-axisymmetric stellarator reactor device, we find that the total pressure surfaces are closely coupled with the magnetic surfaces even when the parallel component of the pressure greatly exceeds its perpendicular counterpart. The shift of the magnetic axis increases with the anisotropy at fixed total and thermal <β> values [5].

Acknowledgments

We would like to thank the support Staff of the Swiss Center for Scientific Computing as well as the on-site NEC application analysts for the kind support provided to this project. This project has been partially sponsored by Euratom and the Fonds National Suisse de la Recherche Scientifique.

References

[1] D.V. Anderson, W.A. Cooper, R. Gruber, S. Merazzi, U. Schwenn Methods for the efficient calculation of the (MHD) magnetohydrodynamic stability properties of magnetically confined fusion plasmas, International J. Supercomp. Appl. 4 (1990) 34-47.

[2] W. Lotz, P. Merkel, J. N ¨uhrenberg, E. Strumberger, Collisionless -particle confinement in stellarators, Plasma Phy. Control. Fusion 34 (1992) 1037-1052.

[3] P. Popovich, W.A. Cooper, L. Villard, Three-dimensional full wave propagation for cold plasma, Fusion Science and Technol. 46 (2004) 342-347.

[4] S. P. Hirshman, W.I. van Rij, P. Merkel, Three-dimensional free boundary calculations using a spectral Green's function method, Computer Phys. Commun. 43 (1986) 143-155.

[5] W. A. Cooper, S. P. Hirshman, T. Yamaguchi, Y. Narushima, S. Okamura, S. Sakakibara, C. Suzuki, K. Y. Watanabe, H. Yamada, K. Yamazaki, Three-dimensional anisotropic pressure equilibria that model tangential neutral beam injection effects, Plasma Phy. Control. Fusion 47 (2005) 561-567.

Quantum chemical studies of the anticancer drug cisplatin

Dr. Dirk V. Deubel

with Justin Kai-Chi Lau
Computational Science, ETH Zurich USI Campus, Switzerland

Description

The anticancer activity of cisplatin, cis-diammine-dichloroplatinum(II) (Figure 1), was serendipitously discovered more than 35 years ago. Today, platinum(II) complexes belong with annual sales of approximate 3 billion Swiss Franks to the most important anticancer drugs. Cisplatin is particularly active against testicular cancer and has also been used to treat other malignancies. Significant drawbacks in cancer chemotherapy with cisplatin including nephro- and neurotoxicity, intrinsic and acquired drug resistance of certain cancer types, and the inconvenience of an intravenous administration called for the development of new drugs.

Since the discovery of the anticancer activity of cisplatin, several therapeutic improvements including the discovery of new anticancer complexes have been made (see Figure 2 for examples): Carboplatin, diammine(1,1-cyclobutane¬dicarboxylato)¬platinum(II), is a second-generation drug that shows less toxic side effects than does cisplatin. Oxaliplatin, trans-R,R-1,2-cyclohexanediamine)¬oxalato¬platinum(II), is a third-generation drug that has been used to treat colorectal cancer, which is intrinsically resistant to cisplatin. Satraplatin, bis(acetato)¬amminedichloro¬(cyclohexylamine)¬platinum(IV) (JM-216), a platinum(IV) complex in phase III clinical trials, can be administered orally and is reduced in vivo to its platinum(II) analogue. The search for new anticancer drugs has extended to trans-Pt(II) complexes, oligonuclear Pt complexes, and complexes of other metals. Understanding their mode of action potentially accelerates the rational development of new drugs.

Computational chemistry provides valuable tools for drug discovery, in particular similarity searching, docking and scoring, de novo design, predictions of administration, distribution, metabolism, and excretion (ADME) parameters, as well as studies of drug-target interactions using force fields. Due to the kinetic control of the reactions of platinum anticancer drugs with biomolecules, however, meaningful computational approaches in the platinum anticancer arena will likely have to consider the transition states for the reactions of the electronically complicated metal complexes.

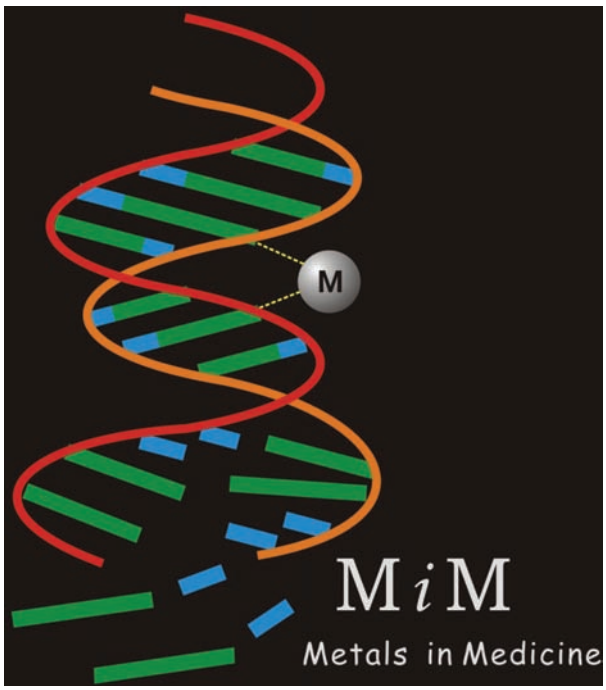

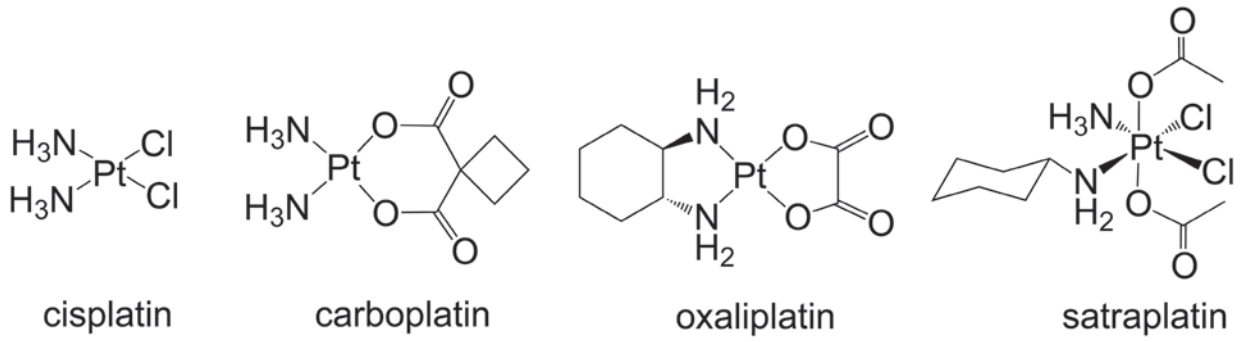

Figure 2: Examples of platinum anticancer complexes

Quantum chemistry is particularly suitable for such studies, because (i) the structures and energies of transition states for reactions of metal complexes can be predicted, whereas a force field parameterization is difficult for both transition states and transition metals, (ii) hypothetical competing reactions can be compared to one other, (iii) multiple-step reactions rather than only the rate-determining step can be investigated, and (iv) the electronic structure of molecules and transition states can be analyzed to obtain information about a possible control of reactivity.

The objective of this project has been to unravel mysteries in the mode of action of platinum anticancer drugs with the help of modern quantum chemistry. Our long-term goal is a contribution to the development of novel metallopharmaceuticals.

Achievements

The reactions of the anticancer drug cisplatin with various biomolecules including purine bases and amino acid residues have been studied computationally using density functional theory (DFT) at the B3LYP level. Our initial work aimed to clarify why cisplatin can finally reach the purine-N7 sites of DNA, the ultimate target of platinum anticancer drugs, despite the presence of sulfur-containing amino acid residues like cysteine (Cys) or methionine (Met) in the cell [1]. Since cisplatin binding to biological targets is kinetically controlled, we have investigated the transition structures and activation barriers for the reaction of the first and second hydrolysis products of cisplatin, i.e., cis-diammineaquachloroplatinum(II) and cis-diamminediaquaplatinum(II), with nitrogen and sulfur ligands including potential biological targets. Both hydrolysis products show a surprising kinetic preference to simple nitrogen nucleophiles (such as ammonia) over sulfur nucleophiles (such as dihydrogen sulfide). However, biologically relevant substituents can mask this intrinsic kinetic preference for nitrogen nucleophiles: The reactions with aromatic heterocycles have higher barriers than do simple alkyl-substituted molecules. To consider the fact that approximately 30 percent of the cell consists of material other than water, we have investigated environmental effects on the activation free energies by using a continuum dielectric model (CDM) at various values of the dielectric constant. The calculations reveal that a low dielectric medium, which is possibly present in DNA-protein complexes, specifically stabilizes the transition states for the reactions of cisplatin hydrolysis products with guanine-N7 sites, whereas the barriers for the reactions with methionine and other nucleophiles are less affected by the environment [1].

While most quantum chemical studies have focused on cisplatin hydrolysis and the binding of the hydrolysis products to biomolecules [2], our recent work aimed to look beyond these initial reactions. Since the ammine ligands remain coordinated at the metal upon formation of the most abundant cisplatin-DNA adducts, whereas they are displaced from the metal upon formation of metab-

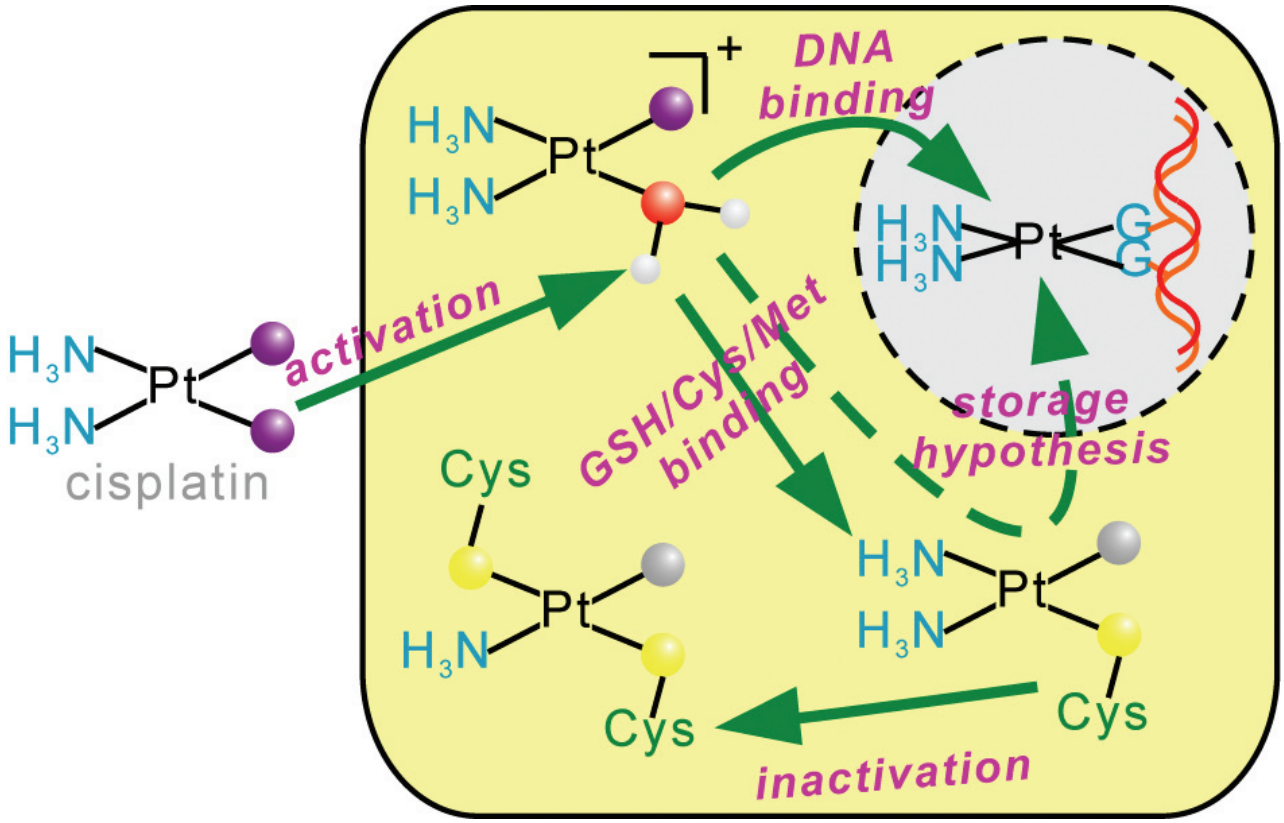

Figure 3. Activation, function, and inactivation of platinum anticancer drugs (simplified).

olites of the drug, we have analyzed the factors governing ammine loss from platinum(II) complexes as a potential pathway of drug inactivation in resistant cancers. The calculations systematically show the effect of (i) the trans ligand, (ii) the charge of complex, (iii) the nucleophile, and (iv) the environment on the thermodynamic instability and kinetic lability of platinum-ammine bonds. The results contribute to an understanding of the modes of cisplatin inactivation prior to DNA binding, for example, by overexpression of glutathione in cisplatin-resistant cancer cells. In particular, the calculations predict intracellular nucleophiles to replace preferentially the ammine trans to a sulfur ligand rather than the sulfur ligand itself. Hence, theory does not support the long-standing storage hypothesis, i.e., the transient platination of sulfur ligands and the subsequent transfer of the diammineplatinum core to genomic DNA, as a predominant mechanism in the mode of action of the drug [3].

Acknowledgements

This project has been supported by Prof. M. Parrinello, the Fonds der Chemischen Industrie (Germany), and the Swiss National Science Foundation.

References

[1] Factors Governing the Kinetic Competition of Nitrogen and Sulfur Ligands in Cisplatin Binding to Biological Targets. Deubel, D. V. J. Am. Chem. Soc. 2004, 126, 5999-6004.

[2] Quantum Chemical Studies of Platinum Anticancer Drugs. Deubel, D. V. Chem. Rev. 2006, 106, in preparation.

[3] Loss of Ammine from Platinum(II) Complexes. Implications for Cisplatin Inactivation, Storage, and Resistance. Lau, J. K.-C.; Deubel, D. V. Chem. Eur. J. 2005, 11, 2849-2855.

Seismic Ambient Recording and Numerical Modelling Applied to Site Effects Assessment

Dr. Donat Fäh

with Ivo Oprsal, Cecile Cornou, Sonia Álvarez-Rubio, Daniel Roten, Swiss Seismological Service, ETH Zürich, Switzerland

Description

Earthquake damage depends on the combined contributions from the earthquake source, the local ground motion amplification and the vulnerability of the buildings. After recent earthquakes however, a priori estimations of site effects became a major challenge for an efficient mitigation of seismic risk. In the case of moderate earthquakes, or moderate motion at some distance from large events, severe damage is indeed often limited to zones of unfavorable geotechnical conditions that give rise to significant site effects. In the case of large events, although damage distribution in the near-source area is also significantly affected by fault geometry and rupture history, there exist famous examples of tremendous site effects even in the near-field of large events (Northridge 1994,

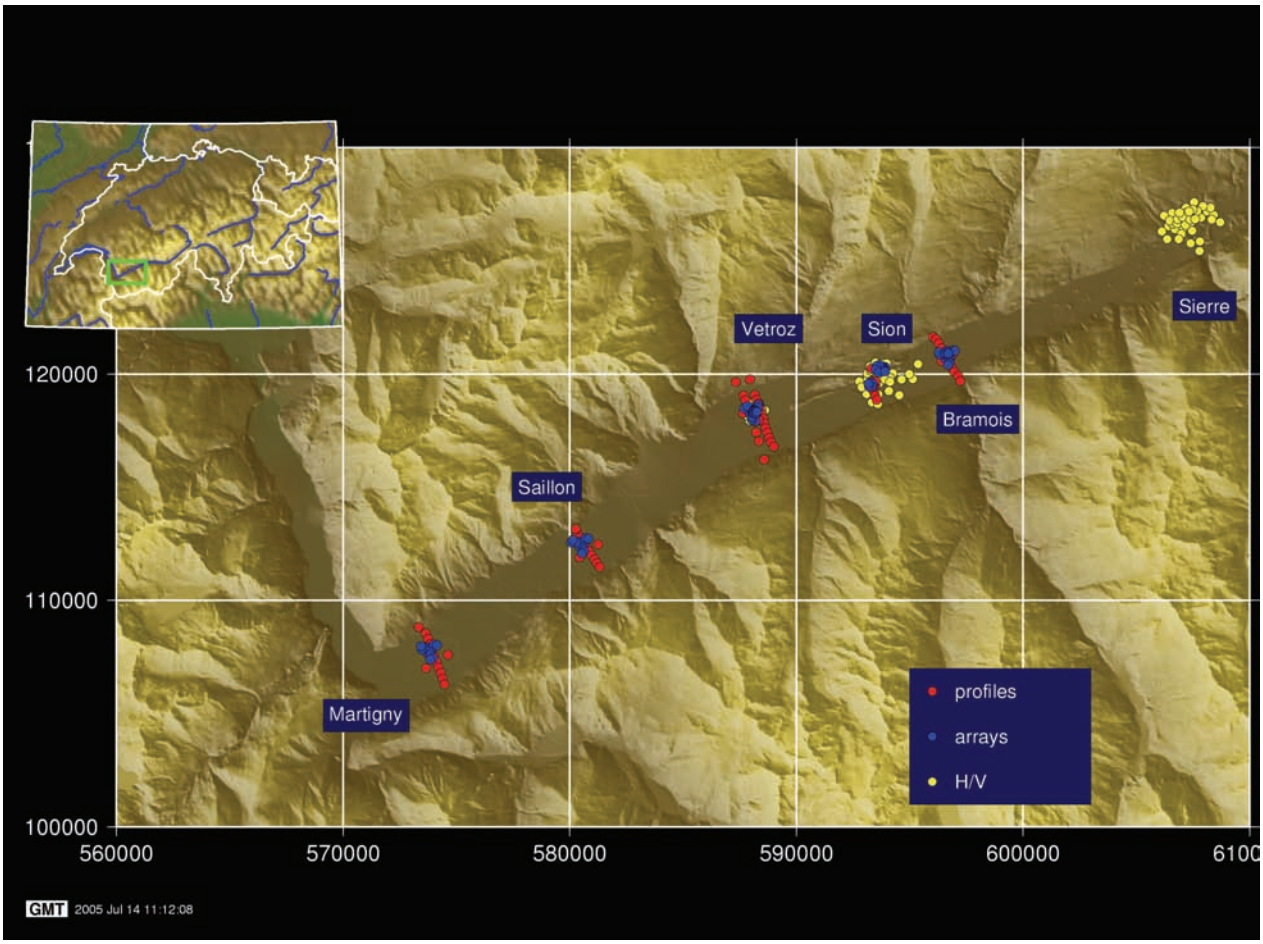

Figure 1: Map showing some of the main sites of the Valais (Switzerland), where the local seismic response is being assessed.

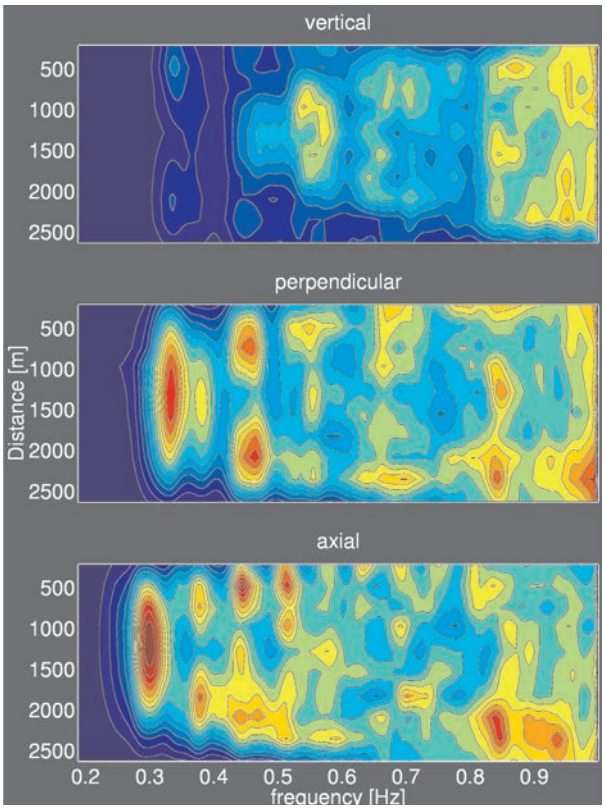

Figure 2. Average spectral ratio as a function of distance for all stations set along the profile at Martigny, Valais. (Roten et al. 2005)

Kobe 1995, Quindio 1999, Kocaeli 1999, Athens 1999, Bhuj 2001, Alger 2003). This underlines how important it is to account for site effects in the design of new constructions and in land use planning as well. This is particularly valid in areas of low and moderate seismicity, as is the case for most European countries.

The numerical prediction of ground motion with a reasonable confidence level is usually possible only if some key parameters such as earthquake rupture process, regional velocity model, and P- and S-wave velocity profiles and geometry of the site are known. Very promising developments based on the use of ambient vibration measurements were launched over the last decade for determining the near-surface geophysical conditions. Ambient vibrations are very easy to obtain in any conditions and much cheaper than classical geophysical site investigations. That is why they have the potential to significantly contribute to effective seismic risk mitigation, in particular in urban areas.

The present research project has dealt with the following issues:

- Investigate thoroughly the reliability of the ambient noise and numerical based techniques in retrieving some useful, qualitative and/or quantitative information on site conditions and/or site effects (SESAME project. EVG1-CT-2000-00026 funded by the Swiss Federal Office for Education and Science BBW Nr. 00.0085-2; SISMOVALP project: Interreg IIIB- Alpine Space Project)

- Precise the seismic velocities profiles within the Rhône valley sediment fill (Wallis area) by using these ambient noise based techniques on simulated noise (SHAKE-VAL project: Swiss National Science Foundation 200021-101920)

Achievements

The finite-difference noise simulations for real sites and cross checking between synthetics and actual noise simulations have been carried out for a few well-known test-sites. The work has focused first on tests on noise synthetics in order to establish a correct parameter set needed for the numerical modeling. Then, canonical models have been defined in order to determine the effects of the source distribution (density, time function, spatial location) on H/V ratios and on spatial correlations. A good representation of observed noise in terms of H/V shape and spatial correlation is achieved. The models for the sites Colfiorito, Liege, Basel, and Grenoble have been used in the modeling.

A numerical 3D method based on a hybrid approach has been applied. This approach combines computational methods in two successive steps. The 1st step uses finite-difference (FD), ray or discrete wave-number (DWN) method, and the 2nd step is a 3D FD method on an irregular grid with topography. The FD hybrid method was successfully tested on a series of models. The modeling technique has then been applied to the Basel area on a newly established P- and S-wave velocity

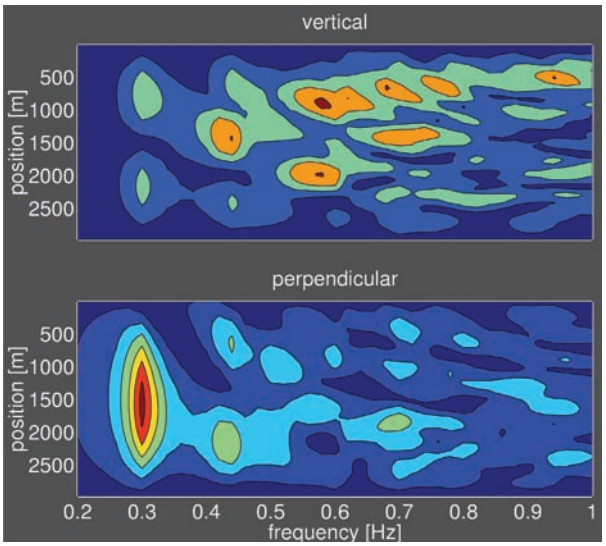

Figure 3 Numerical average spectral ratio computed by the Direct Boundary Element Method, as a function of distance for all stations set along the profile at Martigny, Valais. (Roten et al. 2005)

structure. The modeling for Basel was first done for different point-source models at various depths. Then an earthquake of the size of the 1356 Basel event, with magnitudes Mw ranging between 6.5 and 6.9 was simulated.

In the Valais area, the Swiss Seismological Service has carried out several earthquake and ambient noise recording campaigns. The work has been devoted to define a detailed geophysical and geological model that can explain most of the characteristics of the observed wave motion in the area. Several surveys based on the reference station method and the frequency-wavenumber technique have been carried out. The results have been compared with those obtained from the simulations computed by the Direct Boundary Element Method. Computations of realistic 2D models (Vétroz, Martigny) for different excitation characteristics have been performed.

2D resonance frequencies observed in the recorded ambient noise wave-field are very similar to those obtained from the 2D simulation. Spectral amplification derived from application of the reference station method to ambient noise and simulated spectral amplitudes exhibit a very similar pattern.

The observed phase characteristics of ambient noise at the identified 2D resonance frequencies are confirmed by the phase properties of simulated SH and SV waves.

The simulations therefore help to understand the importance of 2D resonance effects in the observed ambient vibration wave-field.

References

[1] Roten, D.; Álvarez-Rubio, S.; Fäh, D.; Giardini, D. (2005). Revealing the two-dimensional response of a sediment-filled valley from ambient vibration records. European Geosciences Union (EGU) General Assembly, Vienna.

[2] Roten, D., Cornou, C., Steimen, S., Fäh, D. and D. Giardini.(2004). 2D resonances in alpine valleys from ambient vibration wavefields. 13th World Conference on Earthquake Engineering, Vancouver.

[3] Álvarez-Rubio S.,Sánchez-Sesma F.J.,Benito J.J.,Alarcón E. (2004). The boundary element method:2D site effects assesment on laterally varying layered media(methodology). Soil Dyn. Earthquake Engng., 24:167-180.

[4] Cornou, C., J. Kristek, S. Bonnefoy-Claudet, D. Fäh, P.-Y. Bard, P. Moczo,M. Ohrnberger, M Wathelet (2004). Simulation of seismic ambient vibrations: II H/V and array techniques for real sites, 13th World Conference on Earthquake Engineering, Vancouver.

[5] Bonnefoy-Claudet, S., C. Cornou, J. Kristek, M. Orhnberger, M. Wathelet, P.-Y. Bard, D. Fäh, P. Moczo, F. Cotton (2004). Simulation of seismic ambient vibrations: I H/V and array techniques on canonical models, 13th World Conference on Earthquake Engineering, Vancouver.

[6] Roten D., Fäh D., Cornou C., Giardini D (2004). 2D resonances in alpine valleys identified from ambient vibration wavefields. Submitted to Geophys. J. Int.

[7] Oprsal, I:, Fäh, D., Mai, M. and D. Giardini (2004). Deterministic earthquake scenario for the Basel area - Simulating strong motion and site e.ects for Basel, Switzerland. J. Geophys. Res., Vol. 110, B04305, doi:10.1029/2004JB003188, 2005.

[8] Steimen S., D. Fäh, F. Kind, C. Schmid and D. Giardini (2003).Identifying 2-D Resonance in Microtremor Wave Fields. Bull. Seism. Soc. Am., 93, 583 - 599.

[9] Álvarez-Rubio, S; Benito, JJ; Sánchez-Sesma, FJ; Alarcón, E (2005). The use of direct boundary element method for gaining insight into complex seismic site response. Computers & Structures; 83(10-11): 821-835.

Computational Science and Engineering in Microelectronics and Optoelectronics

Prof. Wolfgang Fichtner

with Stefan Röllin, Bernhard Schmithüsen, Beat Sahli, Eduardo Alonso, M. Streiff, Lutz Schneider, Simon Brugger and Andreas Schenk; Institut für Integrierte Systeme ETH Zürich, Switzerland
P. Arbenz and M. Becka; IWR-ETH Zürich
O. Schenk; University Basel
H. Fitze; Paul Scherrer Institute, Villigen

Project Abstract

Computational Science and Engineering is in microelectronics and optoelectronics an established methodology in research as well in development. Physics based process simulation (i.e. simulation of the manufacturing technology) and device simulation (i.e. simulation of the operating of semiconductor devices) is known as «Technology CAD» (TCAD). The benefit of TCAD is not only of technical and economic nature (reduction of the very expensive experimental runs in the development phase, time-to-market of integrated circuits), it is of the same importance for science and findings: physical simulations make it possible to have an insight view in processes or device operating during transient and very fast events, which is closed to experimental techniques. Due to the continuous miniaturization of technology and devices (e.g. research subjects are CMOS transistors in the regime of 65 nm down to 15 nm, quantum structures or material layers below 2 nm) there is an ambitious challenge for research in TCAD (3D simulation, transient events in the pico second regime, complex material structures). This requires more and more number crunching resources per job, i.e. more than 32 GB of memory, several hours of CPU time on high-end compute servers and parallelization in the range of 4 to 8 processors.

This project is structured in 4 research topics:

- Numerics: Robust iterative methods and Harmonic Balance in Semiconductor Device Simulation
- Molecular Dynamics: Ab Initio Simulation of Process and Device Physics
- Optoelectronics: Advanced Numerical Simulation of Optoelectronic Devices
- Device Physics: Deep Submicron and Nano Device Simulation in Microelectronics

Numerics: Robust iterative methods and Harmonic Balance in Semiconductor Device Simulation

The computational simulation of semiconductor micro- and optoelectronic devices has matured to an indispensable tool for the design and development of state-of-the-art highly integrated systems. The research topic of our group currently concentrates on two different aspects of semiconductor device simulations.

Optimized Parallel Incomplete LU-Factorizations for Shared-Memory Multiprocessors

Personnel: Stefan Röllin
Funding: CSE-SEP ETHZ

During a semiconductor device simulation a lot of large sparse linear systems have to be solved.

The best choice for large 3D simulations to solve these linear systems is an iterative solver. The time and memory requirements are much smaller compared to direct methods. For example a simulation with about 320,000 unknowns requires about 12.5 GB of memory, whereas an iterative solver only needs 3.2 GB. Moreover, the simulation time is reduced by a factor of 6 compared to the direct solver.

The wall-clock time for the solution of the linear systems can further be reduced with the use of parallel computers. Most of the time in the iterative solver is spent for the computation of the preconditioner and the iterative method, e.g. BiCGStab. The existing parallel implementation for these parts gave satisfactory results, but there was room for improvements. An optimized version has therefore been implemented, which divides the computation of the Schur complement among the involved processors. As a drawback, one has to take into account slightly increased memory demands and a higher algorithmic complexity.

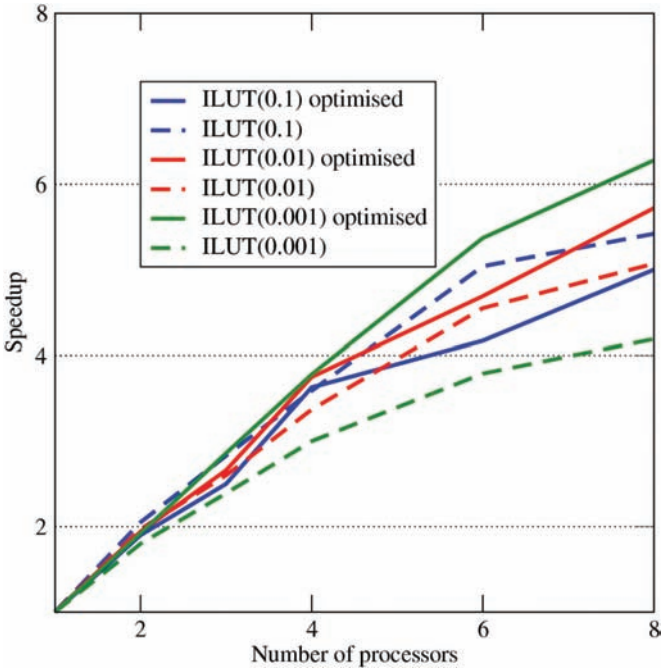

Figure 1: Speedups measured on the IBM SP4 for the optimised incomplete ILUT factorization compared with an older implementation. The performance is significantly increased, especially with a small drop tolerance.

The realized implementation has been tested on several shared-memory multiprocessor architectures for different drop tolerances, i.e., parameters for the factorization. The results show that the performance of the optimized parallel incomplete ILUT factorization scales quite well. With eight processors, speedups up to 6.3 have been measured.

Iterative Solution Procedures for the Harmonic Balance Equation in Device Simulation

Personnel: Bernhard Schmithüsen

Funding: KTI-6378.1 LASSIS

The Fourier transformation of the differential equation describing periodically excited electronic systems leads, using truncated Fourier series, to the harmonic balance (HB) equation, a very large nonlinear algebraic equation containing the Fourier coefficients of the solution variables as unknowns. Compared to DC simulations, with typical system sizes of several ten thousand variables, the number of unknowns grows linearly with the number of approximating harmonics. The use of iterative linear solvers becomes indispensable.

Within our mixed-mode device simulation platform DESSIS Newton-like solving methods for the HB equation have been coupled to the standard parallel linear iterative solver ILS, to the parallel direct solver PARDISO, and a novel block-band preconditioned GMRES solver with memory-less matrix assembly. Experimental simulations show that well established incomplete-LU-factorization-based preconditioners are hardly feasible for the HB problem, while, astonishingly enough, a physically motivated block-band preconditioner for GMRES iterations lead to reasonable convergence even under large signal operation. Compared to Newton-direct methods, the novel Newton-BBP-GMRES iteration scheme requires more Newton steps but reduces significantly the memory consumption of the simulation and enables the use of a larger number of approximating harmonics.

Molecular Dynamics: Ab Initio Simulation of Process and Device Physics

The topic of the research of our group is the diffusion (and clustering) of dopants and intrinsic defects in silicon. Our project consists of two parts. The first part is developing better physical models for the diffusion (and clustering) of dopants and intrinsic point defects in silicon. The second part is developing and implementing a new kinetic Monte Carlo (KMC) solver which can deal with more complex diffusion/clustering models than the continuum based solvers currently used in process simulators.

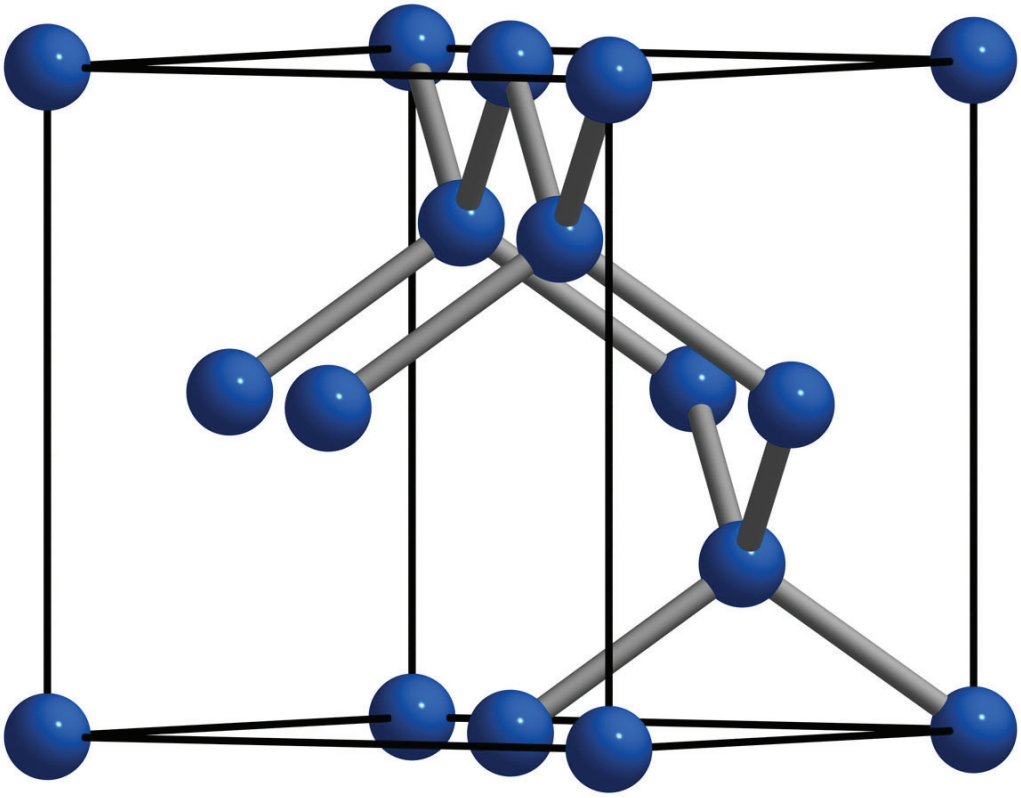

Figure 2: This picture shows a vacancy in the silicon crystal lattice: One silicon atom is missing.

Vacancy Diffusion in Silicon

Personnel: Beat Sahli

Funding: TOP NANO 21 5779.2 MOLDYN

In a previous project phase the diffusion coefficient of the self-interstitial was calculated for different temperatures with ab-initio molecular dynamics simulations. The method worked well and indeed proved to be indispensable. In the current phase the same method is applied to the diffusion of the vacancy in silicon.

The vacancy and the self-interstitial are the two intrinsic point defects in silicon. It is necessary to know their properties for modeling dopant diffusion in silicon and for modeling silicon crystal growth with the Czochralski method. But their diffusion coefficients and many other of their properties are very difficult to measure. Accordingly, many studies have tried to determine the diffusion coefficients of the vacancy and the self-interstitial with theoretical methods. But the required amount of computing power to do this with an accurate potential energy function and without additional assumptions about the defect dynamics has only recently become available.

The simulations are done with the Vienna Ab-initio Simulation Package (VASP). The particle trajectories produced by the molecular dynamics simula-

tions are analyzed in order to determine the trajectory of the defect in the simulation cell. From the defect trajectory the diffusion coefficient is calculated. The procedure is repeated for several different temperatures and a prefactor and a migration energy are extracted by fitting to an Arrhenius curve.

Integration of Kinetic Monte Carlo Module in Continuum Process Simulator

Personnel: Eduardo Alonso
Funding: TOP NANO 21 5779.2 MOLDYN

The kinetic Monte Carlo (KMC) code ATOMISE developed in the MOLDYN project has been integrated as a module into the continuum based process simulator FLOOPS. Its TCL interface allows for the implementation of diffusion and oxidation models at user level. ATOMISE is a diffusion solver based on the KMC method with charged defects and Fermi level effects, that can now substitute the diffusion processing steps in FLOOPS. Like in FLOOPS, different diffusion models can be constructed in ATOMISE without modifying the source code.

During the coupling stage, the FLOOPS supported diffusion models have been implemented in ATOMISE. Direct comparisons between finite element simulations by FLOOPS and KMC by TOMISE have been conducted in order to assess the charges implementation. The results have been very encouraging since the agreement between continuum and atomistic simulations has been excellent, while performance has not been affected. Further work geared towards extending the coupling between FLOOPS and ATOMISE to all the processing steps, such as etching and oxidation, are planned. In this manner, the whole atomistic picture can be conserved throughout the entire process simulation.

Optoelectronics: Advanced Numerical Simulation of Optoelectronic Devices

Optoelectronic manufacturing processes have matured to such a degree of reproducibility that it becomes feasible to use computer aided design tools to explore the design parameter space for an optimum device design. In this way many costly production trial runs become obsolete and device design becomes more efficient in terms of cost and time. The optoelectronic devices that have been investigated in the present project are destined at applications in sensing, optical storage technology, biotechnology, medical applications, data- and telecommunications.

Wavelength Tuning Behavior of Sampled-Grating DBR Laser

Personnel: Lutz Schneider
Funding: TOP NANO 21 5785.1 MQW

Covering all the physical effects in widely-tunable sampled-grating DBR (SGDBR) lasers requires full 3D device simulation. In this project, the numerically challenging task of acquiring a wavelength tuning map through self-consistent electro-optical simulation has been mastered.

While tunable lasers such as DFB and three-section DBR lasers exhibit a smooth and continuous tuning behavior widely-tunable lasers with sampled gratings are known for their discontinuous wavelength jumps of up to more than 5 nm depending on the specific mirror design. A new approach had to be developed to deal with this particularity within the self-consistent device simulation framework. Comparison with experimental data shows very good agreement. A tuning map proves to be an important tool for industrial device design.

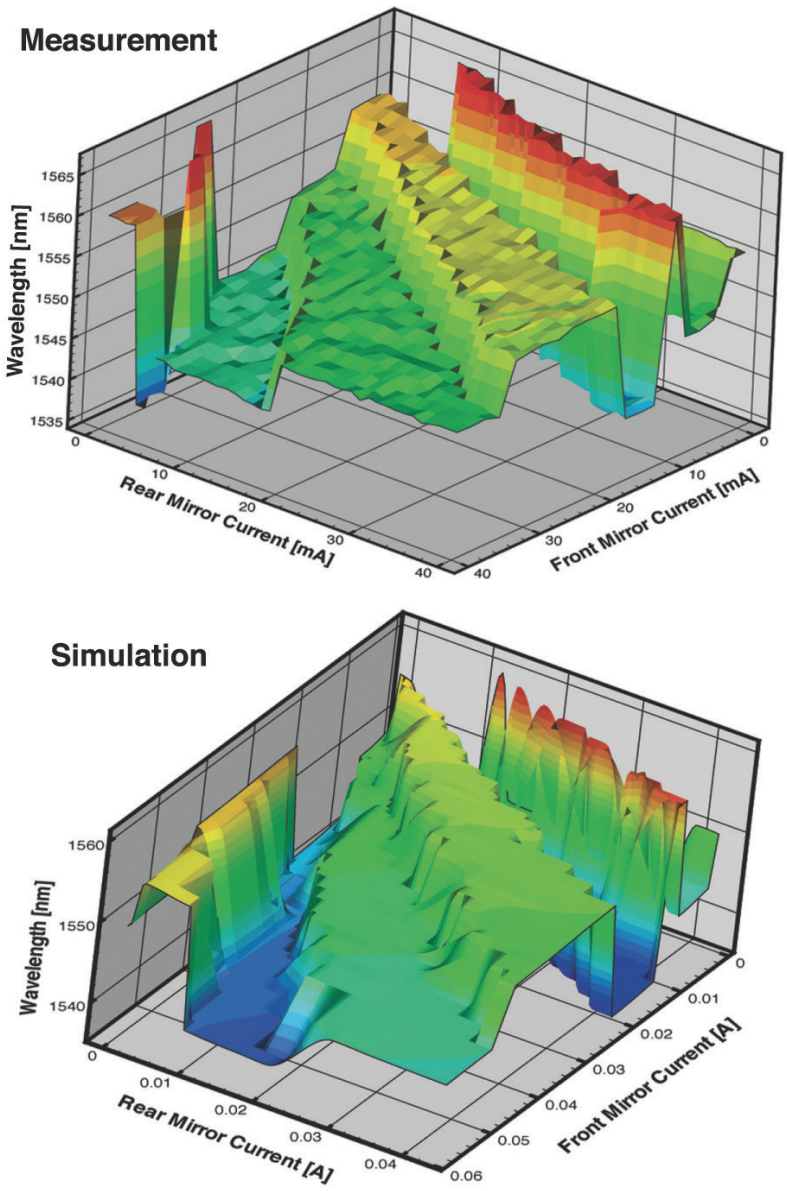

Figure 3: Measured (top) and simulated (bottom) wavelength tuning map versus front and rear mirror tuning currents as obtained from 3D device simulation.

Large Scale Eigenvalue Problems in Optoelectronic Semiconductor Lasers and Accelerator Cavities

Personnel: S. Röllin, M. Streiff, B. Schmithüsen, P. Arbenz, M. Becka, O. Schenk, H. Fitze

Funding: CSE-SEP ETHZ

Solving large scale eigenvalue problems is a major task in the numerical simulation of optoelectronic semiconductor lasers, as well as of accelerator cavities. The discretization of the homogeneous Maxwell equations leads to generalized eigenvalue problems that have more than one million of unknowns and therefore are very challenging to treat. The Jacobi-Davidson eigensolver is used to solve these problems. In order to reduce the solution time, this method has been parallelised for distributed memory architectures. The most difficult part has been the parallelization of the two-level hierarchical preconditioner. The realized implementation shows very good speedups.

The solution of large sparse linear systems arising in the electronic part is another major computational part in a semiconductor laser simulation

apart from the solution of the eigenvalue problems. The increasingly complex devices and the need to carry out 3D simulations lead to dozens of linear systems with more than 100,000 unknowns. Iterative solvers are the only viable solvers for these systems. In this part of the project, a fully parallel iterative solver has been implemented for shared memory architectures with the help of OpenMP. The numerical experiments on different architectures show that good speedups are achieved with a modest number of processors.

Device Physics: Deep Submicron and Nano Device Simulation in Microelectronics

As devices are scaled down, the usual assumption of local thermodynamic equilibrium does not hold anymore and the usual transport models, i.e. Drift-Diffusion (DD), Hydrodynamic (HD) and noise models, become less reliable. Therefore more accurate and complicated models are needed to describe this «new reality».

Hierarchical Physics-based RF Noise Modeling for Silicon Devices

Personnel: Simon Brugger, Andreas Schenk

Nowadays different methods are available to compute noise figures of merit for semiconductor devices.

In an effort to compare all those methods with each others a device simulator for noise computation called SimnIC was developed and validated. SimnIC is a simulator for silicon devices which can compute both the steady states and small signal behaviors using the drift-diffusion, energy-balance, one-particle and many-particle Monte Carlo (MC) methods. It is, therefore, not only able to compute noise figures using the impedance field method (IFM) coupled with MC generated- or thermodynamic noise sources, but also using the one-particle and many-particle MC methods. The simulator is fully parallelized and can run on many processors on shared memory architecture. It is therefore possible to simulate millions of particles in a reasonable amount of CPU time.

SimnIC enables to determine the cases where the IFM breaks down and offers, in those cases, alternative ways to compute the needed figures of merit.

Inverse modelling to monitor source regions of air pollutants in Europe

Dr. Doris Folini

with S. Ubl, Empa Dübendorf, Switzerland

Frame of the project

Various climate relevant gases (greenhouse effect, ozone layer depletion) are emitted more or less continuously into the earth's atmosphere. The release of some of these gases is regulated or banned by the Montreal- and Kyoto-protocols. Given their climate impact and the need to verify the imposed regulations on some of them, monitoring the emission of such gases is a key issue today, and the motivation for our project. There are essentially two ways to establish such emission inventories. The 'traditional' way is to compile emission inventories based on sales numbers, taxes etc. However, for various substances this procedure yields unsatisfying results or is barely feasible at all.

In our project we follow the second, alternative approach. This approach relies on numerical models to derive regionally resolved emission estimates from long term concentration measurements of various gases, taken at a few permanent measurement stations. The basic idea is to use an atmospheric transport model to link emissions and measured concentrations, and then to determine a regionally resolved emission scenario such that the long term (several years) concentration measurements are best reproduced. On the European scale, we currently use as transport model the Lagrangian Particle Dispersion Model (LPDM) of MeteoSwiss.

One advantage of this approach is its relative independence. Data from a few monitoring sites is used instead of data from national reports. Also, the approach allows fast reaction to newly developed chemical substances. As soon as a new substance can be measured, for example by gas chromatography-mass spectrometry, emission estimates become possible. 'Traditional' inventories take a few years to include a new substance.

The ultimate goal is to derive regionally resolved emission maps for various gaseous substances, in particular halocarbons and other greenhouse gases. Halocarbons are of special interest for several reasons. Substances of this class are listed in both, the Montrealand Kyoto-protocol. Nevertheless, 'traditional' inventory data is relatively scarce, partly due to the existing wide variety of substances. From a modeling point of view they are attractive as their chemical reaction time scales are much longer than the relevant transport time scales.

Lagrangian Particle Dispersion

To model atmospheric transport of passive tracers (for example halocarbons) we use the LPDM of MeteoSwiss in backward mode. In this model, a large number of particles are released at one point (the measurement site) during some time (the measurement period) and are then traced backward in time. Their motion is governed by meteorological wind fields plus a turbulent velocity component. The wind fields stem from the alpine model of MeteoSwiss and are given on a grid with 7km x 7km horizontal spacing and 45 vertical

levels. The turbulent velocity component is obtained as the solution of a Langevin equation.

As output of the LPDM we get a 3D residence time map which, in essence, gives the probability that an air parcel reaches the measurement site during the measurement period. From this 3D data we can extract the 2D footprint: the residence time at each horizontal grid point, summed over a boundary layer of a certain height, for example 500 m. The footprint basically gives a probability map of what boundary layer air (thus possibly polluted air) will reach the measuring site. The footprint thus contains information on what geographical region can be how well monitored by a particular measuring site.

LPDM in complex terrain

We currently focus on measurement data from the high Alpine station Jungfraujoch, 3580 m asl. Jungfraujoch is particularly suited to monitor central European emissions as it is reached by both, clean background air masses at one time and polluted boundary layer air from central Europe at other times. This allows to estimate the net contribution from central Europe to the measured concentrations.

Running an atmospheric transport model at this site is, however, demanding because of the complex topography. Consequently, it is crucial to analyze the performance of our LPDM under these conditions. One way to do this, is to compare a real, measured data series with a corresponding, synthetically generated data series. To obtain the latter we first compute, by means of our LPDM, one footprint every three hours, for each day of the years 2003 and 2004. Multiplying each footprint with the EMEP CO inventory data (50 km x 50 km horizontal grid spacing, http://www.emep.

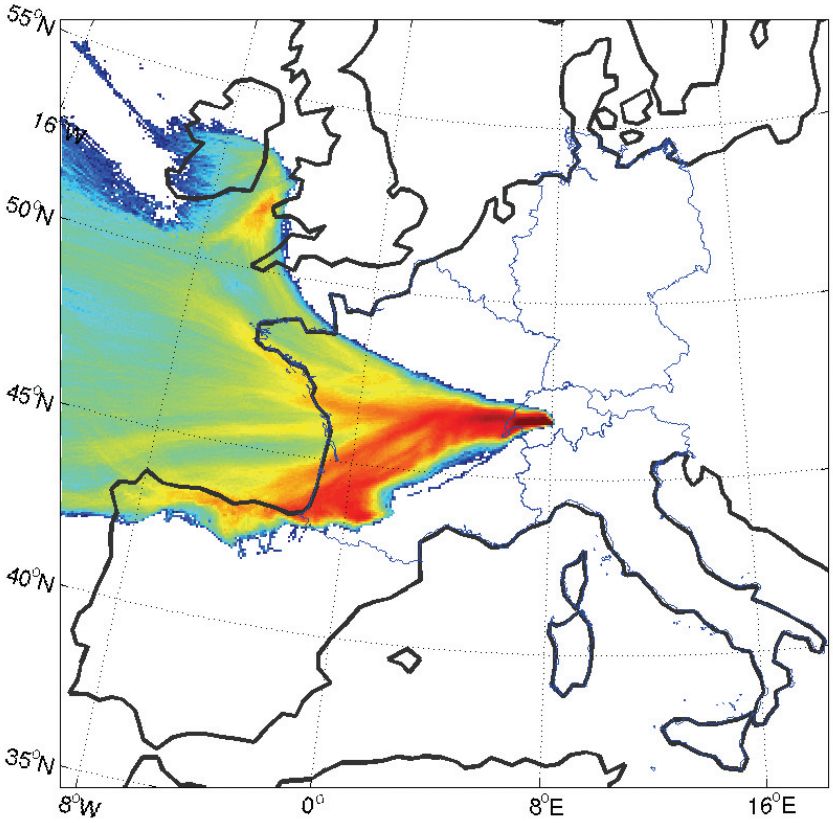

Figure 1: Footprint for station Jungfraujoch, July 4, 2002, measurement period between 03:00 and 06:00. Measured concentrations during this time contain signatures of sources that are located in the western part of Switzerland and in the central part of France. Red indicates high residence time, blue is low residence time.

int) yields our synthetic data series. Comparison shows that the average magnitude of the measured and synthetic data agree quite well. Also captured well on average is thermally induced uphill flow in summer. Correlation between the two data series is highly sensitive to the assumed boundary layer height of the footprint.

European emission maps from inverse modeling
Consider a relatively long living substance. A measured concentration value at a particular measurement site can, in principle, be decomposed into a set of contributions from a variety of different sources (like different cities or industrial regions) that lie in different places and have different source strengths, i.e. emit a different amount of the substance per time. Likewise, if we cover Europe by a rectangular grid, the measured concentration can be decomposed into a set of contributions from different grid cells. The average emission per time of each cell, i.e. the emission strength of each cell, is the emission map we want to determine.

The footprints (residence time maps) we obtain from our LPDM basically relate the measured concentrations and the emission map we want to determine. Footprint times emission map should yield the measured concentration value. Therefore, to obtain the desired emission map an inverse problem has to be solved. One possibility to do this is simulated annealing, where the emission map is adjusted more and more such as to obtain optimum agreement between the modeled and measured concentration data.

Representativeness of measurement sites
To obtain emission maps based on measurements from a particular station, it is important to determine the representativeness of the station. What sources can actually be recovered from the measured concentrations? How far away can a source be such that it still contributes often and strongly to the measured data? How many measurement sites would we needed to cover the whole of Europe? And where would they have to be placed? With regard to the last question it goes without saying that a station that is to monitor a wider region must not be placed close to strong pollution sources, like cities or industrial plants. Apart from this pre-requisite, the answer to the above questions lies to a good part in the footprint of a measurement site. For example, analysis of the footprint data of Jungfraujoch shows that sources up to a distance of roughly 400 km contribute frequently to the measured concentrations at Jungfraujoch. Extrapolating from this one station, several tens of stations thus would be needed to cover the whole of Europe.

Full QCD with 2+1 Light, Chiral Fermions

Prof. Peter Hasenfratz

with F. Niedermayer, A. Hasenfratz and K.J. Juge
Institute of Theoretical Physics, University of Bern, Switzerland
Physics Department, University of Boulder, Colorado,USA
Physics Department, Trinity College, Dublin, Ireland

Description

Quantum Chromodynamics (QCD) is one of the four fundamental interactions in nature. QCD is believed to describe exactly the properties of hadrons, like those of protons, neutrons, pions, etc. The theory contains a small number of fundamental parameters only. Most of the phenomena in QCD are non-perturbative and standard analytic quantum field theoretical methods fail.

Lattice QCD opens the way towards numerical techniques. Due to the universality property of quantum field theories, there is a considerable freedom to discretize the action of QCD. As the lattice becomes fine (continuum limit) the different formulations produce identical results. The speed of approach towards the continuum limit, however, depends on the details. QCD actions which approximate the fixed point of a renormalization group transformation have good theoretical and numerical properties. The present form of the fixed point action has been tested in detail in the quenched approximation and the results were very encouraging: the action shows small scaling and chiral symmetry violations.

The main numerical problem of QCD simulations is the need to calculate repeatedly the determinant of a huge sparce matrix D, where D is the Dirac operator which describes the interaction between quarks and gluons in QCD. It is practically impossible to calculate this determinant exactly, but there exist several local updating algorithms to treat det(D) stochastically. The complex structure of the fixed point action makes it difficult to use these local algorithms, however. We have constructed, coded and tested a new global updating procedure. The algorithm works for small quark masses also which allows to simulate the system with parameters close to that of in nature.

In the algorithm a global gauge field update is followed by several accept/reject steps, where parts of the determinant are switched on gradually in the order of their expenses.

In the ongoing runs the spatial sizes are Ls = 1.2 fm and 1.8 fm with a lattice resolution a = 0.15 fm. One of the important questions we want to investigate is the autocorrelation length in the Markov chain of generated configurations. Another question is whether the algorithm is able to change effectively the topological charge Q of the gauge configurations. Most of the existing local updating algorithms have serious problems with creating and annihilating topological charge whose presence is important to the physics of QCD. The to-pological charge density depends on the quark masses and should go to zero as the quark masses are tuned to zero. The topological charge is reflected by the small real eignevalues of the spectrum of the Dirac

operator D. In Fig. 1 a part of the spectrum is shown for infinitely heavy quark masses, equivalent to a pure Yang-Mills gauge theory, (on the left) and QCD with closely massless quarks (on the right). The figure shows the first 48 low lying (smallest absolute value) part of the spectrum in the complex plane from 50 subsequent configurations from the Markov chain for these two extreme cases. The presence of small real eigenvalues in the Yang-Mills case shows clearly a non-zero topological susceptibility Q2 , while in closely massless QCD the real modes disappeared indicating that the algorithm deals with the topology effectively.

The larger lattice with Ls = 1.8 fm is sufficiently large to allow light hadron spectroscopy, calculate the physical quark masses and low energy matrix elements. The remaining finite volume distortions can be removed with the help of chiral perturbation theory. While on the smaller lattice we generate configurations since several months already, on the larger lattice the starting configurations have not even equilibrated yet and a serious, competitive simulation requires computing power significantly beyond our present possibilities.

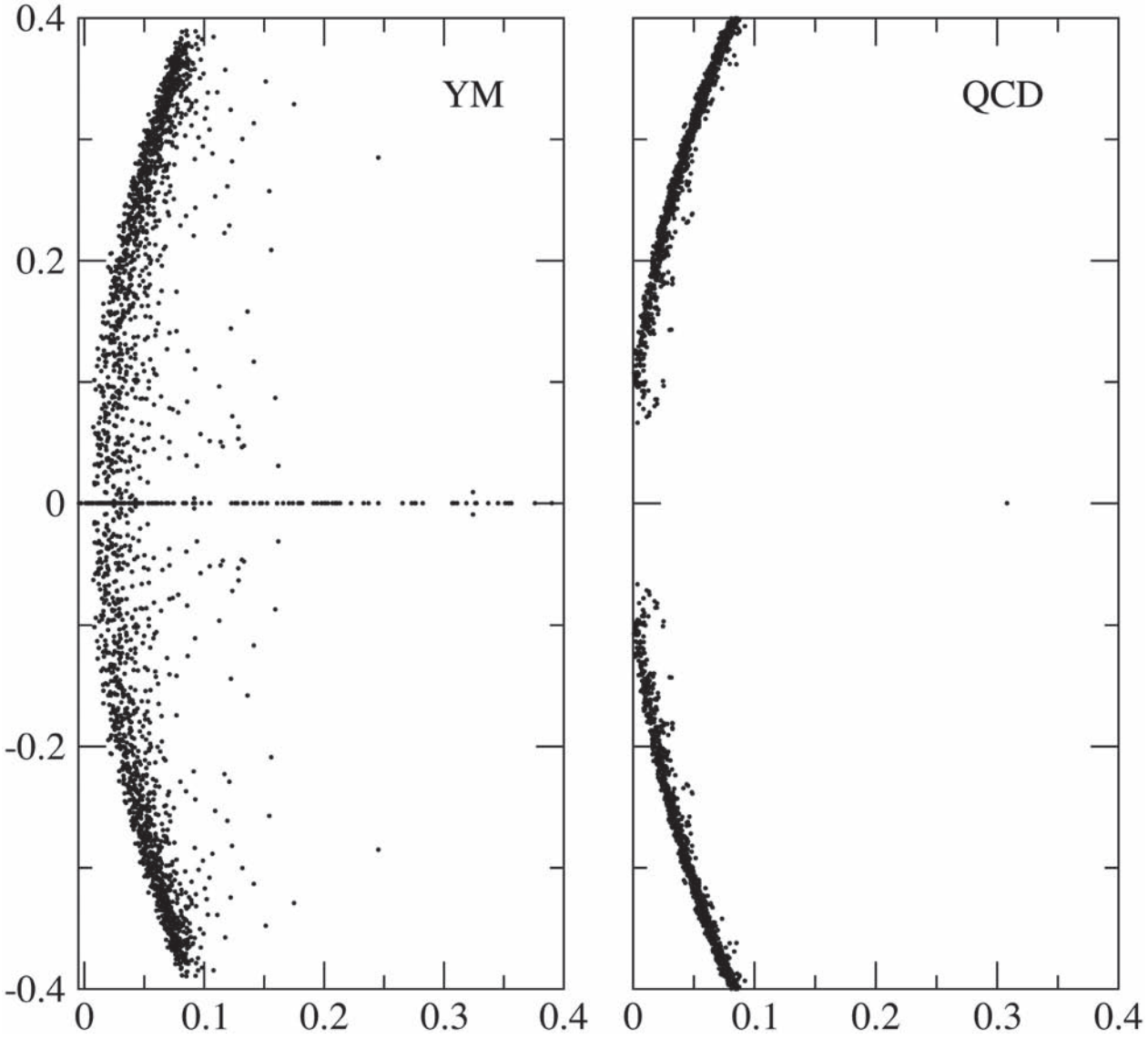

Figure 1: The low lying eigenvalue spectrum of the Dirac operator on 50 pure Yang-Mills (left) and 50 equilibrated dynamical (right) configurations. Both panels correspond to 83 ×24, a ≈ 0.14 fm lattices with the same lattice quark masses.

References

[1] P. Hasenfratz, K. J. Juge and F. Niedermayer, (BGR collaboration) New results on cut-off effects in spectroscopy with the fixed point action, JHEP 0412 (2004) 030, hep-lat/0411034.

[2] A. Hasenfratz, P. Hasenfratz and F. Niedermayer, (BGR collaboration) Simulating Full QCD with the Fixed Point Action, hep-lat/0506024.

Photophysics and photochemistry of transition metal compounds: theoretical approaches

Prof. Andreas Hauser

with L. M. Lawson Daku and A. Vargas
Département de chimie physique, Université de Genève, Switzerland

Description

Photophysical and photochemical properties of transition metal compounds are increasingly being made use of in advanced technological applications. It is thus of more than just academic interest to achieve an in-depth understanding of the fundamental photophysical and photochemical processes, such as laser-induced luminescence, intersystem crossing (ISC), internal conversion, excitation energy transfer or light-induced electron transfer, and the parameters which govern their rates and quantum efficiencies. Our research interests are focussed on establishing relationships between structural, electronic and energetic parameters, and the dynamics of elementary radiationless processes at a molecular level, using time-dependent optical spectroscopy in condensed media at temperatures between 4.2 and 300 K [1] along with theoretical methods based on density-functional theory (DFT).

Achievements

During 2004/2005, the resources allocated to our project allowed significant progress in the understanding of the photophysics of several transition metal complexes to be achieved. For the low-spin (LS) iron(II) complexes $[Fe(bpy)3]^{2+}$ and $Fe(tpy)2]^{2+}$ (bpy = 2,2'-bipyridine; tpy = 2,2':6',2"-terpyridine) DFT characterisation in the LS $^1A_{1g}(t^6_{2g})$ ground state and metastable high-spin (HS) $^1T_{2g}(t^4_{2g}e^2_g)$ states helped gain major insight into the dynamics of the HS → LS relaxation that occurs after the photo-induced population of the HS state.

For $[Fe(bpy)3]^{2+}$, the low-temperature tunnelling in the HS → LS ISC is quite fast, varying between 10^4 and 10^6 s^{-1} depending on the host in which the complex is embedded. Assuming for this complex a HS-LS Fe-N bond length difference of $\Delta r_{HL} \approx 0.2$ Å as for iron(II) spincrossover complexes with the same $[Fe\text{-}N_6]$ coordination sphere, a zero-point energy difference $\Delta E°_{HL}$ of 2500-5000 cm^{-1} could be deduced from the low-temperature tunnelling dynamics on the basis of the inverse gap low (Figure 1A). The DFT characterisation of $[Fe(bpy)_3]^{2+}$ in both spin-states validated this structural assumption. However, with the exception of the RPBE and B3LYP* density functionals, most of the functionals used failed to correctly reproduce the HS-LS energy difference (Figure 1). Hence the ability of the different density functionals to give estimates of the HS-LS energy gap close to the experimental values was used to assess the performance of these functionals [2]. In that respect, the DFT study of $[Fe(bpy)3]^{2+}$ parallels our DFT studies of $[Fe(H_2O)_6]^{2+}$ [3] and $[Fe(NH_3)_6]^{2+}$ [4] targeted at assessing the performance of modern functionals for energy and structural differences between the LS and HS states of iron(II) complexes against *ab initio* CASPT2 results.

The low-temperature tunnelling dynamics of the HS → LS relaxation of $[Fe(tpy)_2]^{2+}$ embedded in crystalline hosts can be drastically slower than the one of the chemically similar $[Fe(bpy)_3]^{2+}$ complex ($k_{HL}(T \rightarrow 0) \sim 10^{-4}$ s^{-1}), and gives rise to the light-in-

duced trapping of $[Fe(tpy)_2]^{2+}$ in the HS state similar to spin-crossover complexes. The DFT study of $[Fe(tpy)_2]^{2+}$ showed that the HS-LS energy gap in this complex is as large as in $[Fe(bpy)_3]^{2+}$, in agreement with the experimental observation that the HS states cannot be thermally populated up to ~500 K for both complexes. The main difference turned out to reside in the structural variations which go with the change of spin-states. Indeed, in contrast to $[Fe(bpy)_3]^{2+}$ for which the structural changes take place along the totally symmetric breathing mode, that is a symmetric elongation of the Fe-N distance Δr_{HL} of ~0.2 Å, the geometry of $[Fe(tpy)_2]^{2+}$ undergoes a strongly anisotropic distortion after the photoinduced population of the HS state. Hence, the return to the LS state requires a large structural reorganisation along several internal coordinates which, in turn, slows down the relaxation and which is responsible for the light-induced spin-state trapping phenomenon observed for $[Fe(tpy)_2]^{2+}$ [5].

The allocated resources have also allowed us to characterise the cobalt(II)tris(2,2'-bipyridine) $[Co(bpy)_3]^{2+}$ complex in the HS $^4A_1$ and LS ^2E states in the gas phase using DFT methods. We could thus investigate the ability of the density functionals to correctly predict the HS ground state of the complex and also to describe the Jahn-Teller effect in the LS state. The absorption and CD spectrum of $[Co(bpy)_3]^{2+}$ could be anlysed using time-dependent DFT (TDDFT) calculations [6].

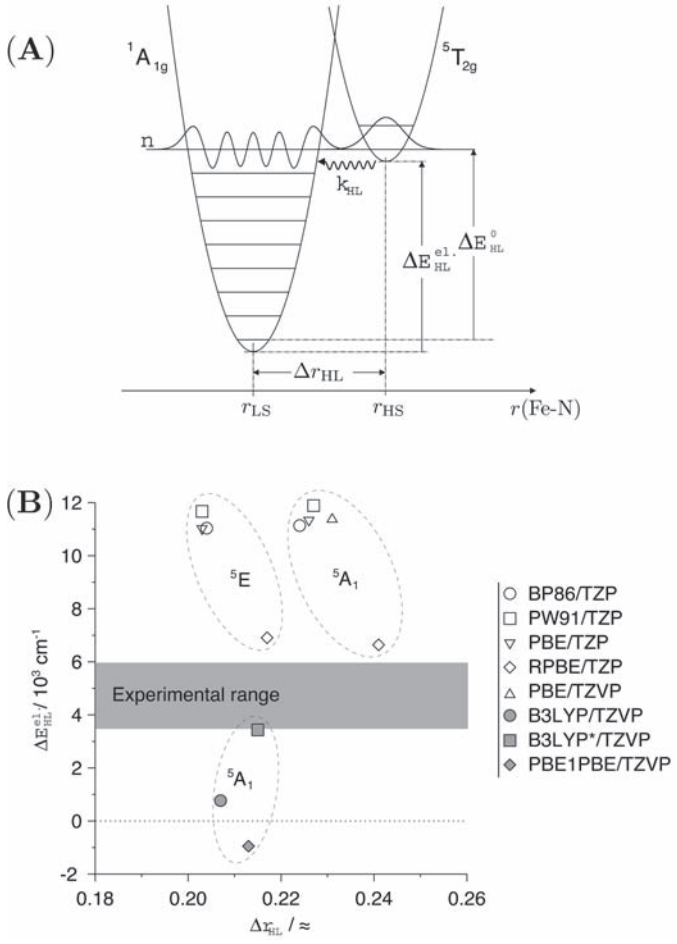

Figure 1: (A) Configurational coordinate diagram for an octahedral iron(II) complex with a $[FeN_6]$ coordination sphere and a LS ground state along the Fe-N distance coordinate. The low-tempera ture tunnelling occurs exclusively from the lowest vibrational level of the HS state. For $[Fe^{II}N_6]$ spin-crossover complexes, the low-temperature tunnelling rate constant, ΔE°_{HL} and Δr_{HL} are related through the inverse energy gap law: $kHL(T \to 0) = f(\Delta r_{HL}, \Delta E^{\circ}_{HL})$. (B) Plot for $[Fe(bpy)_3]^{2+}$ of calculated HS-LS energy differences against HS-LS Fe-N distances for the $^5A_1$ and ^5E trigonal components of the octahedral HS $^5T_2$ state [2].

References

[1] A. Hauser, N. Amstutz, S. Delahaye, S. Schenker, A. Sadki, R. Sieber and M. Zerara, in Structure and Bonding, edited by Th. Schönherr, vol. 106, p. 81 (Springer, 2004).

[2] L. M. Lawson Daku, A. Vargas, A. Hauser, A. Fouqueau, M. E. Casida, ChemPhysChem 2005, 6, 1393-1410.

[3] A. Fouqueau, S. Mer, M. E. Casida, L. M. Lawson Daku, A. Hauser, T. Mineva, F. Neese, J. Chem. Phys. 2004, 120, 9473-9486.

[4] A. Fouqueau, M. E. Casida, L. M. Lawson Daku, A. Hauser, F. Neese, J. Chem. Phys. 2005, 122, 044110.

[5] A. Hauser, C. Enacescu, M. Lawson Daku, A. Vargas, N. Amstutz, Coord. Chem. Rev. 2006, in press.

[6] A. Vargas, L. M. Lawson Daku, M. Zerara, A. Hauser, E. Krausz, submitted.

Hyperfine interaction anisotropy on first and second coordination sphere water molecules in paramagnetic metal ion solution

Dr. Lothar Helm

with O. Yazyev
Institute of Chemical Sciences and Engineering,
EPF Lausanne, Switzerland

Description

Our research performed with the help of CSCS computational facilities involves quantum chemical modeling of hyperfine interactions in complex paramagnetic systems. Started in the summer of 2004 the project was focused on the magnetic properties of water solutions of paramagnetic metal ions. Later, the scope of our scientific activity performed at the CSCS was broadened. We started to be involved in the development of new methods for modelling magnetic properties. Also, new objects like conducting carbon materials appeared in our interests. Three main sub-projects of our Large User Project are following:

A. Methods for accurate calculation of hyperfine interaction with in pseudopotential-based electronic structure calculations.

An important parameter in electron paramagnetic resonance (EPR) and nuclear magnetic resonance (NMR) experiments on paramagnetic systems is the isotropic (Fermi contact) hyperfine coupling constant, which describes the magnetic interaction between the nuclear and electronic spins under isotropic averaging conditions. This property is related to electron spin-density at the point of nucleus under consideration. While all-electron approaches based on localized basis sets (e.g. Gaussian or Slater type atomic orbitals) have already proven to give good results for the calculation of isotropic hyperfine coupling constants, there is still a lack of methods for its calculation in pseudopotential based approaches which are particularly important for condensed matter physics and plane wave based first-principles dynamics applications in chemistry and biology. We proposed a simple scheme[1] for the evaluation of the core spin-polarization contribution within pseudopotential electronic structure methods. The core contribution to the spin-density at the point of the nucleus corrects for the leading error in the Fermi contact hyperfine coupling constants within pseudopotential based electronic structure calculations[2]. The correction is implemented in the framework of pseudopotential plane-wave DFT theory. Comparison with all-electron Slater-type orbital calculations on a number of molecular radicals containing first-row elements proves the accuracy of this approach.

B. Hyperfine interactions of water solutions of paramagnetic transition metal and lanthanide ions

An important manifestation of hyperfine interactions is their decisional in NMR relaxation of solvent nuclei in solutions of paramagnetic species. Such paramagnetic complexes are utilized in medicine as magnetic resonance imaging (MRI) contrasts agents[3]. Currently, the typical representatives of MRI contrast agents are gadolinium complexes because of high spin state (^{8}S state, half-filled f-shell) and slow electronic relaxation rate of Gd(III) ion. The MRI contrast agents are probably one of the striking examples where the purely quantum nature of hyperfine interactions directly

turns into its pharmaceutical properties and these properties cannot be described by means of any kind of classical theory. Other paramagnetic metal ions, like majority of the first-row transition metal ions, are also of large interest. In spite of the decisive role of hyperfine interactions in these phenomena, only very small amount of knowledge concerning the electronic structure details of these magnetic properties is accumulated. We perform Car-Parrinello molecular dynamics[4] simulations of paramagnetic metal ions (currently, Gd^{3+}, Cr^{3+} and Mn^{2+}) in order to study details of these fascinating magnetic interactions and dynamics of solvatation shells.

C. Isotropic Knight shifts of conducting carbon nanotubes

Carbon nanotubes (CNTs) attracted enormous interest during the past decade due to their unusual physical properties[5]. For instance, many topological varieties of CNTs possess metallic conductivity which is not typical for carbon-based organic compounds. This promises many applications of CNTs in technology and suggests new methods to investigate the atomic and the electronic structure of these nanoscale objects. One of the possibilities to study conductors is the investigation of the magnetic interaction between the conduction electron spin and the nuclear spin. This interaction can be observed experimentally using nuclear magnetic resonance (NMR) measurements of the Knight shift[6]. We study isotropic Knight shifts using all-electron periodic boundary conditions DFT approach[7]. We show that its magnitude depends on the particular structure of the conducting CNT, which opens a number of new possibilities for future structural studies of carbon nanostructures using NMR[8].

Achievements

A. The proposed method relies on the reconstruction of the all-electron wavefunctions and the frozen valence spin-density approximation to solve the Kohn-Sham equations for core electrons only. The reconstruction part was implemented in CPMD code[9] while the frozen valence spin-density DFT calculations are carried out using the modified atomic code of ESPRESSO package[10]. The availability of CSCS computers permitted us to carry out extensive benchmark tests of our method on a set of molecular radicals. This method will be used in other project (B).

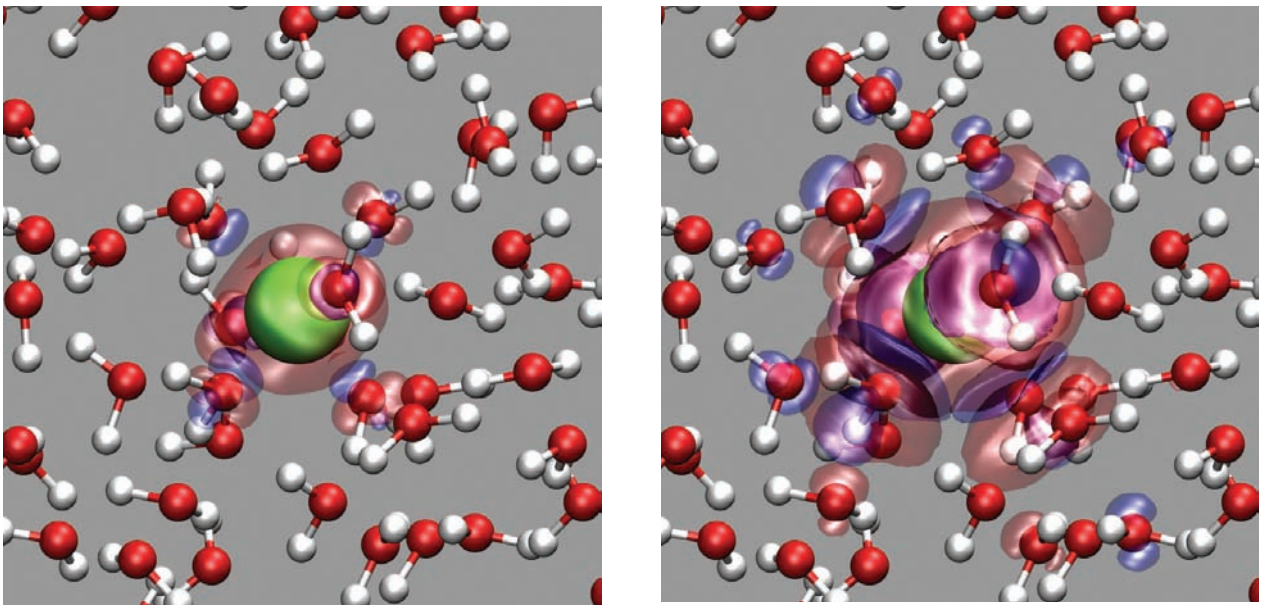

Figure 1: Isosurface plots of the spin-density distribution around the paramagnetic Cr^{3+} for an isovalue of 0.002 a.u.$^{-3}$ (left) and 0.0001 a.u.$^{-3}$ (right). The positive (excess spin) spin-density is shown in red and the negative spin density is shown in blue. The spin-polarization of second coordination sphere water molecules can be observed (right).

B. In this sub-project, we perform Car-Parrinello molecular dynamics simulations of the paramagnetic metal ions, Cr^{3+}, Gd^{3+} and Mn^{2+} until now. Then, calculations of hyperfine parameters are performed for a set of configurations since better pseudopotentials and higher values of plane-wave kinetic energy cutoffs are required. The Cr^{3+} aquaion is an interesting example for which the hyperfine couplings of water molecules in second coordination sphere are known experimentally. We were able to prove the accuracy of the approach comparing with this experimental data[11]. First sphere 1HI and second sphere $^{17}O_{II}$ hyperfine coupling constants are in excellent agreement with experimental results (computed -0.20±0.02 MHz versus experimental value of -0.215 MHz)[12]. Thus, the value of the second coordination sphere water molecule ^{17}O isotropic hyperfine coupling shows significant unpaired electron delocalization even in the second coordination sphere of Cr^{3+} (Fig. 1). The simulation of lanthanide ions for our application requires explicit presence of f-electrons which are highly localized. This results in very high plane-wave cutoffs necessary for calculations of magnetic properties. We perform Car-Parrinello molecular dynamics simulations using pseudopotentials which include 4f-shell in core, while calculations of magnetic properties are performed using 140 Ry plane-wave cutoff for treatment of explicit f-electrons[13] . The time consuming simulations of Gd^{3+}-water model are now finished and the results are being analyzed. The results of molecular dynamics simulations are also very important for estimation of other important NMR parameters, e.g. quadrupolar coupling constants[14] .

C. We implemented a method for density functional theory calculation of isotropic Knight shifts of periodic metallic systems in GAUSSIAN03 package[15]. Our approach relies on self-consistent calculation of hyperfine interactions in response to a finite uniform magnetic field[16]. The wide range of metallic single-wall carbon nanotubes and example of chemically modified carbon nanotube are considered. Our results show that the isotropic Knight shifts of metallic CNTs, except ultranarrow ones, reflect the density of states at the Fermi level. High-resolution NMR can be used to study the distribution of diameters of the conducting CNTs in a sample. Ultranarrow zigzag CNTs possess large positive isotropic Knight shifts characteristic of their chirality indices. Knight shifts can

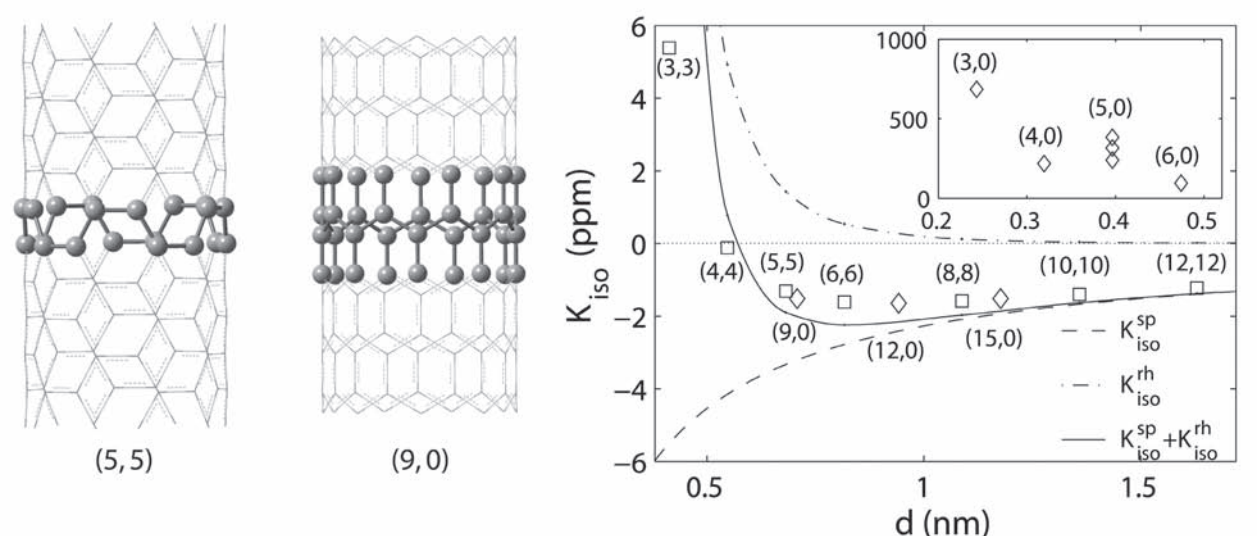

Figure 2: Isotropic Knight shifts of conducting single-wall CNTs. In regular metallic nanotubes Knight shift shows dependence on the nanotube diameter as a result of interplay between the spin-polarization (K^{sp}) and the rehybridization (K^{rh}) contributions. The squares and diamonds indicate the calculated shifts for armchair and metallic zigzag CNTs, correspondingly. The curves show estimated shift as a function of CNT diameter and its individual contributions. The examples of zigzag and armchair topological varieties of conducting CNTs are shown on the left (unit cells are highlighted).

serve as the unambiguous spectroscopic signatures of these unusual structures. Finally, Knight shift measurements can be useful to study chemically functionalized CNTs. The results of our theoretical study provide a new perspective for studying carbon nanostructures using NMR.

References

[1] O. V. Yazyev, I. Tavernelli, L. Helm, U. Röthlisberger, Phys Rev B 71, 115110 (2005) .

[2] C. G. Van de Walle and P. E. Blöchl, Phys. Rev. B 47, 4244 (1993).

[3] Tóth, É.; Helm, L.; Merbach, A. E. In The Chemistry of Contrast Agents in Medical Magnetic Resonance Imaging; Tóth, É., Merbach, A. E., Eds.; Wiley: Chichester, 2001.

[4] R. Car and M. Parrinello, Phys. Rev. Lett. 55, 2471 (1985).

[5] S. H. Baughman, A. A. Zakhidov and W. A. de Heer, Science 297, 787 (2002).

[6] W. D. Knight, Phys. Rev. B 76, 1259 (1949).

[7] K. N. Kudin and G. E. Scuseria, Phys. Rev. B 61, 16440 (2000).

[8] O. V. Yazyev and L. Helm, Phys. Rev. B 72, 245416 (2005)

[9] CPMD version 3.9.1, Copyright IBM Corp 1990-2004, Copyright MPI für Festkörperforschung Stuttgart 1997-2001, http://www.cpmd.org.

[10] http://www.democritos.it/scientific.php

[11] P. Bergström, J. Lindgren, M. C. Readand M. Sandström, J Phys Chem 95, 7650 (1991).

[12] O. V. Yazyev and L. Helm, Theor. Chem. Acc, in press.

[13] O. V. Yazyev and L. Helm, in preparation.

[14] O. V. Yazyev and L. Helm, in preparation.

[15] M. J. Frisch et. al., GAUSSIAN03, Revision C.01, Gaussian, Inc., Wallingford, CT, 2004, http://www.gaussian.com.

[16] M. Weinert and A. J. Freeman, Phys. Rev. B 28, 6262 (1983).

Development and Application of ab initio Molecular Dynamics

Prof. Jürg Hutter

Institute of Physical Chemistry
University of Zurich, Switzerland

General Interests

The basic theme of our research is development and application of novel methods in computational chemistry. The focus is on large systems, mostly in the condensed phase and on density functional theory. The systems studied range from simple liquids to chemical reactions in complex solvents. We are the leading group in the development of the software packages CPMD (www.cpmd.org) and CP2K (cp2k.berlios.de). Both packages are freely available to the scientific community and widely used.

Ab initio molecular dynamics simulations need large amounts of computer time. Fortunately, our computer codes are highly optimized and can make efficient use of almost all kinds of modern computer architectures from vector machines to massively parallel computers. Currently, the CPU time provided by CSCS covers 10% of our needs for computational resources.

Research projects at CSCS

An ab initio Investigation of the DNA Photolyase Repair Activity

The most common type of DNA damage caused by UV radiation is the [2+2] cycloaddition of two adjacent pyrimidine bases which yields cyclobutane pyrimidine dimers (CPDs). Kinetic studies suggested that the formation of the photodimer arises from the reaction of one molecule in a triplet state with a second one in its ground state. DNA photolyases use light energy to repair the CPD lesions by transferring an electron to the cyclobutane ring. The resulting radical anion then splits into two pyrimidines and transfers back the excess electron to the enzyme. However, the atomistic details of the reaction mechanism that transforms the dimer anion into a monomer and a monomer radical anion are still not well understood. The purpose of our work is to shed light on the details of the dimer formation and dissociation process, first in vacuo and then in its natural environment,

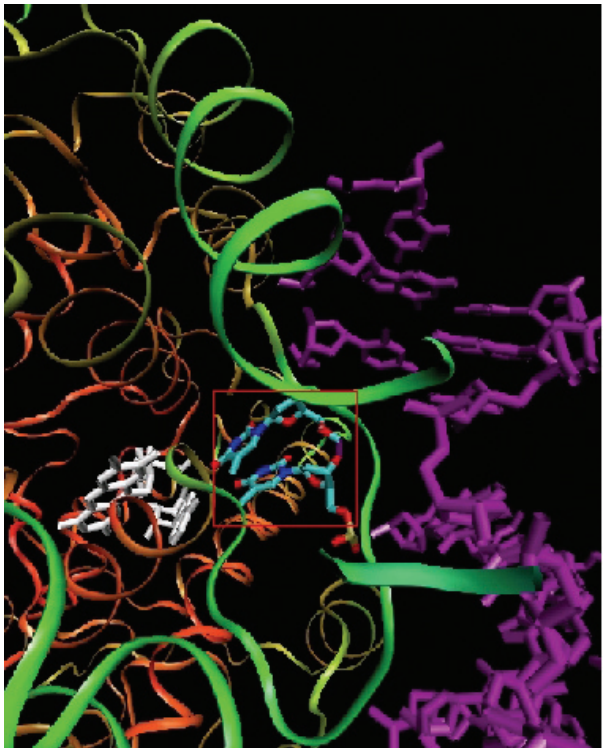

Figure 1: Ribbon model of DNA photolyase bound to CPD-comprising DNA in stick representation after in situ repair. The quantum mechanics (QM) part of the system, i.e. the CPD lesion, is highlighted in a red box. The flavin cofactor which transmits an electron to the cyclobutane ring is shown in white.

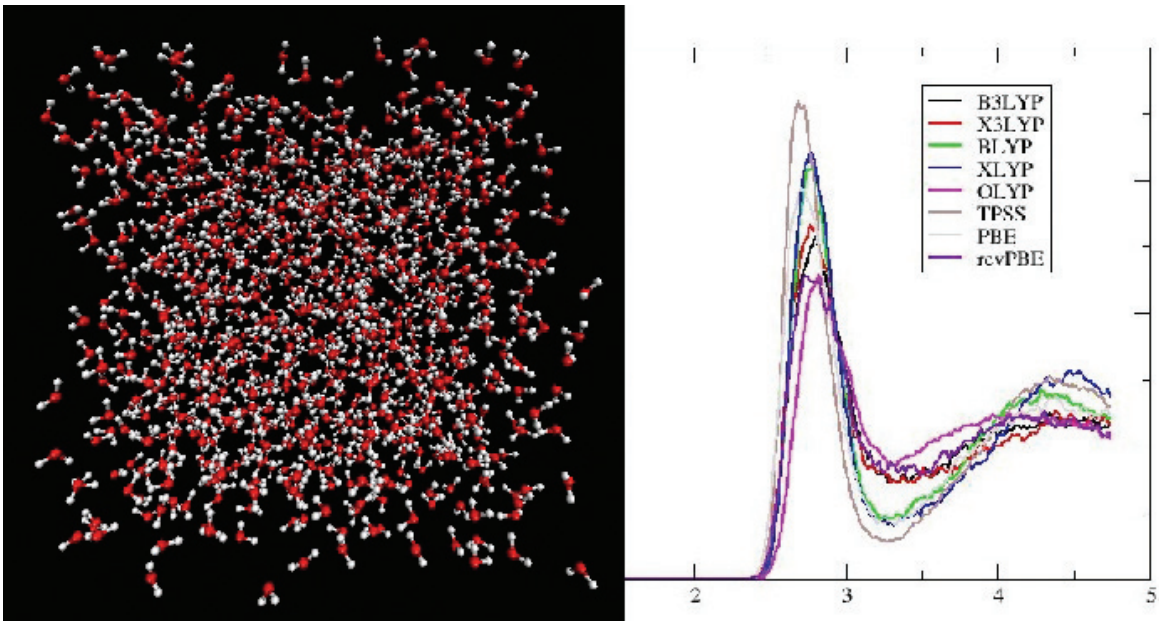

Figure 2: Oxygen-oxygen radial distribution function of liquid water at 350 K calculated with different density functionals.

i.e. within DNA. We address this issue by using a hybrid Car-Parrinello quantum mechanical/molecular mechanical (QM/MM) approach, in which the complex DNA environment is treated with a classical force field and the ground state potential energy surface and the excitation energies of the dimer are described within density functional theory (DFT) and time dependent (TD) DFT, respectively.

Liquid Water from First Principles

Water holds a unique role among liquids, not only because of its ubiquity and importance on earth but also because of its anomalous liquid properties. Thus, understanding its properties has been a grand challenge for liquid state theory and molecular simulation. The first particle-based simulations of liquid water using pairwise empirical potentials were carried out almost 40 years ago. However, the strong dipole moment and large polarizability of water and its participation in many chemical processes, particularly its self-dissociation, pose a challenge for empirical potentials. Although great strides have been made in the development of empirical force fields for water, none of these has yet succeeded to yield a quantitative description of the thermodynamic, structural, and dynamic properties of water over its entire liquid range. In contrast, an ab initio representation of water affords the opportunity to study both physical and chemical properties of water.

At the current stage of the project, we investigate the influence of different density functionals on the structure of the liquid state. Most importantly the inclusion of exact exchange contributions are tudied. From a series of simulations employing a large variety of different functionals we compare radial distribution functions, diffusion coefficients and dipole moment distributions.Further projects are concerned with the solvation of simple ions in water. We investigate the dependence of the structure on technical details, like the treatment of excess charge or the inclusion of counter ions. An important tool to study electronic effects upon solvation are maximally localized Wannier functions. We have implemented an efficient parallel scheme that allows to calculated these functions along a molecular dynamics trajectory with only small additional cost. This has been used for the study of polarization effects in the solvation of dimethyl sulphoxide in water.

Time-dependent density functional studies

Time-dependent density-functional theory (TD-

Initial State

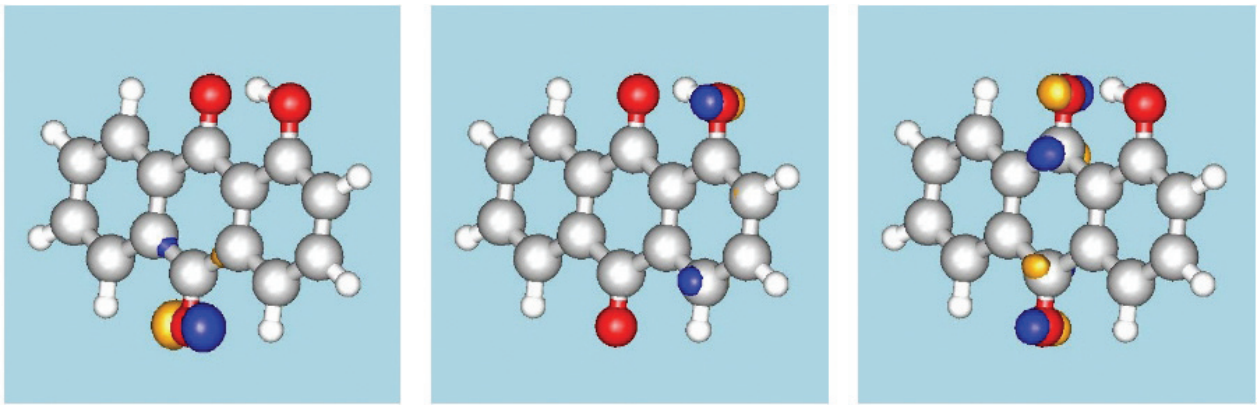

Final State

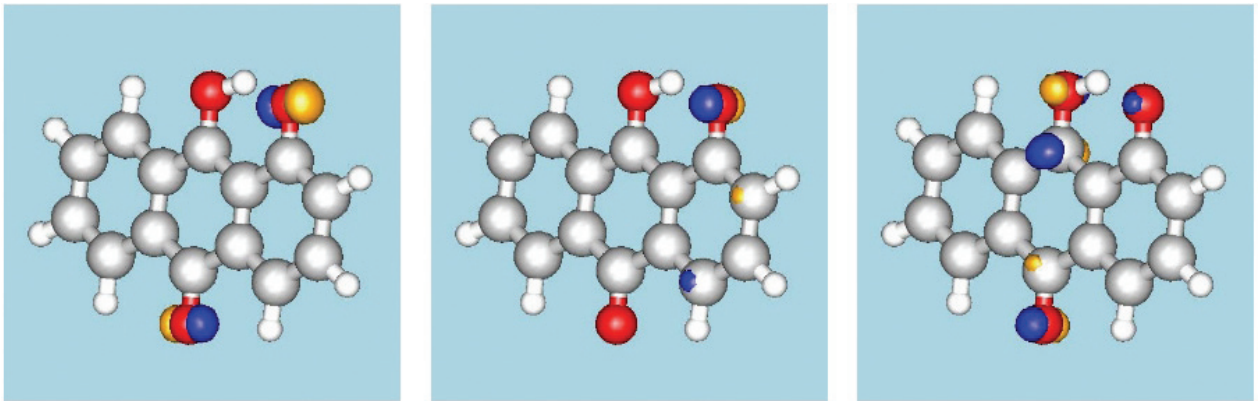

HOMO-1 **HOMO** **LUMO**

Figure 3:The figure shows the relevant molecular orbitals of 1-HAQ (1-hydroxyanthraquinone) for the Excited State Proton Transfer (ESPT).

DFT) allows for the calculation of electronic excitation energies. We have applied the implementation in CPMD to study the excitations in small molecules in gas phase and solvated in water. We studied the solvation of s-tetrazine in water by first calculating tetrazine-water clusters, and then the molecule in liquid water. The resulting excitation spectrum agrees well with the experimental one. In water-solvated acetone we found the intra-molecular excitation to underly excitations with water-derived and mixed character. These are due to artificial solutions of non-local excitations, and are prone to semi-local approximations such as the BLYP-GGA functional used in this study. To correct for this short-coming calculations with hybrid functionals were carried out. They yield improved excitations with increased energies for the mixed inter-molecular excitations, whereas the intra-molecular excitation energy of acetone hardly changes, staying close to the experimental values.

We have applied TDDFT to study proton transfer in the hydroxyanthraquinones. The optically active excitation in the initial (ground) state is the HOMO to LUMO transition, but the excitation leads to a proton transfer from to the central oxygen, shown as the final state. In the final state the excitation is starts from the HOMO-1 state which follows a lower potential energy surface than the original transition but is optically dark.

Molecular modelling of radionuclide mobility and retardation in clay materials

Dr. Sergey V. Churakov

under project leader Dr. Andreas Jakob

Laboratory for Waste Management, PSI Villigen, Siwtzerland

Description

Clay minerals occur as colloidal aggregates of tiny particles. Their large surface area is responsible for unique physical and chemical properties like swelling, cation exchange and pH dependent sorption. Because of the strong cation retardation ability, clay sediments are considered as appropriate host rocks for radioactive waste repositories. The safety and performance of such repositories depend entirely on our understanding of the mechanisms controlling the radionulides mobility and retardation in clays.

The basic structure element of phyllosilicates can be imagined as a hexagonally ordered layer of octahedra sandwiched between two tetrahedral siloxane planes, commonly referred as TOT-layer (Fig. 1). Various isomorphic substitutions in the octahedral and tetrahedral layers of the clay minerals result in a permanent structural charge in the TOT unit which in turn enables the swelling and the sorption by cation exchange mechanism. Additionally, the sorption processes take place on the edge sides of the TOT layer. The structure, the composition and the charge of the edges change as a function of pH due to the dynamic proton exchange between the surface and the solution. Thus the sorption capacity and the mechanism of cation uptake on the edge sites depend on pH in the solution.

Different macroscopic models for the surface complexation have been proposed to describe the sorption of cations on clays from aqueous solutions. Most of them consider two major contributions to the electrostatic potential, namely, the electric field produced by a permanent structural charge in the TOT layer, and a pH dependent potential due to proton sorption/desorption at edge sites. To a first approximation, both contributions can be considered independent. The calculation of the electrostatic potential due to a permanent structural charge is straightforward since it is determined by the extent of the isomorphic substitution in the TOT layer only. An accurate estimation of the pH-dependent potential requires several fundamental parameters which are poorly, if at all, constrained: 1) the effective surface area and the structure of the edge sites; 2) the density of sites involved in the protonation/deprotonation reactions; 3) the equilibrium absorption constants for

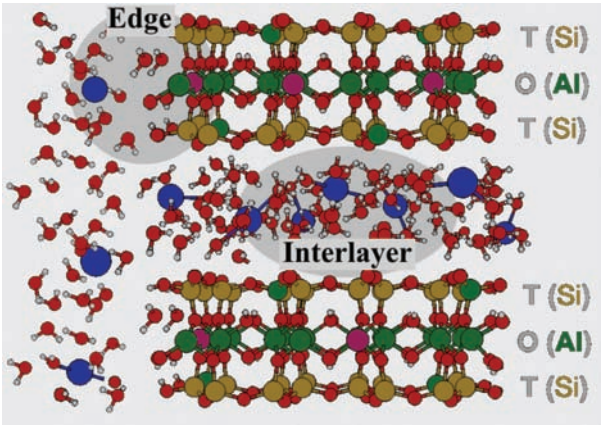

Figure 1: Schematic view of the TOT unit in clay minerals and the water-clay interfaces. Large spheres in the fluid represent counter ions compensating permanent charge in the TOT layer. Shadowed areas emphasize two regions of particular interest: interlayer fluid and the fluid-solid interface at the edges sites.

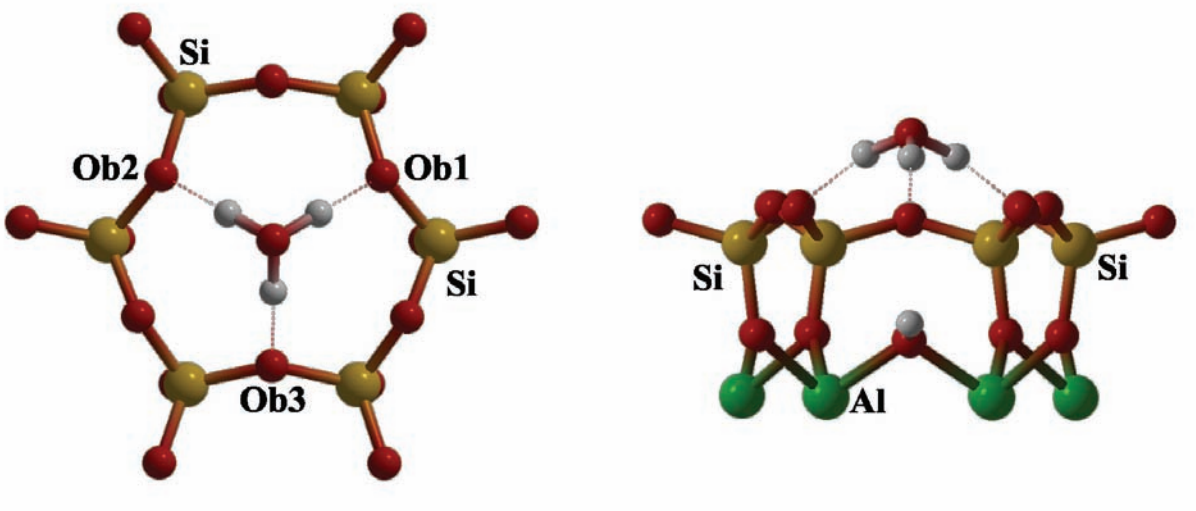

Figure 2: Most stable configuration of hydronium complex on the basal plane of pyrophyllite. Only the uppermost tetrahedral layer is shown. Thin lines indicate hydrogen bonds

the reactive sites.

Achievements

Using ab initio calculations we predict the structure and the surface energy of the different facets of pyrophyllite as function of water coverage. The calculations suggest that at the pH of zero charge the edges of the pyrophyllite particles should be preferentially formed by the (110) and (-110) facets. This conclusion is in agreement with the high resolution images of the pyrophyllite nano-particles where the crystals of the pseudorhombic form were observed.

Knowing the structure of the most common edge facets the density of the functional groups is calculated. The (110) edge contains 1.6 nm^{-2} ≡Si-1H, ≡Si-O2H, ≡Al-OH_2, ≡Al-(OH)-Al≡, and ≡Al-O-Si≡ groups. The proton affinity of the surface groups were analysed using the Fukui indexes. The calculation allowed us to establish a linear relationship between the electronic properties of the surface groups and their pK values [1,2]. Using this relation we constrain relative acidities of the edge sites. The absolute values of the pK should be obtained using the experimental data, however. Several different configurations of the hydronium ion on the basal plane were found. In the most stable configuration (Fig. 2) the hydronium ion is situated parallel to the surface within the siloxane plane. The ion dips into the siloxane cavity so that the oxygen atom is situated just 1.35 Å above the outermost basal oxygen. Hydronium forms two strong hydrogen bonds with Ob1 and Ob2 sites. A somewhat weaker bond is directed to the Ob3 site [2].

Bringing together the site densities and the relative proton affinities of the surface sites obtained in ab initio calculations and the conventional thermodynamic modelling with GEMS package the titration data of montmorillonite were modelled using Basic Stern Multi-Site Triple Layer model [3]. The results show that the mechanism of the proton sorption depends on pH. At high pH the proton equilibria is controlled by concurrent de-protonation of the edge sites while at low pH the capacity of the edge sites is used up and the protonation fulfilled by inner sphere complexation on the basal plane. The density of the edge sites along is not sufficient to explain the behaviour of the titration curve at low pH. The thermodynamic model for proton sorption on pyrophyllite based on ab-initio calculations will be extended on the more complex systems with isomorphic substitutions in tetrahedral and octahedral layers of clays.

References

[1] S.V. Churakov 2005: Ab initio modelling of surface site reactivity and fluid transport in clay minerals case study: Pyrophyllite. PSI Scientific Report 2004/Volume IV. ISSN 1423-7334. pp. 109-120.

[2] S.V. Churakov 2006: Ab initio study of sorption on Pyrophyllite: Structure and acidity of the edge sites. Journal of Physical Chemistry B - ASAP Web Release.

[3] D. A. Kulik and S. V. Churakov 2005: Matching a surface complexation model with ab initio molecular dynamics: montmorillonite case. 2th International meeting: Clays in Natutal and Engineered Barriers for Radioactive Waste Confinement. March 14-18, Tours

Modelling CARBOn Cycle CLIMate Feedbacks (CARBOCLIM)

Dr. Fortunat Joos

with Thomas Frölicher, Markus Gerber and Gian-Kasper Plattner

Climate and Environmental Physics, Physics Institute, University of Bern, Switzerland

Project Overview

The presently observed and projected future climate change poses a significant risk to the human society. Adequate response strategies to mitigate greenhouse gas emissions and to adapt to climate change require scientific information based on our best understanding of the Earth System (e.g. Edmonds et al., 2004). The project CARBOCLIM is targeted to provide such information.

The primary research tool in the Large User Project CARBOCLIM is the Climate System Model (CSM) developed by the National Centre for Atmospheric Research (NCAR). CSM is a state-of-the-art 3-dimensional coupled atmosphere-ocean climate-carbon cycle model. CARBOCLIM is a contribution by the division of Climate and Environmental Physics (CEP) to two European projects within the Framework Programme Six: the Integrated Project CARBOOCEAN and the Network of Excellence EUR-OCEANS. Both projects will start in 2005 and have a duration of five years. CARBOCLIM is part of a collaboration with the National Centre for Atmospheric Research, Boulder, institutionalised through an NCAR affiliate scientist position of the project leader.

The goal of CARBOCLIM is to perform simulations with the fully coupled ocean-atmosphere climate-carbon cycle model over the industrial period and over this century to study carbon cycle climate interactions. The understanding of the coupling between the carbon cycle and the physical climate system is a prerequisite for global warming projections. The main focus of CARBOCLIM is on the ocean carbon cycle. The uptake of anthropogenic carbon, the impact of carbon cycle climate feedbacks on the CO_2 uptake, and marine ecosystem changes are investigated. CARBOCLIM is addressing spatial scales ranging from regional to the global and temporal scales ranging from seasonal to centennial.

The project CARBOCLIM is currently in the start-up phase. The biogeochemical version of CSM has been installed on the IBM mainframe and first test simulations have been performed. First scientific results will be delivered in summer 2006. In the following, the primary scientific themes and questions of the project are discussed and the links with other projects outlined.

Scientific Background

Projections of future climate change require models that incorporate mechanistic descriptions of the climate system and that are evaluated using the broad range of available observational data. State-of-the-art, coupled carbon cycle climate models that represent the major climate system components (atmosphere, ocean, land, sea ice) in three dimensions allow us to investigate current and future climate change and climate variability in a spatially and temporally resolved setting. This

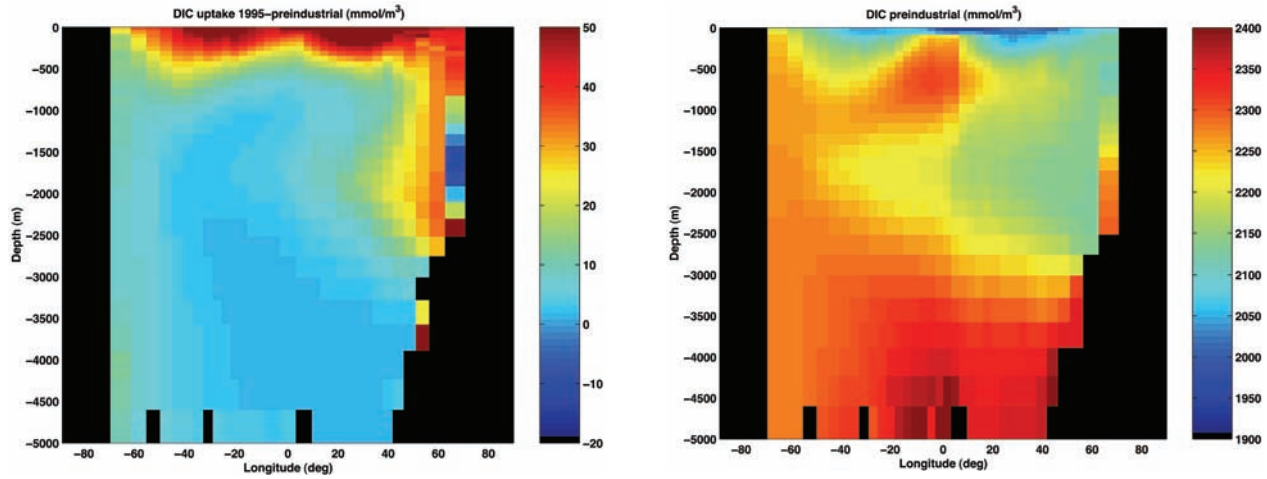

Figure 1: Simulated zonally-averaged concentrations of dissolved inorganic carbon in the Atlantic (left) and the increase over the industrial period (right) in mmol m^{-3} (Müller et al., 2005).

is required for a comprehensive comparison with available data and for detailed spatial information on future climate change and its impact.

Carbon dioxide (CO_2) is the most important anthropogenic greenhouse gas and its radiative forcing contributes significantly to current and future global warming. CO_2 is emitted through burning of fossil fuel and due to land use and land use change activities. Presently, about half of the current carbon emissions stays airborne, whereas the rest is taken up by the ocean (Figure 1) and the land biosphere. The atmospheric CO_2 rise and climate change would proceed at much higher rates than observed if these natural sinks were not operating. It is key for climate change projections to understand how the present marine and terrestrial carbon sinks will evolve in the future and how climate change itself will affect atmospheric CO_2 (Joos et al, 1999; Joos et al., 2001). CARBOCLIM will enhance our understanding in this direction

Uncertainties in the response of the carbon cycle to future warming lead to uncertainties in projected warming of several degree Celsius. This is the same order of magnitude as uncertainties associated with the response of the physical climate system to a prescribed greenhouse gas forcing (Knutti et al., 2003). Recent simulations with coupled carbon cycle - climate models yielded conflicting results about the strength of the carbon cycle – warming feedback. The projected increase in atmospheric CO_2 was found to be higher by a factor of 1.1 to 2 in simulations with global warming than in simulations without global warming (Friedlingstein et al., 2005). The scientific challenge is to understand such model differences and to reduce the associated uncertainties.

Marine (and terrestrial) ecosystems will be affected in a variety of ways by global warming. Marine ecosystem changes are likely to change the biogeochemical cycling of carbon and other elements (nitrogen, iron, silica etc) within the ocean and to feed back on the evolution of atmospheric CO_2. Ecosystem changes will also have impacts on fish stocks and global fishery. Global warming will lead to changes in the spatial distribution of sea surface temperature and salinity that will lead to shifts in ecosystem distribution and ecosystem composition. For example, cold dwelling organisms in the high latitude may loose competitive advantages in a warming environment. Another important variable influencing ecosystem composition is carbon uptake. The uptake of the acid CO_2 by the ocean lowers the pH of seawater and increases the aquatic concentrations of CO_2, $[CO_2]$, and of bicarbonate, $[HCO_3^-]$, whereas the concen-

tration of the carbonate ion, [CO_3^{--}] is lowered. Many marine organisms produce a shell consisting of calcite or aragonite (two different forms of the mineral $CaCO_3$). Recent projections by a range of carbon cycle models within the framework of the international Ocean Carbon Model Intercomparison Project (OCMIP), including a model of the division of Climate and Environmental Physics, revealed that aragonite will become undersaturated over the coming decades in the high latitude ocean (Orr et al., 2005). Then, the aragonite shells of many species (e.g. pteropods) will be prone to dissolution. The scientific community is just at the beginning of investigating the impact of anthropogenic activities on natural marine ecosystems and the links between ecosystem changes and biogeochemical cycles and the climate. CARBOCLIM comes timely to contribute to the necessary effort.

Links to International and National Reseach Efforts

CARBOCLIM, carried out by staff of the Climate and Environmental Physics Division, University of Bern, is closely tight to international research efforts. CARBOCLIM is aimed to provide deliverables to two projects within the European Community (EC) Framework Programme and is part of a collaboration with the National Centre for Atmospheric Research (NCAR), Boulder, USA, and linked to the Large User Project MONALISA.

The Integrated Research Project CARBOOCEAN is coordinated by Dr. C. Heinze, Bergen, and consists of a consortium of 40 groups. The project will include a variety of measurements from the coastal system as well as measurements from targeted ship tracks in order to quantify air-sea exchange of carbon and to improve estimates of ocean carbon inventories. Targeted experiments will investigate the response of individual plankton species to changes in environmental conditions. The leading European modelling groups will perform coordinated coupled climate-carbon cycle simulations. CARBOCLIM will contribute to this effort by applying the NCAR CSM to simulate climate change, carbon cycle-climate feedbacks, and ocean carbon uptake over the industrial period and the next hundred years.

The Network of Excellence EUR-OCEANS is coordinated by Drs. P. Treguer and L. Legendre and links a consortium of 69 institutes. Climate and Environmental Physics leads Workpackage 3.3 «Large-scale Earth System Modelling». CARBOCLIM will deliver fields of biogeochemical variables relevant to ecosystem models to the other project members and investigate biological export production from the regional to the global scale using the NCAR CSM.

CARBOCLIM is closely tied to the Large User Project MONALISA carried out by the climate modelling group at Climate and Environmental Physics. In MONALISA, a physics-only version of the NCAR model is applied to investigate climate variability over the past five hundred years.

Climate and Evnironmental Physics has a longstanding collaboration with the National Centre for Atmospheric Research. Recent joint work includes the completion of two simulations over the period 850 AD to 2000 AD to address natural climate variability.

References

[1] J. Edmonds, F. Joos, N. Nakicenovic, and R. Richels. Scenarios, Targets, Gaps and Costs. In The Global Carbon Cycle: Integrating Humans, Climate and the Natural World, C. Field and M. Raupach (Eds.), SCOPE series 62, Island Press, Washington DC, USA, 77-102, 2004.

[2] Friedlingstein, P., P. Cox , R. Betts, L. Bopp, W. von Bloh, V. Brovkin, S. Doney, M. Eby, I. Fung, B. Govindasamy, J. John, C. Jones, F. Joos, T. Kato, M. Kawamiya, W. Knorr, K. Lindsay, H. D. Matthews, T. Raddatz, P. Rayner, C. Reick, E. Roeckner, K.-G. Schnitzler, R. Schnur, K. Strassmann, S. Thompson, A. J.Weaver, C. Yoshikawa, and N. Zeng. Climate-carbon cycle feedback analysis, results from the C4MIP model intercomparison. J. Climate , submitted, 2005.

[3] F. Joos, I. C. Prentice, S. Sitch, R. Meyer, G. Hooss, G.-K. Plattner, S. Gerber, and K. Hasselmann. Global warming feedbacks on terrestrial carbon uptake under the Intergovernmental Panel on Climate Change (IPCC) emission scenarios. Global Biogeochemical Cycles , 15, 891-908, 2001.

[4] F. Joos, G.-K. Plattner, T.F. Stocker, O. Marchal, and A. Schmittner. Global warming and marine carbon cycle feedbacks on future atmospheric CO2. Science , 284, 464-467, 1999.

[5] R. Knutti, T. F. Stocker, F. Joos, and G.-K. Plattner. Probabilistic climate change projections using neural networks. Climate Dynamics, 21, 257-272, 2003.

[6] S. A. Müller, F. Joos, N. R. Edwards, and T. F. Stocker. Water mass distribution and ventilation time scales in a cost-efficient, 3-dimensional ocean model. J. Climate , submitted, 2005.

[7] J. C. Orr, V. J. Fabry, O. Aumont, L. Bopp, S. C. Doney, R. M. Feely, A. Gnanadesikan, N. Gruber, A. Ishida, F. Joos, R. M. Key, K. Lindsay, E. Maier-Reimer, R. Matear, P. Monfray, A. Mouchet, R. G. Najjar, G.-K. Plattner, K. B. Rodgers, C. L. Sabine, J. L. Sarmiento, R. Schlitzer, R. D. Slater, I. J. Totterdell, M.-F. Weirig, Y. Yamanaka, and A. Yool. Decline in high-latitude ocean carbonate by 2100. Nature , in press, 2005.

Numerical Simulation of Transitional, Turbulent and Multiphase Flows

Prof. Leonhard Kleiser

Institute of Fluid Dynamics, ETH Zurich, Switzerland

1. Large-Eddy Simulation of compressible wall-bounded and massively separated flows

Supersonic boundary-layer flow at moderately high Reynolds numbers

The correct representation of zero-pressure-gradient flat plate boundary layers is an obvious prerequisite before applying a subgrid-scale model to geometrically and physically more complex flows. Supersonic spatially developing turbulent boundary layer flow was computed by means of Large-Eddy Simulation (LES) with the HPF Smagorinsky model. The Reynolds numbers were chosen to match the range where experimental data are available. We have shown that the results agree well with the experimental data and data obtained previously with Approximate Deconvolution Model(ADM).

Compact upwind-biased finite-difference schemes

To simulate flows in complex geometries with explicit finite-difference schemes domain decomposition is an established approach. For higher-order finite-difference discretization a compact upwind-biased scheme has been further developed which has stability properties suitable for block coupling and has wave propagation properties which minimize reflections on the boundaries. The scheme has been successfully applied to the simulation of 2D eigensolutions of compressible Couette flow.

Massively separated flows

The applicability of ADM subgrid-scale model for LES in complex industrial-type configurations is currently investigated. Of particular relevance are the massively separated flows. All numerical simulations of this project are performed with the semi-industrial solver NSMB, in which the compressible Navier-Stokes equations are discretized with the finite-volume method.

The streamwise-periodic hill channel is a standard test case for separated flows from curved surfaces. This configuration is especially challenging, since the separation location is not prescribed but is often spatially fluctuating. Also, the separation process naturally exerts great influence on the downstream flow. By comparing the LES results with high-resolution LES and DNS data, the capability of ADM to yield high-quality results is demonstrated. A number of LES computations of the streamwise-periodic hill channel at different Reynolds and Mach numbers for various mesh resolutions have been undertaken. The comparison to results from literature at significantly higher resolution yielded good agreement of the mean quantities and the second-order statistics for all cases.

A second flow case focuses on a turbulent jet issuing into oncoming boundary layers («jet in cross-flow»). Particular attention will be paid to the flow topology, i.e. the formation of counter-rotating vortices, and the mixing properties of the mean flow. Preparatory work comprised the multiblock implementation of ADM into the NSMB solver, the adaptation of passive scalar transport and the creation of a mesh converter, as well as the choice of suita-

ble initial and boundary conditions. Some preliminary simulations with smaller mesh and domain size, and Dirichlet inlet conditions for the jet nozzle were conducted. Already with this simplified approach the counter-rotating vortex pair can be observed. The next step consists of the simulation of the full setup, including a parallel simulation of turbulent pipe flow, which provides the inlet data for the jet.

2. Large-eddy simulation of jet flows and aeroacoustic computations

LES of swirling jet flows

In this project the capability of advanced LES methods for prediction of swirling flows is investigated and a better understanding of the complex flow physics of swirling jet flow is sought.

In order to validate the Navier-Stokes solver, an eigenvalue solver accounting for viscous effects was developed. This program solves the linearized compressible equations in a cylindrical frame of reference with various numerical schemes. It was successfully used to complete the validation of the Navier-Stokes solver where excellent agreement with linear theory was achieved. Furthermore, appropriate mappings in radial as well as in the axial direction were implemented. This enables local grid refinement, for example in the area of the shear layer or at the point where the potential core of the jet closes.

Compressible circular swirling jets flows exhibit instability features that differ fundamentally from their swirl-free counterparts. A detailed analysis was performed with respect to spatial linear stability. The effects of varying different parameters such as Mach number, Reynolds number, swirl intensity and coflow intensity were examined. The corresponding base flow solutions were computed by solving the boundary layer equations in cylindrical coordinates. It was shown that the addition of a modest amount of swirl significantly enhances the maximum growth rate in circular mixing layers. Ana-lyzing the energy disturbance budgets of the disturbance modes allowed to further characterize the different instability types.

After implementation of ADM into the Navier-Stokes solver, first simulations of swirling mixing layers using this solver have been performed. In this simulations, the inflow plane is defined by a laminar compressible boundary layer solution superposed with instabilities from linear stability theory.

Computational aeroacoustics

The objective of this project is to explore ways of using LES for jet noise prediction. In previous studies noise in the acoustical far-field of a rectangular jet flow was predicted using Lighthill's acoustic

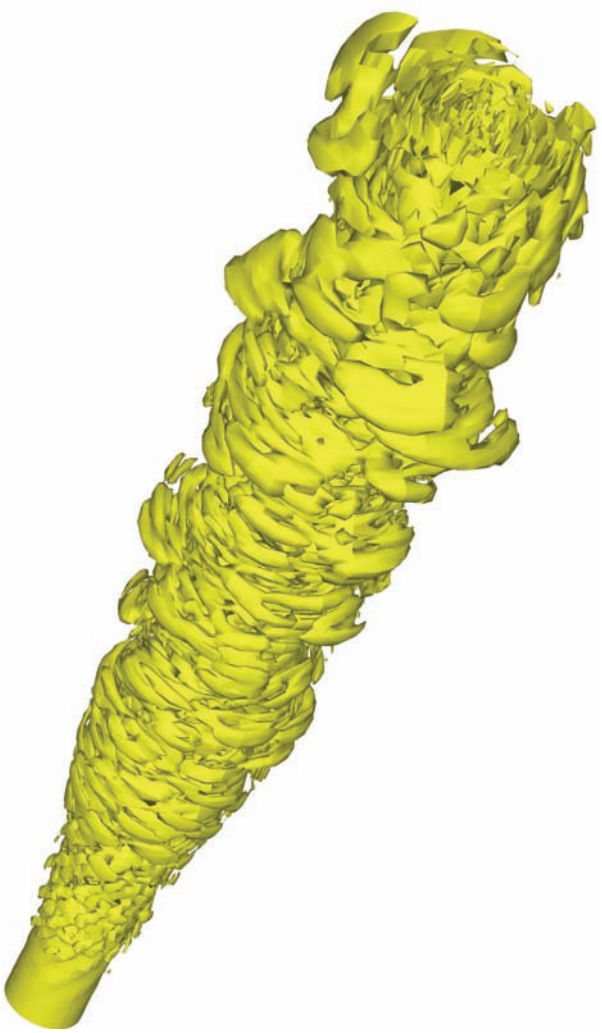

Figure 1: Vortical structures in a subsonic swirling mixing layer.

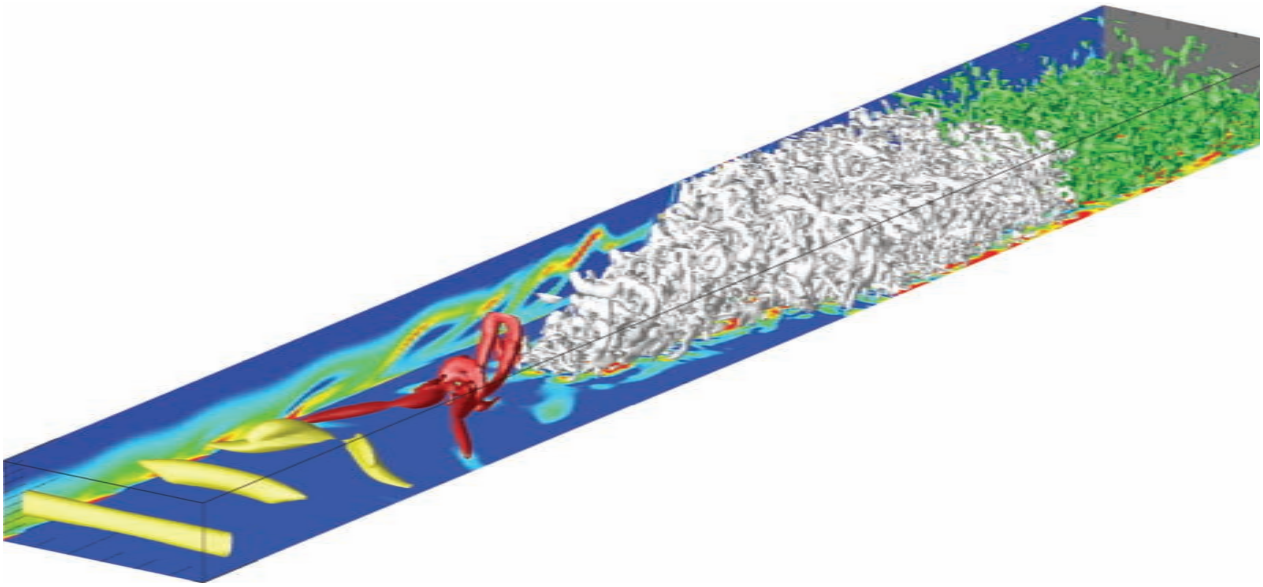

Figure 2: Visualization of the vortical structures of a spatial laminar-turbulent transition in plane channel flow obtained from a large-eddy simulation (only one channel-half is shown).

analogy. In order to assess the capability of the subgrid-scale model to correctly predict noise in the acoustic near-field, a direct noise computation of a round jet flow is being performed. Then the computational domain is extended into the acoustic near-field and the acoustical noise is directly computed without additional models or acoustic analogies. To avoid the numerical difficulties and computational costs associated with the explicit representation of the jet nozzle itself the flow just downstream of the nozzle is modeled as an inflow boundary condition. Instabilities are seeded in a physically motivated way by superimposing instability modes taken from a linear stability analysis of the inflow profile. To prevent spurious noise from being generated, sponge layers are employed.

With the previously mentioned LES code a simulation of an isothermal jet flow at Ma = 0.9 is being performed. Five azimuthal modes are superimposed at the inflow. The disturbances seeded by the inflow forcing in the shear layer become evident downstream, where the rolling-up of the shear layer starts. The mixing intensifies with the growing distance from the inflow.

3. Large-Eddy Simulation of transitional wall-bounded shear flows

LES of transitional incompressible channel flows

LES computations of transitional and turbulent incompressible channel flow and homogeneous isotropic turbulence were performed using spectral methods. For the transition simulations, both the temporal and the spatial approach have been employed. Various classical and newly devised subgrid-scale closures have been implemented and evaluated, including ADM, the relaxation-term model (ADM-RT), and the new class of high-pass filtered (HPF) eddy-viscosity models.

The standard ADM methodology was revisited due to observed destabilizing properties of the deconvolution operation on coarse grids in the wall-normal direction. The appropriate definition of the relaxation term causes the model contributions to vanish during the initial stage of transition and, approximately, in the viscous sublayer of wall turbulence. An analysis of the energy budget for HPF models including the SGS terms revealed that the contribution to the mean SGS dissipation is nearly zero, while it is significant for other SGS models.

Moreover, unlike the classical eddy-viscosity models, the HPF eddy-viscosity models are able to predict backscatter. On the basis of spectral discretization a close relationship between the modeling approach of the HPF models and the relaxation term of ADM and ADM-RT could be established. The HPF eddy-viscosity models have also been applied successfully to incompressible forced homogeneous isotropic turbulence with microscale Reynolds numbers up to 5500 and to fully turbulent channel flow at moderate Reynolds numbers up to the skin friction Reynolds number of 590.
The different SGS models have been tested for both the temporal and the spatial transition simulation approach. For the model problem of temporal transition in channel flow, spatially averaged integral flow quantities can be predicted reasonably well by LES even on comparably coarse meshes. However, it is equally important to faithfully represent the physically dominant transitional flow mechanisms and their three-dimensional vortical structures. The temporal results transfer readily to the spatial simulation method, which is more physically realistic but computationally much more expensive. For the spatial simulations the ADM-RT model, the dynamic Smagorinsky model, the filtered structure-function model and the different HPF models are able to predict the laminar-turbulent changeover. However, the accuracy of the various models in respect of e.g. the transition location and the characteristic transitional flow structures differs considerably.

Subharmonic transition in supersonic boundary layers

The forced subharmonic transition process of a flat-plate boundary layer at high Mach number was analyzed by means of LES with ADM and HPF eddy-viscosity models. The HPF eddy-viscosity models have been extended by an HPF eddy-diffusivity approach in order to allow for the computation of compressible flows. Both models are able to correctly predict the subharmonic transition in supersonic boundary layers and reasonable agreement in terms of integral quantities and structures with DNS data could be established.

4. Turbulent spot propagation in compressible boundary layers

A transitional flow phenomenon of major interest is the growth of turbulent spots. For high Mach number boundary layer flow turbulent spots are investigated with the focus on growth rate, skin friction and heat transfer. The self-similarity properties of spots reported in the literature are still being investigated. Different spot triggering mechanisms are compared with respect to similarity of the developing turbulence. The simulations are carried out using a high-order finite-difference code with ADM for the non-resolved scales.

A series of LES computations at Mach numbers Ma=2, 3, and 5 was performed. As corresponding Reynolds numbers the values Re=950, 1500, and 2550 were chosen which are close to the stability limit. The spots were triggered using a vortex pair. After an initial transient the spots become turbulent. Their further growth in streamwise and lateral direction is approximately linear. This also applies for the wall normal case but for later stages the spot height is expected to be limited by the boundary layer thickness. A strong Mach number dependence of the growth rate is confirmed. For comparison the Ma=2 case has also been investigated performing a DNS. The spot growth and the structures of the spot compare well between LES and DNS.

5. Simulation of particulate flows

In this project a special class of disperse two-phase flows is studied, in which the particles are much smaller than the smallest relevant scales of the fluid motion. This allows for the particles to be modeled as point--forces without resolving their finite size. In the simulations a Eulerian-Lagrangian approach is used. The fluid equations are solved

in a Eulerian framework, whereas the particles are individually tracked along their trajectories.

Settling and break-up of suspension drops
A highly accurate pseudo-spectral method with two-way coupling (to account for the feedback force) was implemented and optimized for the SX-5. In order to study fundamental aspects of particle suspensions, the numerical method was applied to investigate the settling and break--up of suspension drops under the influence of gravity. Here, the fluid motion remains laminar providing a test case for low and moderate Reynolds number flows. In this Reynolds number range an initially spherical suspension drop usually deforms into a torus that eventually becomes unstable and breaks up into a number of secondary blobs. With increasing Reynolds number the torus breaks up into a growing number of sub-structures. At a fixed Reynolds number the instability involved in the break-up process was shown to depend primarily on the number of particles and their distribution inside the settling torus. For the visualization of the results a close collaboration with CSCS was pursued, leading, among other things, to an award-winning video entry to the Gallery of Fluid Motion at the 57th APS/DFD annual meeting.

Particle settling in homogeneous turbulence
In this project the settling of an initially random particle suspension in homogeneous turbulence was studied with the focus on the mean particle settling velocity. In the case of one-way coupling, when the fluid motion is not affected by the presence of the particles, the mean particle settling velocity is increased by the preferential sweeping effect: due to their inertia the particles are swept towards the peripheries of turbulent eddies in the carrier flow. Under gravity the particles accumulate preferably in regions of downward fluid motion on their way through the turbulent carrier flow. In the case of two-way coupling an additional enhancement of the particle settling velocity is observed, which increases with growing particle volume fraction. This is because of a collective particle effect in regions of increased particle concentration. Here, the particles exert a collective downward drag force on the surrounding fluid, such that the downward fluid velocity increases. This, in turn, yields are larger particle settling velocity in these regions.

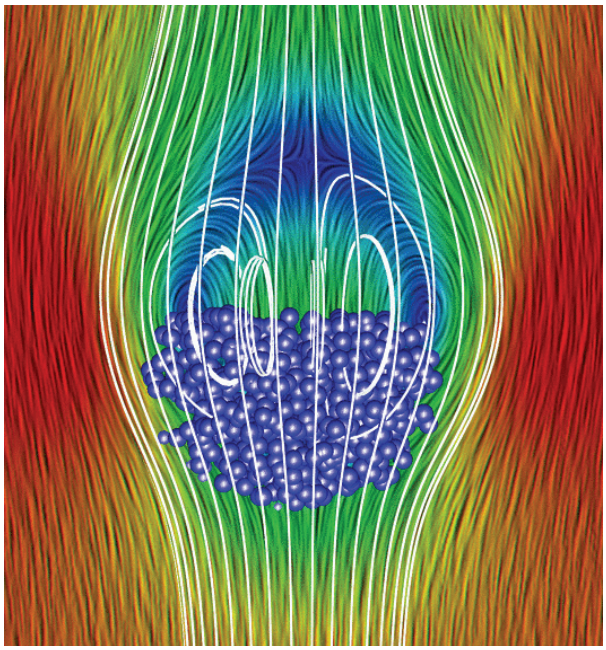

Figure 3: Visualization of the flow around an initially spherical cloud of solid particles (blue spheres) settling in a fluid under gravity.

Particle-laden flow over a backward-facing step
This project covers turbulent, wall-bounded particulate flows with separation. To account for the wall--particle interaction models of this process were extended and refined. A newly developed unified model -- covering elastic and non-elastic wall-particle collisions, increased drag coefficient close to the wall, and the deposition of the particles -- compared favorably to the older models, in terms of accuracy as well as in efficiency. Two-way coupling for the particulate flow was implemented allowing for studies of turbulence attenuation. The examination of the various forces acting on solid particles in laminar and turbulent flow over a backward-facing step (BFS) was conducted for a variety of flow and particle characteristics. The investigation took into account the distinct flow regimes of the BFS flow. Generally, the find-

ings confirmed the presumption that a simplified particle force model will be sufficient for larger calculations thereby saving computational time as well as disk space. In the BFS flow seeding can introduce a significant bias into the calculation. Developed particle-laden channel flow was found to be the most favorable inflow condition for BFS flow. The first studies of channel and BFS flows yielded good results for mean, instantaneous, and statistical quantities. Partially, comparisons with literature were possible, where good agreement was obtained between all quantities.

Identifying genetic determinants of bone strength – a high-throughput phenomics approach in mice

Dr. Harry van Lenthe

with P. Morley, R. Voide and R. Müller

Institute for Biomedical Engineering, ETH and University of Zürich, Switzerland

Abstract

Osteoporosis is a disease characterized by low bone mass and deterioration of bone microarchitecture, leading to increased bone fragility and risk of fracture, particularly of the hip, spine and wrist. It has become evident from twin, multigenerational family and sib-pair studies that bone strength, the most important skeletal determinant for fracture risk, is under genetic control. Our research aims at identifying genes that affect bone strength. Of critical importance to such analyses is the availability of methodologies with marked sensitivity and precision to accurately determine both genotype and phenotype. Where techniques to determine genotype have received much attention over the last years, high-throughput analyses of skeletal phenotype remains a rather unexplored field. We have implemented a functional phenomics approach, a novel, non-destructive, high-throughput computational technique to determine bone strength from bone structure. Using this approach, we are evaluating a large set of bones from mice for which the genetic make-up is known; specifically, we are analyzing their femora and vertebrae. These analyses will allow us to locate genetic determinants of femoral and vertebral bone strength. Furthermore, we will be able to identify whether bone strength is regulated differently in males and females, and whether bone strength is regulated differently for different skeletal sites.

Osteoporosis leads to fractures

Osteoporosis is a disease characterized by low bone mass and structural deterioration of bone tissue, leading to bone fragility and an increased susceptibility to fractures [1], especially of the hip, spine and wrist. Osteoporotic fractures are a major cause of severe long-term pain and physical disability, and have an enormous impact on the individual, society and health care social systems. Osteoporosis is second only to cardiovascular disease as a leading health care problem (World Health Organization): one in two women and one in four men over age 50 will have an osteoporosis-related fracture in her/his remaining lifetime. The estimated direct expenditures (hospitals and nursing homes) for osteoporotic hip fractures was $18 billion in 2002, in the US alone.

Of mice and men

At present, bone mass is the measure most often used to predict fracture risk. Although multiple environmental and hormonal components influence bone mass and adult bone loss, it has now become evident that the genetic regulation of bone mass is a major determinant of an individual's subsequent risk for fracture. Our knowledge about the heritable aspects of bone mass have been derived principally from twin, multigenerational family and sib-pair studies. Collectively, such studies have shown that 60-70% of the normal variability in bone mass is genetically determined.

Thanks to recently developed genome-wide screening techniques major research efforts have

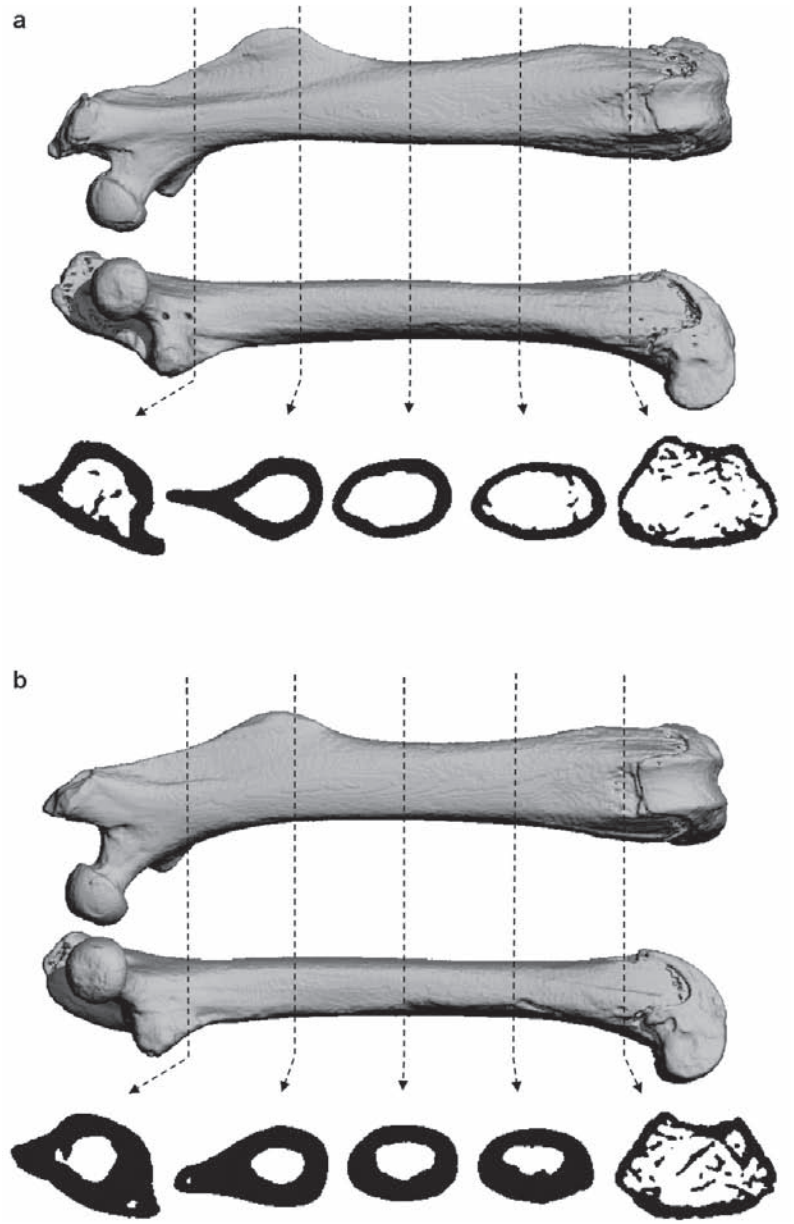

Figure 1: Top view, frontal view, and several cross sections of the femur of two different inbred strains of mice, C57BL/6J (a) and C3H/HeJ (b). Femoral geometry is markedly different, while body weight for these animals is similar. Distance between the dashed lines is 2.5 mm

been started to identify the genetic influence on bone mass, and also on bone structure and function, which are major determinants in assessing fracture risk. Animal models are critical for these studies, as the environmental influences can be largely controlled. Because of the recent deciphering of the mouse and human genome and the high homology between them, the mouse is a perfect model to study the influence of different genes on skeletal phenotypes. Inbred strains are particularly useful, because the genetic make-up is identical for each animal, yet, there is genetic difference between strains. This can be exploited using genetic breeding strategies for two genetically distinct strains. Of critical importance to such analyses is the availability of methodologies with marked sensitivity and precision to accurately determine both genotype and phenotype.

Assessment of bone structure

Where techniques to determine genotype have received much attention over the last years, high-throughput analyses of skeletal phenotypes remains a rather unexplored field. Traditionally, bone

geometrical and architectural phenotypes have been assessed in two dimensions; the structural parameters are measured in histological sections and the third dimension is extrapolated on the basis of stereology [2]. This typically entails substantial specimen preparation, including embedding in a plastic resin, sectioning and staining. While offering high spatial resolution and image contrast, this established technique is both tedious and time-consuming. Particularly limiting is the destructive nature of the procedure, excluding the specimen from use for other measurements. Micro-computed tomography (µCT) is a new, emerging alternative technique to non-destructively image and quantify bone in three dimensions that has been pioneered in our institute. The current systems provide high isotropic spatial resolution of 6 µm. Desk-top µCT has been used by our group extensively to study the microstructural organization of bone and explore genetic effects on bone structure (Fig. 1). This has allowed investigators to gain new insights into trabecular bone micro-architecture and the influence of age-related bone loss on bone architecture.

Assessment of bone strength

Although bone mass and bone architectural parameters are commonly measured in patients, these are only surrogate measure: the ultimate aim of any bone measurement is to assess bone strength, the most important skeletal phenotype to determine whether a bone is at risk of fracture. The gold standard to determine bone strength is direct mechanical testing of bone. Biomechanical testing is a straight-forward procedure but has its limitations, as it is a destructive test, indicating that a sample can only be tested once; in patients it cannot be applied at all. Furthermore, these tests are prone to errors, especially in view of the small size of murine bones, and they are laborious, hence, not applicable to test the large numbers of bones needed in genetic studies.

We recently used microstructural finite element (µFE) analysis to determine bone strength directly from bone structure, as obtained from µCT images. In short, we measured a mouse femora with a µCT40 (Scanco Medical, Bassersdorf, Switserland) using a 20 µm resolution (Fig 2). The recon-

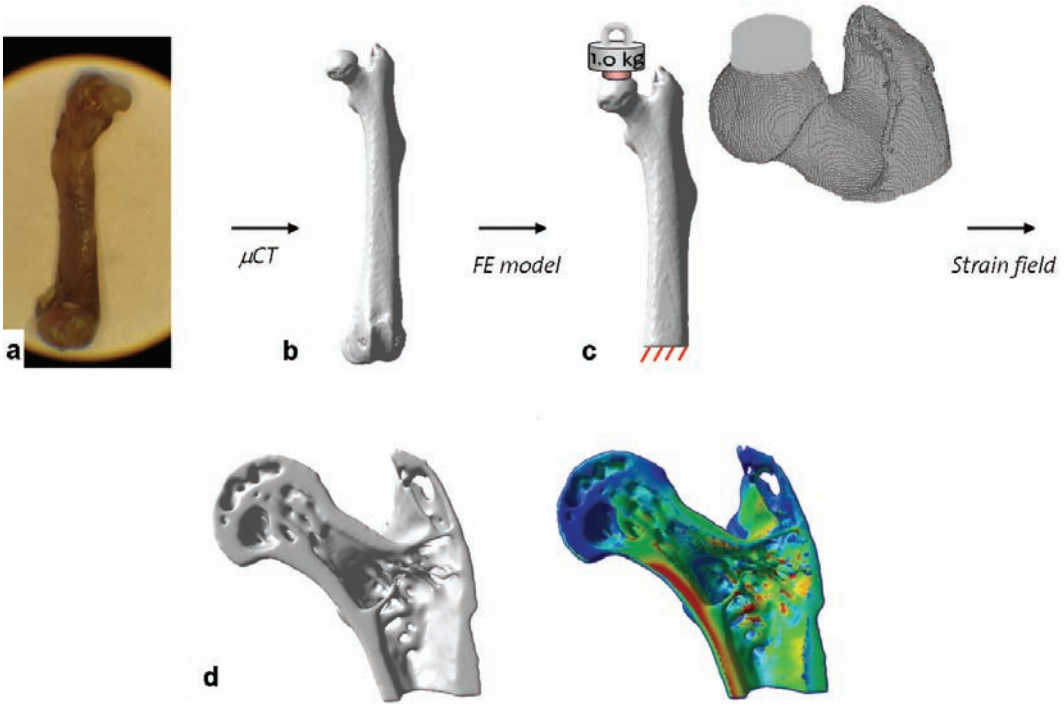

Figure 2: Computational strength analysis of a murine femur. The femur (a) was three-dimensionally reconstructed using micro-computed tomography (b). Using a direct voxel conversion technique, a µFE model was created that simulated loading at the femoral head (c); all elements had identical size and shape (c, inset). The models were solved for displacements from which the strains were calcu-lated. The three-dimensional nature of the models allow to visualize internal bone structure and strains at arbitrary planes (d).

structed images were filtered using a constrained three-dimensional Gaussian filter to partially suppress noise in the volumes (σ=1.2 and support =1) and binarized using a global threshold (22.4% of maximum possible gray scale value). Morpho-metric parameters, such as bone volume, trabecular thickness, trabecular spacing, and cortical thickness, were determined for the bone as a whole and for selected volumes of interest. Then, a μFE model was created that simulated a loading at the femoral head. For that purpose, the μCT-reconstructed femora were automatically aligned in a vertical position. The distal 30% was removed, and a direct voxel conversion technique was used to create the μFE models. The models were loaded at the femoral head with a Hertzian force distribution, and fixed at the distal end. This loading situation causes a fracture at the femoral neck, which is a common fracture location in humans. The models were solved for displacements using in-house written software that uses the iterative preconditioned conjugate gradient element-by-element method [3, 4]. Based on the displacements, the stresses and strains in each element were calculated, and strength in the femoral neck was assessed. Strength was determined as the force needed such that 1% of the elements in the neck had effective strain values greater than 0.7% [5]. FE analysis is a computational technique that has become an essential part of biomechanical investigations focused on better understanding the structure-function relationships associated with tissue adaptation and failure. The advantages that computer modeling has over direct destructive testing, such as the preservation of the test specimen and the possibility of conducting a variety of different tests on the same specimen, make FE modeling an attractive option for investigating the mechanical properties of materials. Even more so, we showed that its precision was 50% better [6] than for traditional experimental testing [7]. We have applied μFE analysis to femora of two growth-hormone deficient inbred strains of mice (B6-lit/lit and C3.B6-lit/lit), and found that although having higher bone volume and thicker cortices, C3.B6-lit/lit had lower femoral strength than B6-lit/lit. Our analyses revealed that this is caused by a weaker femoral neck (Fig. 3). This is an intriguing result as it shows that bone mass alone is not sufficient to have strong bones.

To further investigate the genetic background causing these phenotypic differences the two strains were crossed to obtain an F2 population

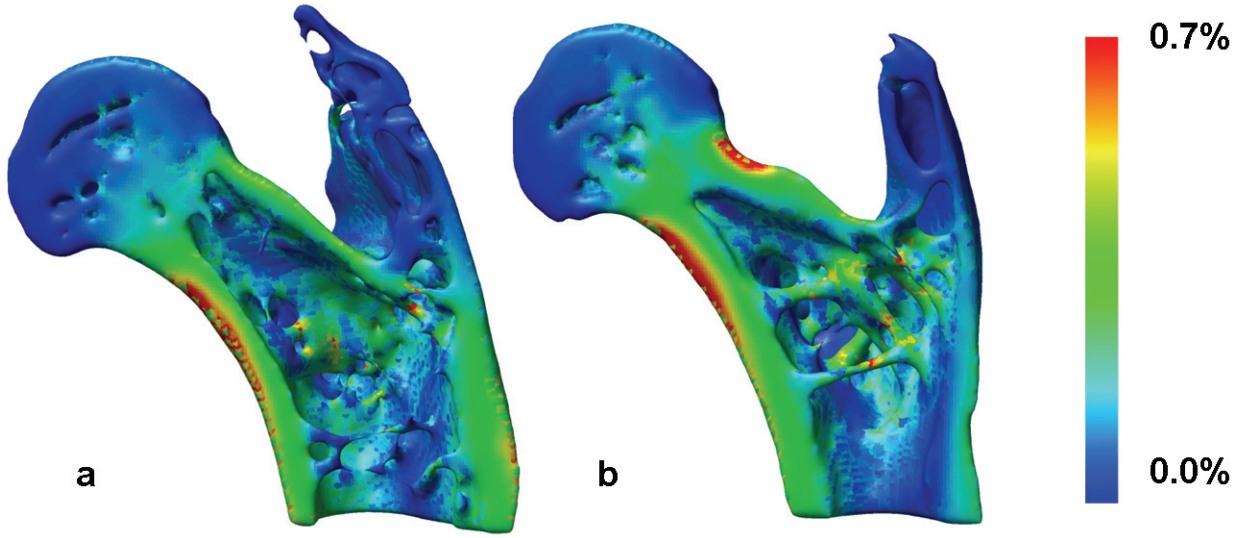

Figure 3: Effective strains in the proximal femur of two genetically different mice. The strains resulting from equal loading at the femoral head were determined from micro-finite element models.

of 2,000 mice; the mice were raised to the age of 4 months. At present, the 2,000 right femora are being scanned using micro-computed tomography with a resolution of 20 µm in three dimensions. After reconstruction, the femora are automatically aligned and convert to microstructural finite element (µFE) models, as described before. The µFE models have around 850.000 elements, and possess 3.000.000 degrees of freedom. This work is unique in its computational aspects: it is the first to apply microstructural finite element analysis to a large set of (bone) samples, hence, it is the first to use these techniques in a high-throughput manner for the assessment of mechanical properties.

The results of the genome-wide screening of all 2,000 mice, which will be performed at The Jackson Laboratory (Bar Harbor, Maine, USA), will be combined with our results on bone strength for these mice. This will provide us the means to determine chromosomal regions (quantitative trait loci, QTL) influencing femoral bone strength. This will give more insight into the regulatory pathways of bone strength rather than simple measures of bone density. Furthermore, we will assess any gender specificity.

Site-specific regulation of bone strength

In these same 2,000 animals we have also started to investigate the fifth lumbar (L5) vertebra. There are two important reasons for also investigating the vertebrae. First of all, because this is a major location where many of the osteoporosis-related fractures occur, they are difficult to treat and they cause reduced quality of life. And second, in a previous study we have shown that trabecular bone volume is regulated differently for femur and vertebra [8]. We have recently assessed the geometry and architecture of the L5-vertebrae using µCT, and found that in our present growth-hormone deficient animal model there are also huge differences in trabecular bone microarchitecture within the vertebral body.

To assess vertebral bone strength we follow a similar approach as for the analysis of femoral neck strength. The 2,000 L5-vertebra are being scanned with a resolution of 12 µm in three dimensions. The segmented µCT data will be used to convert directly to µFE models. Large-scale high-throughput computational techniques similar to the ones described before to assess vertebral bone strength directly from geometry and internal architecture. The data on the genomic markers will be combined with our mechanical and structural data to determine chromosomal regions (QTL) related to vertebral bone strength. By comparing the QTL for femoral bone strength with the QTL for vertebral bone strength we can determine which QTL effect both, hence, have a systemic effect, and which ones have site-specific effects.

References

[1] Osteoporosis prevention, diagnosis, and therapy, in NIH Consensus Statement. 2000. p. 1-45.

[2] Parfitt, A.M., et al., Relationships between surface, volume, and thickness of iliac trabecular bone in aging and in osteoporosis. Implications for the microanatomic and cellular mechanisms of bone loss. J.Clin.Invest, 1983. 72(4): p. 1396-1409.

[3] Smith, I.M. and D.V. Griffiths, Programming the finite element method. third ed. 1998, Chichester: John Wiley & Sons.

[4] Boyd, S.K., R. Müller, and R.F. Zernicke, Mechanical and architectural bone adaptation in early stage experimental osteoarthritis. J Bone Miner Res, 2002. 17(4): p. 687-694.

[5] Pistoia, W., et al., Estimation of distal radius failure load with micro-finite element analysis models based on three-dimensional peripheral quantitative computed tomography images. Bone, 2002. 30(6): p. 842-848.

[6] van Lenthe, G.H., et al., Functional phenomics in bone: high-throughput assessment of genetic differences in murine inbred strains. J. Bone Miner. Res., 2004. 19: p. S390.

[7] Turner, C.H., et al., Genetic regulation of cortical and trabecular bone strength and microstructure in inbred strains of mice. J Bone Miner Res, 2000. 15(6): p. 1126-1131.

[8] Bouxsein, M.L., et al., Mapping quantitative trait Loci for vertebral trabecular bone volume fraction and microarchitecture in mice. J Bone Miner Res, 2004. 19(4): p. 587-99.

Direct Numerical Simulation of the Buoyancy-Driven Turbulence in a Cavity: the DNSBDTC project

Dr. Emmanuel Leriche

Laboratoire d'Ingénierie Numérique
Institut des Sciences de l'Energie
Faculté des Sciences et Techniques de l'Ingénieur
EPF Lausanne, Switzerland

Description

When a fluid enclosed in a cavity is heated over one vertical wall and cooled over its opposite at equal rates – all other walls being adiabatic –, a complex flow develops. The flow characteristics depend on the non-dimensional system parameters known as the Rayleigh (Ra) and Prandtl (Pr) numbers. This problem is one of the classical heat and mass transfer problems with significance for fundamental fluid mechanics, as well as for engineering – the cavity domain is a good approximation to the geometries commonly found in practice – and geophysical applications, like for instance, industrial cooling systems, crystal growth procedures, building insulation or buoyancy-induced horizontal mass transfer in geophysical flows.

Estimates for the attainable turbulent Reynolds/ Rayleigh number by the method of direct numerical simulation have been known for several decades. The evolution in computer hardware and algorithmic developments make it now possible to extend this technique to transitional turbulent flows that are inhomogeneous in all space directions. At present, this is at the limit of what can be achieved with confidence. The present project is concerned with the numerical and physical aspects of the direct simulation of incompressible turbulence within a side-heated cubical cavity. The goal of this project is to reach the highest Rayleigh number but in a very simple domain, a cubical cavity. This simple geometry leads to a very efficient code.

The flow phenomena encountered within such systems are many and poorly understood. At sufficiently high Ra numbers the ascending layer which develops on the heated side undergoes transition to turbulence. A corresponding flow pattern develops on the cooled wall where a descending layer also undergoes transition. The action of these two streams combine to generate a global circulation pattern that sets up a positive vertical temperature gradient over the central part of the cavity which tends to suppress turbulence. As a result some of the turbulent energy generated near the walls is used into setting up a set of internal gravity waves. Another strange phenomenon that is sometimes found in turbulent buoyant flows under density stratification is that of counter-gradient heat transfer (the mean heat flux due to the turbulent fluctuations is against the mean temperature gradient.) This has been studied in the context of homogeneous flows but not within a complex flow domain. The scientific aims are the study of the transition process by buoyancy forcing, the enhanced heat transfer due to the development of turbulence, the collapse of the turbulence under stable stratification conditions, the role of the gravity waves in the global circulation and, if possible, the heat transfer scaling laws.

The objective is to study in detail the three-dimensional turbulent and laminar flow properties within a side-heated cubical cavity by means of direct simulation at high Rayleigh numbers: between 10^5 and 10^9. The simulation will be based on the numerical solution of the Navier-Stokes equations with a Boussinesq buoyancy forcing by spectral methods. The resolution to be used, at least 3.0 million modes, will enable the detail representation of all dynamically significant scales of motion. To our knowledge, such detailed study of this type of complexity is not available from the scientific literature.

Achievements

1. A recent numerical study of natural convection in a side heated cavity has been carried out. The geometry is that of an 'open' cavity meaning that the domain in the direction parallel to the heated walls but normal to the gravity vector is infinite. The usual approximation of such domain is to assume periodicity at some predetermined wavelength along this open direction. The method used for the numerical solution of this problem is Fourier expansions for the periodic direction with Legendre spectral element discretisation for the two inhomogeneous directions. In order to maintain the separability of the pressure operator in the two inhomogeneous directions, the time marching scheme is fully explicit. This limits the highest Ra number that can be simulated due to time step limitation from the diffusive part of the problem. A related problem is the time step limitations due the collocation point distribution within each element. This is because the main flow direction is in the plane of the spectral element grid with the smallest grid size being determined by near wall diffusion. It turns out that in a number of locations, specially near the corners, the Courant limit imposes severe time step limitations. The highest Ra attained with this method is $3x10^8$. The flow is unsteady but not turbulent. Figure 1 shows the instantaneous temperature field in a cross section of the natural convection in a 2:1 cavity with one homogeneous (periodic) direction. The number of collocation points is 64 in the homogeneous direction and 211x311 in the inhomogeneous ones. This is about the limit of what can be achieved with this particular combination of space and time schemes and computer resources provided by EPF Lausanne.

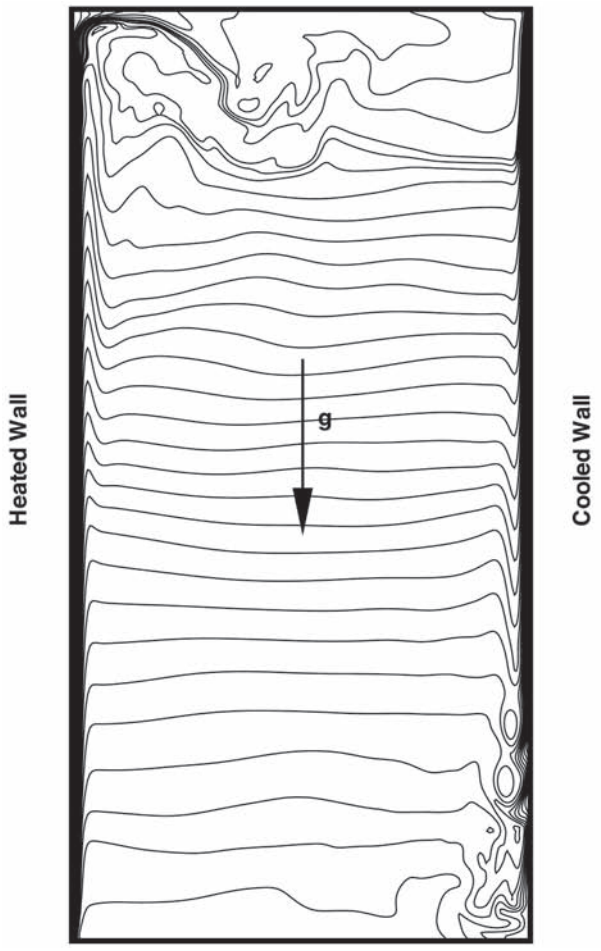

2. A fully three-dimensional Chebyshev collocation method with a projection-diffusion algorithm has been validated in the range of Ra up to 10^6. The agreement with published data is very good. With this code, the time step limits is less stringent and it is therefore possible to tackle higher Ra numbers. This will allow simulations into the turbulent regime.

3. From the previous large user project (the DNSTLDCC project, Direct Numerical Simulation of Turbulence within a Lid-Driven Cubical Cavity), three databases at high Reynolds numbers (12000,18000 and 22000) has been generated , and statistics on meaningful sample are still currently analysed see Figure 2, [2, 7]. It turns out that the statistics for the case of Re=22000 require much more longer sample than the one at Re=18000. The sizes of the databases are of the order of 1.7 Tbytes (Re=18000) and 6.2 Tbytes (Re=22000). Those databases are also used in the framework of the large eddy simulation (LES) to validate filtering approaches and a priori / a posteriori simulation tests [6].

4. Eigenvalues analyses for the Stokes operators have been carried out. The scope of the present work is to provide the first deep insight into the Stokes eigenspace in simple confined geometries like the square [3, 4] or the cube. The eigenvalues and eigenmodes are accurately computed by sevral different means, namely, a Chebyshev Projection-Diffusion solver (2D/3D), a Galerkin Reid-Harris expansion of the stream function (2D), and a Lattice-Boltzman approach (2D/3D). The symmetries which underlie the eigenmode patterns are also identified. The spectra evolution laws are in excellent qualitative agreement with the theoretical asymptotic predictions, $\lambda_k \approx k^{2/n} + O(k^{1/n})$, with n = 2; 3 for 2D or 3D problems. The slopes are evaluated from the computed spectra and are found to be specific to the eigenmodes symmetry family. The dynamic equilibria are analyzed and show a linear relationship between the vorticity and the potential vector in the core of the eigenmodes. These features of the Stokes eigenmodes in the confined geometries are shared by the fully periodic Stokes eigenmodes. The knowledge and interpretation of the Stokes eigenmodes should thus bring an interesting point of view over the resulting dynamics of closed flows, complementary to what is well known regarding the inviscid regions. Analyzing the 3D Stokes eigenmodes in the cube will likely provide valuable understanding of the 3D corners eddies which is the generalisation of the analytical theory of Moffatt in the sixties. Figure 3 shows the 3D corners eddies by streamlines tracking.

5. An extension to higher-order direct Stokes solvers with or without temporal splitting has been investigated numerically [5]. The temporal stability and effective order of two different direct high-order Stokes solvers are examined. Both solvers start from the primitive variables formulation of the Stokes problem, but are distinct by the numerical uncoupling they apply on the Stokes operator. One of these solvers introduces an intermediate divergence free velocity for performing a temporal splitting while the other treats the whole Stokes problem through the evaluation of a divergence free acceleration field [1]. The second uncoupling is known to be consistent with the harmonicity of the pressure field ([1]). Both solvers proceed by two steps, a pressure evaluation based on an extrapolated in time (of theoretical order J_e) Neumann condition, and a time implicit (of theoretical order J_i) diffusion step for the final velocity. These solvers are implemented with a Chebyshev mono-domain and a Legendre spectral element collocation schemes. The numerical stability of these four options is investigated for the sixteen combinations of (J_e; J_i), $1 \le J_e$; $J_i \le 4$. The common result is that

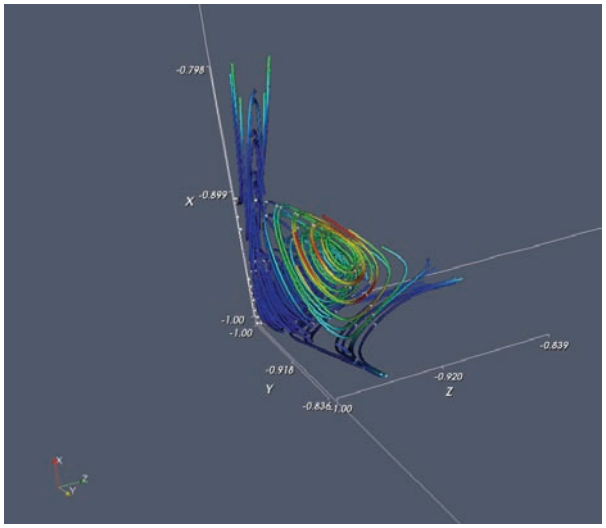

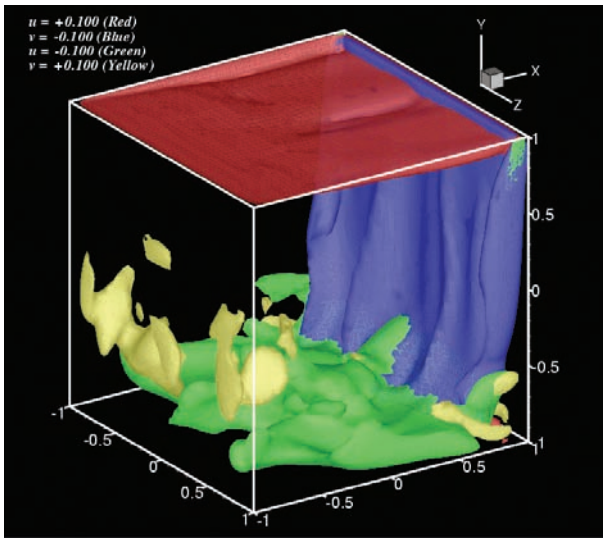

Figure 2: Instantaneous u and v velocity isosurfaces (u/U_o = +0.1 and v/U_o =+ 0.1)

the schemes are unconditionally stable for $J_e \leq 2$, whereas a time step criterion of explicit type occurs – $\Delta t < O(N^{-4})$ –, when $J_e > 2$, slightly less restrictive for the consistent scheme than for the other. The effective time orders are then measured with $1 \leq J_e \leq 2$ and $1 \leq J_i \leq 4$. For the consistent solver the effective and expected time orders are in excellent agreement, and some discrepancies occur for the other scheme which turns out to provide slightly more accurate orders.

References

[1] E. Leriche and G. Labrosse. High-Order Direct Stokes Solvers with or without Temporal Splitting : Numerical Investigations of their Comparative Properties. SIAM J. Scient. Comput., 22(4):1386–1410, 2000.

[2] E. Leriche and S. Gavrilakis. Direct Numerical Simulation of the Flow in a Lid- Driven Cubical Cavity. Physics of Fluids, 12(6):1363–1376, 2000.

[3] E. Leriche and G. Labrosse. Stokes eigenmodes in the square: which expansion is more accurate, Chebyshev or Reid-Harris ?. Numerical Algorithms, 38(1-2):111-131, 2005. [4] E. Leriche and G. Labrosse. Stokes eigenmodes in square domain and the stream function – vorticity correlation. Journal of Computational Physics, 200:489-511, 2004.

[5] E. Leriche, E. Perchat, G. Labrosse and M.O. Deville. Numerical evaluation of the accuracy and stability properties of high-order direct Stokes solvers with or without temporal splitting. J. Sci. Comput., on line, 2006, DOI: 10.1007/s10915-004-4798-0.

[6] R. Bouffanais, M.O. Deville, P. Fischer, E. Leriche and D. Weill. Large-Eddy Simulation of Lid-Driven Cubic Cavity Flow by the Spectral Element Method. 6th International Conference on Spectral and High Order Methods (ICOSAHOM), J. Sci. Comput., in press, 2005.

[7] E. Leriche. Direct Numerical Simulation of Lid Driven Cavity at High Reynolds Numbers. J. Sci. Comput., on line, 2006, DOI: 10.1007/s10915-005-9032-1.

Computational Mineral Physics and Crystallography

Dr. Artem R. Oganov

with D.Y. Jung, D. Adams, K. Hassdenteufel, C.W. Glass and F. Zhang

Laboratory of Crystallography, Department of Materials ETH Zurich, Switzerland

Using ab initio simulations, we study the structure and properties of minerals and other systems of fundamental interest at high pressures and teperatures. The main hallmarks of our approach are the use of highly accurate methods (e.g., the all-electron PAW methodology) and efficient state-of-the-art codes (VASP and ABINIT), novel breakthrough methodologies (e.g., metadynamics method of Martonak and colleagues), development of our own methods and codes (USPEX code – Glass & Oganov, in prep.; Oganov & Glass, in prep.), and active collaboration with experimentalists (in Japan, France, USA, Russia, Switzerland).

We have been the first group to explore systematically the potential of density-functional perturbation theory as a tool to simulate phase diagrams [1-6]. A number of up-to-date reviews of computational methods and codes can be found in the recent special issue «Computational Crystallography» of Zeitschrift für Kristallographie [7]. We have also published several more focussed reviews dealing with studies of planet-forming materials using ab initio simulations [6,8-11]. In 2004-2005 our research focussed on the following directions:

A. Studies of the Earth's mantle minerals, especially those of the D" layer (2700-2890 km depths). In particular, through a combination of ab initio simulations and high-pressure experiment we have discovered [1] the post-perovskite phase of $MgSiO_3$, the main mineral of the Earth's D" layer (Figure 1), and reported detailed studies [1,4,12] of its structure, properties, stability, and defects. This discovery has greatly changed the views on the interior of our planet and its evolution. It has attracted much attention from public media, resulting in a radio interview, article in Tages Anzeiger, and numerous articles in other newspapers and magazines. Although the discovery is very recent (2004), there had already been three international conferences and symposia dedicated to this new mineral.

Resolving the previous dispute among experimental groups, we have found [3] that $MgSiO_3$ polymorphs remain stable against decomposition into $MgO + SiO_2$ throughout the Earth's lower mantle conditions (depths 670-2890 km). Additionally, we have studied surface properties of $MgSiO_3$ perovskite [13] and thermal behaviour of its analogue material, $NdGaO_3$ [14].

For SiO_2 we have determined the ab initio phase diagram and elucidated the nature of the high-pressure pyrite-structured phase [2]. Its chemical bonding was studied using the topological analysis of electron density distribution and using electron localization function and localized orbital locator (Figure 2).

For Al_2O_3 we have found a new phase isostructural with the post-perovskite phase of $MgSiO_3$ [4]. This phase was again discovered in close collaboration

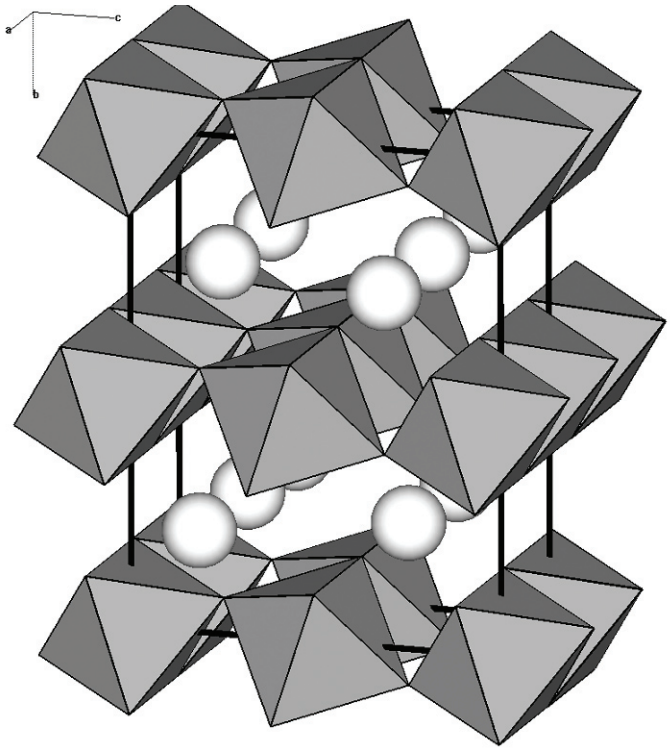

Figure 1: Crystal structure of $MgSiO_3$ post-perovskite (from [1]). Spheres – Mg atoms, polyhedra – Si-centred octahedra.

with experimentalists. In fact, for all the three materials, $MgSiO_3$, SiO_2 and Al_2O_3, high-pressure behaviour is counterintuitive. In particular, close packing motifs in these materials unexpectedly break down at high pressure. For $CaSiO_3$ perovskite, another major mantle-forming phase, we found that it is stable against decomposition into CaO + SiO_2, and that there is no stable post-perovskite-type structure at high pressure [15].

B. Other activities. We have suggested a new formalism for intrinsic anharmonic effects in solids [16,17] based on thermodynamic perturbation theory. This has been used, together with reliable models for other contributions to the thermal equation of state, to analyse experimental data on reference materials and propose a new improved ruby pressure scale [18]. Additionally, we have been involved in studies of high-pressure isosymmetric phase transitions in molecular crystals [19], where our ab initio simulations have been crucial for interpreting experimental results.

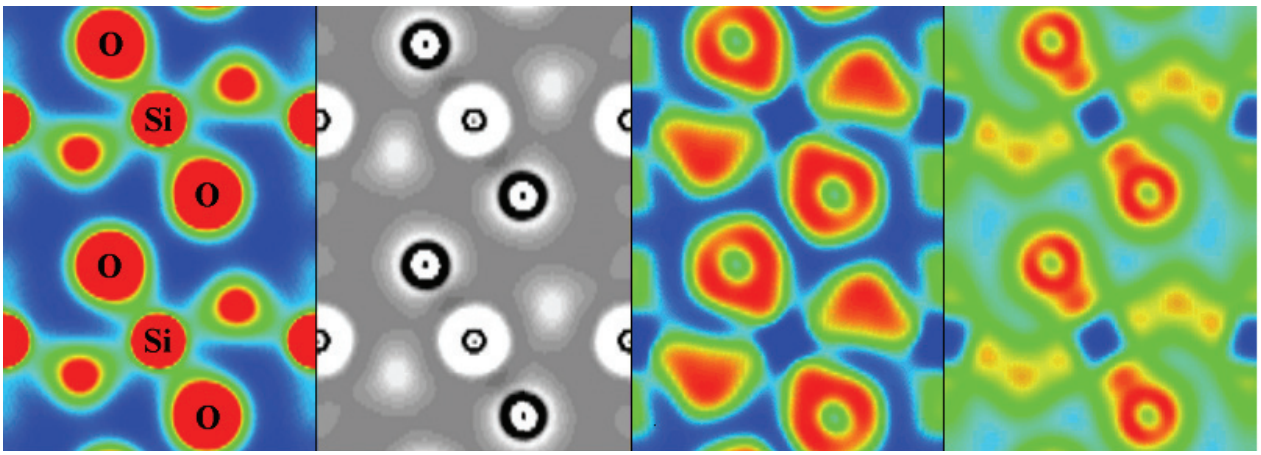

Figure 2: Chemical bonding in pyrite-type phase of SiO_2, stable above 200 GPa, from left to right: total electron density, its Laplacian, valence electron localization function and localized orbital locator. From [2].

Our publications in 2004-2005

[1] Oganov A.R., Ono S. (2004). Theoretical and experimental evidence for a post-perovskite phase of MgSiO3 in Earth›s D» layer. Nature 430, 445-448.

[2] Oganov A.R., Gillan M.J., Price G.D. (2005). Structural stability of silica at high pressures and temperatures. Phys. Rev. B71, art. 064104.

[3] Oganov A.R., Price G.D. (2005). Ab initio thermodynamics of MgSiO3 perovskite at high pressures and temperatures. J. Chem. Phys 122, art. 124501.

[4] Oganov A.R., S. Ono (2005). The high-pressure phase of alumina and implications for Earth's D" layer. Proc. Natl. Acad. Sci. 102, 10828-10831.

[5] Ghose S., Krisch M., Oganov A.R., Beraud A., Bossak A., Gulve R., Seelaboyina R., Yang H., Saxena S.K. (2006). Lattice dynamics of MgO at high pressure: theory and experiment. Phys. Rev. Lett. 96, art. 035507.

[6] Oganov A.R. (2004). Phase diagrams of minerals from first principles. Proceedings of the CECAM Workshop «First-Principles Simulations: Perspectives and Challenges in Mineral Sciences» (Berichte aus Arbeitskreisen der DGK, Nr. 14, German Crystallographic Society), pp. 53-62.

[7] Oganov A.R., editor (2005). Zeitschrift für Kristallographie 220, issue 5/6 „Computational Crystallography".

[8] Oganov A.R. (2004). Theory of Minerals at High and Ultrahigh Pressures: Structure, Properties, Dynamics, and Phase Transitions. In: High-Pressure Crystallography, NATO Science Series: II: Mathematics, Physics and Chemistry, vol. 140, p.199-215 (edited by A.Katrusiak, P.F.McMillan). Kluwer Academic Publishers, Dordrecht.

[9] Jung D.Y., Oganov A.R. "Basics of first-principles simulation of matter under extreme conditions". EMU Notes in Mineralogy v.7 ("High-Pressure Behaviour of Minerals", edited by R. Miletich), 124-145.

[10] Adams D.J., Oganov A.R. "Theory of minerals at extreme conditions: predictability of structures and properties". EMU Notes in Mineralogy v.7 ("High-Pressure Behaviour of Minerals", edited by R. Miletich), 441-457.

[11] Oganov A.R., Price G.D., Scandolo S. (2005). Ab initio theory of planetary materials. Zeitschrift fuer Kristallographie 220, 531-548.

[12] Ono S., Oganov A.R., Ohishi Y. (2005). In situ observations of phase transition between perovskite and CaIrO3-type phase in MgSiO3 and pyrolitic mantle composition. Earth Planet. Sci. Lett. 236, 914-932.

[13] Alfredsson M., Dobson D.P., Oganov A.R., Catlow C.R.A., Brodholt J.P., Parker S.C., Price G.D. (2005). Crystal morphology and surface structures of the orthorhombic MgSiO3 perovskite. Phys. Chem. Minerals 31, 671-682.

[14] Senyshyn A., Oganov A.R., Vasylechko L., Ehrenberg H., Bismayer U., Berkowski M., Matkovskii A. (2004). Crystal structure and thermal expansion of the perovskite - type Nd0.75Sm0.25GaO3 - powder diffraction and lattice dynamical studies. J. Phys.: Cond. Matter. 16, 253-265.

[15] Jung D.Y., Oganov A.R. (2005). Ab initio study of the high-pressure behaviour of CaSiO3 perovskite. Phys. Chem. Minerals 32, 146-153.

[16] Dorogokupets P.I. & Oganov A.R. (2004). Intrinsic anharmonicity in equations of state of solids and minerals. Doklady Earth Sciences 395, 238-241.

[17] Oganov A.R. & Dorogokupets P.I. (2004). Intrinsic anharmonicity in thermodynamics and equations of state of solids. J. Phys.: Cond. Matter. 16, 1351-1360.

[18] Dotogokupets P.I., Oganov A.R. (2005). Ruby pressure scale: revision and alternatives. In: Proc. Joint 20th AIRAPT & 43th EHPRG Int. Conf. on High Pressure Science and Technology, 27 June – 1 July 2005, Karlsruhe, Germany. Collected papers (CD-ROM version).

[19] Boldyreva E.V., Ahsbahs H., Chernyshev V.V., Ivashevskaya S.N., Oganov A.R. (2005). Effect of hydrostatic pressure on the crystal structure of sodium oxalate: X-ray diffraction study and ab initio simulations. Z. Krist., in press.

Prof. Michele Parinello

Departement of Chemistry and Applied Biosciences, ETH Zürich, Switzerland

Charge Localization in DNA Fibers

Francesco Luigi Gervasio

Charge transfer in DNA is currently the subject of intense theoretical and experimental investigation [1, 2]. This is motivated both by a possible use of DNA as a component in nanoelectronic and electrochemical devices[3] and by the fundamental role of conductivity in the oxidative damage and possibly repair of DNA [4]. A number of experiments have studied conducdance of DNA in different contexts providing seemingly contradictory results, ranging from a highly conducting wire [5] and a proximity induced superconductor [6] to a semiconductor[7] or an insulator[8].

Two different mechanisms have been proposed to explain long-distance positive charge transport in duplex DNA: a coherent single step transport from donor to acceptor or a hopping mechanism where the radical cation, initially trapped on one or several bases, moves to a different location when triggered The possibility of a long-range coherent single step transport can probably be ruled out by the disorder of DNA Hopping can in principle work via two mechanisms: tunnelling when it is through only a few bases, or a phonon assisted polaron-

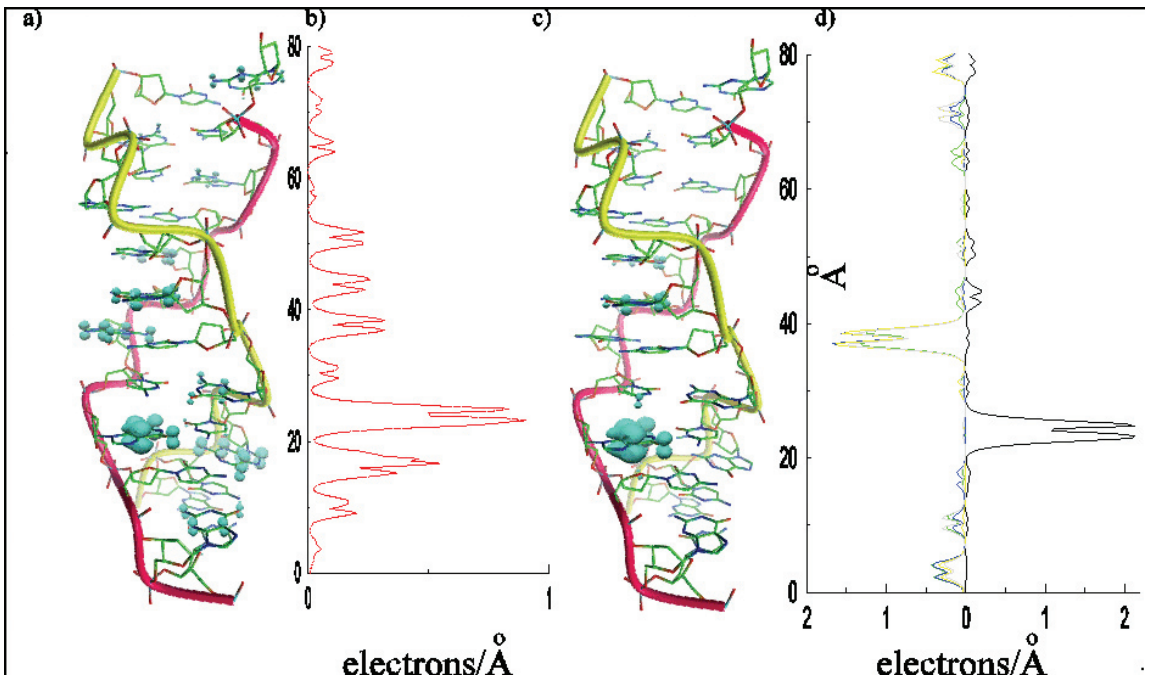

Figure 1: a) View of the three-dimensional structure of the polyd(GpCp) and of the spin density isosurface (in cyan) associated to the radical cation state at zero kelvin. The isosurfaces represented have a value of 10^{-4} electrons $Å^{-4}$ b) Projection of the electronic spin density $\rho_s(z)$ along the z axis for the unit cell (cyan) and for the replicated cell (black). c) Helical parameters of the structure in the local basis frame. The propeller twist is represented in blue, the tip in green.

like hopping model, where the introduction of a charge defect in DNA is accompanied by a structural change that stabilizes the defect [9].

While the role of uctuations in tuning DNA conductivity and a possible polaron-like hopping mechanism has been investigated in several experiments, our knowledge of the microscopic changes induced by the charge defect and its transfer is mostly based on indirect evidence. Theory could be of great help in understanding these phenomena, but given the computational cost of full-scale calculations on realistic DNA systems, theoretical efforts to date have mostly been limited to small and medium-sized model systems or to dry DNA molecules or to larger systems using model Hamiltonian and semi-empirical studies. Recent studies [10] have underlined the need to include the full complexity of the system and in particular the effect of solvation by water and counter-ions. In the present work [11], by performing first-principles calculations on a fully hydrated laboratory realizable system, we found direct evidence that in a polyd(GpCp) fiber the hole can be localized either by proton shift or by a change in the solvation shell of the counter-ions. Distortion of the helical parameters, on the other hand, is ineffective at room temperature.

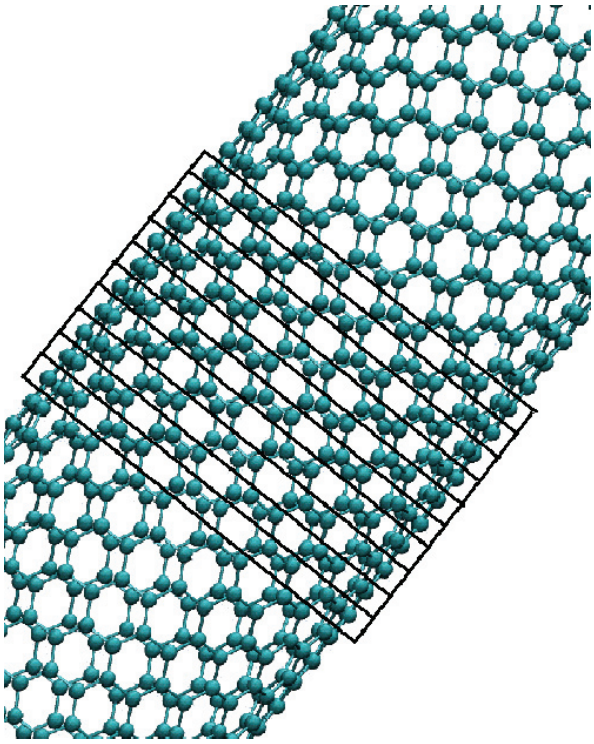

Figure 1: Illustration of a (12,12) carbon nanotube which is subdivided into slices of z=24 atoms. The prefactor of the scaling law showed in figure 2 is proportional to z^2.

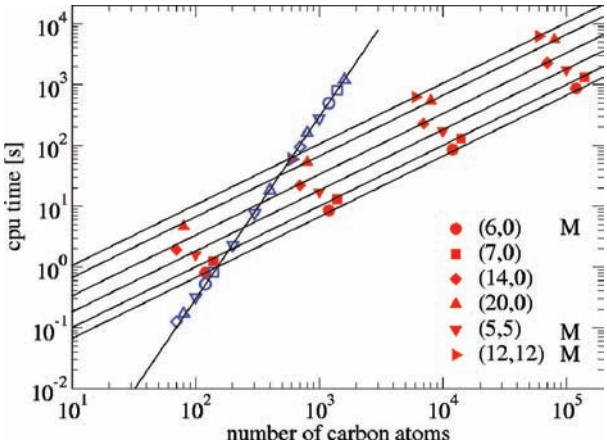

Figure 2: Scaling of the CPU time needed for one electronic structure calculation of a carbon nanotube. Filled symbols correspond to our LS scheme and open symbols are obtained form the timing of the standard method.

Development of new linear scaling electronic structure methods and advanced sampling techniques

Florian R. Krajewski

Atomistic simulations that calculate the atomic interactions on the fly from an electronic structure calculation using an independent particle approximation are nowadays the most important ab-initio simulation scheme. A major limiting factor of these methods is the cubic scaling of the algorithms used. We developed a new class of linear scaling algorithms which are all based on a new expression for the grand canonical potential describing a system of uncorrelated fermions. The new expression used is an exact decomposition of the fermionic determinant and applicable to metals and insulators [12]. It leads to a stochastic algorithm which scales linear with the system size in all dimensions and to a deterministic algorithm scaling linearly for quasi one-dimensional problems and quadratic in all other dimensions. We used the determistic scheme to perform electronic structure calculations for carbon nanotubes (fig.1) and

found perfect linear scaling (figure 2). Using the stochastic linear scaling method the problem of sampling the Boltzmann distribution with noisy energies and forces appears. This is solved by the development of a new sampling scheme that allows to sample the Boltzmann distribution using only noisy forces [13]. The sampling scheme developed is exact in the limit of uncorrelated noise and applicable to all problems where the interaction can only be evaluated stochastically. For illustration we apply the new methods to an ab-initio model system and tight binding silicon in the liquid and the solid phase.

Simulating chemical reactions with Car-Parrinello metadynamics

András Stirling

Within this project we applied the metadynamics method (M. Iannuzzi, A. Laio, M. Parrinello, Phys. Rev. Lett. 90 (2003) 238302) to study the reaction mechanism of different intra- and intermolecular chemical transformation. For the azulene-naphthalene rearrangement we obtained several intramolecular and radical pathways and on the basis of the activation free energies we selected the preferred ones [14]. We also obtained a number of interesting metastable structures derived from

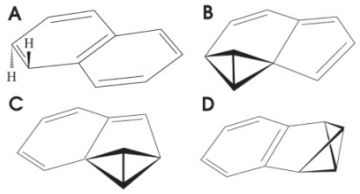

Figure 1: Selected metastable structures on the azulene-naphthalene energy surface

azulene.

In the study of a homogeneous catalytic process (β-lactone formation from epoxide and CO in the presence of a Lewis acid and $Co(CO)_4$) we obtained a very complex reaction mechanism and showed how the nature of the Lewis acid can effect the mechanism [15].

In a redox reaction taking place between hydrated NO_3 ion and defective pyrite surface we obtain a multistep reaction path. We pay particular attention to clarify what role the excess spin density on the surface plays in the mechanism [16].

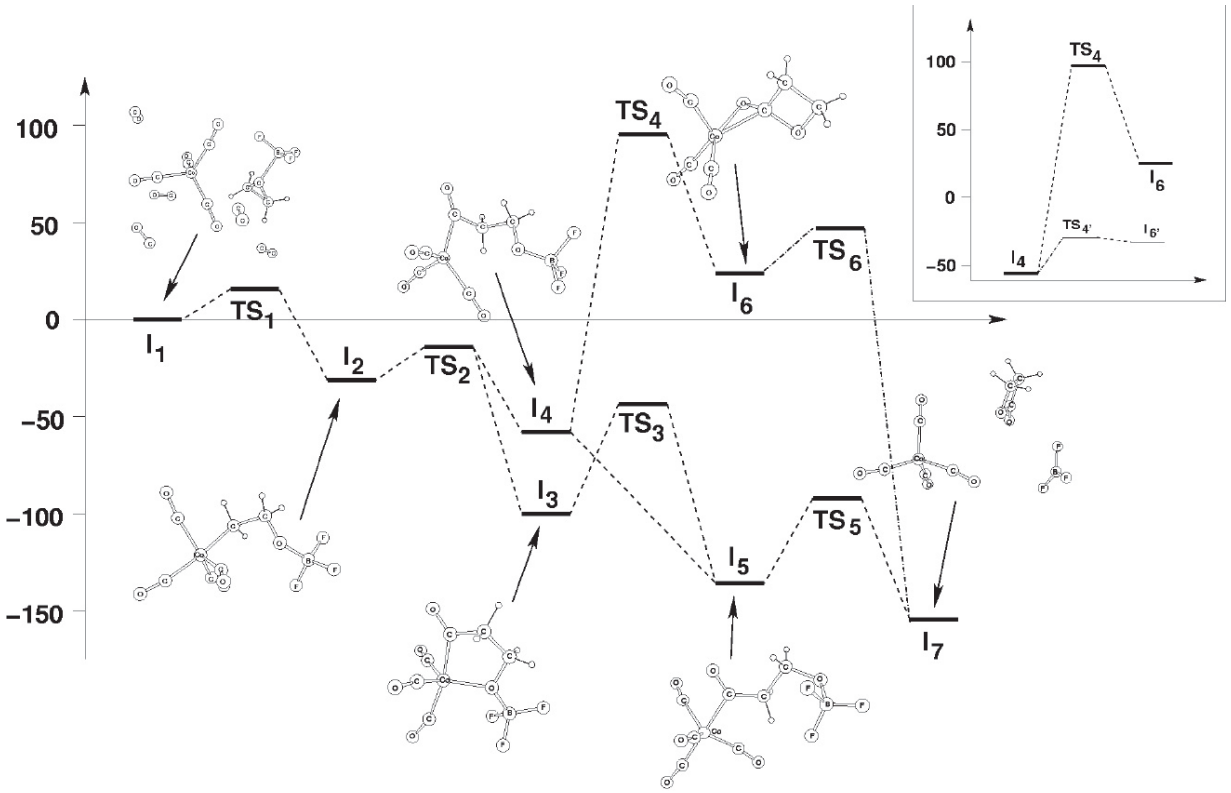

Figure 2: Complete energy profile for the reaction routes. Inset: comparison of TS_4 for two different Lewis acids

References

[1] G. B. Schuster, ed., Longe-Range Charge Transfer in DNA I, vol. 236 of Topics in Current Chemistry (Springer-Verlag,Heidelberg, 2004).

[2] G. B. Schuster, ed., Longe-Range Charge Transfer in DNA II, vol. 237 of Topics in Current Chemistry (Springer-Verlag, Heidelberg, 2004).

[3] S. O. Kelley, N. M. Jackson, M. G. Hill, and J. K. Barton, Angew. Chem. Int. Ed. 38, 941 (1999).

[4] E. M. Boon, Proc. Natl. Acad. Sci. U.S.A. 100, 12543 (2003).

[5] R. Holmlin, P. Dandliker, and J. Barton, Angew. Chem. Int. Ed. 36, 2714 (1997).

[6] A. Y. Kasumov, M. Kociak, S. Gueron, B. Reulet, V. T. Volkov, D. V. Klinov, and H. Bouchiat, Science 291, 280 (2001).

[7] D. Porath, A. Bezryadin, S. deVries, and C. Dekker, Nature 403, 635 (2000).

[8] P. J. de Pablo, F. Moreno-Herrero, J. Colchero, J. G. Herrero, P. Herrero, A. M. Bar, P. Ordejn, J. M. Soler, and E. Artacho, Phys. Rev. Lett. 85, 4992 (2000).

[9] G. B. Schuster, Acc. Chem. Res. 33, 253 (2000).

[10] F. L. Gervasio, P. Carloni, and M. Parrinello, Phys. Rev. Lett. 89, 108102 (2002).

[11] F. L. Gervasio, M. Boero, A. Laio, and M. Parrinello, Phys. Rev. Lett. 84, 158103 (2005).

[12] Stochastic linear scaling for metals and non metals, F. R. Krajewski and M. Parrinello, Phys. Rev. B 71, 233105 (2005).

[13] Linear scaling electronic structure calculations and accurate sampling with noisy forces, F. R. Krajewski and M. Parrinello, cond-mat/0508420, to be published in Phys. Rev. B.

[14] A. Stirling, M. Iannuzzi, A. Laio, M. Parrinello, ChemPhysChem 5 (2004) 1558.

[15] A. Stirling, M. Iannuzzi, M. Parrinello, F. Molnar, V. Bernhart, G.A. Luinstra, Organometallics 24 (2005) 2533.

[16] A. Stirling, M. Bernasconi, M. Parinello, manuscripts in preparation.

The work of the EFLUM Lab of EPFL on the CSCS clusters in 2005

Prof. Marc Parlange

with Ben Rogers, Jan Overney and Elie Bou-Zeid

Environmental Fluid Mechanics Laboratory, EPF Lausanne, Switzerland

Introduction

Understanding the transport of momentum, heat, water vapor, and chemicals in the atmospheric boundary layer (ABL) is crucial to many scientific disciplines such as: hydrology, meteorology, and air quality management. The turbulent nature of the ABL flow controls this transport and significantly complicates its measurements and simulations.

Large-Eddy Simulation (LES) has become increasingly popular as a tool for a physical understanding of the ABL dynamics (Hechtel et al., 1990; Chen and Leclerc, 1995; Avissar et al., 1998; Albertson and Parlange, 1999a; 1999b). By resolving the large scales of motion in turbulent flows, LES can be more faithful to the physics of complex flows than alternative numeric simulations techniques such as Reynolds-Averaged Navier-Stokes (RANS) simulations. This allows simulation of very complex flows such as flow in urban areas and flow over hills. Moreover, LES can capture non-linear effects associated with turbulent mixing much better than RANS where the turbulence is not resolved at all; these effects are very important in simulations of ABL flow over «real» terrain. In that regard, the work of EFLUM on the CSCS clusters has so far consisted of running LES simulations using a new generation Lagrangian scale dependent SGS model to address the following problems

1) Simulating flow in urban environments (EPFL campus to start with).
2) Validating the code for flow over a single hill as a first step to study flow over complex hilly terrain.

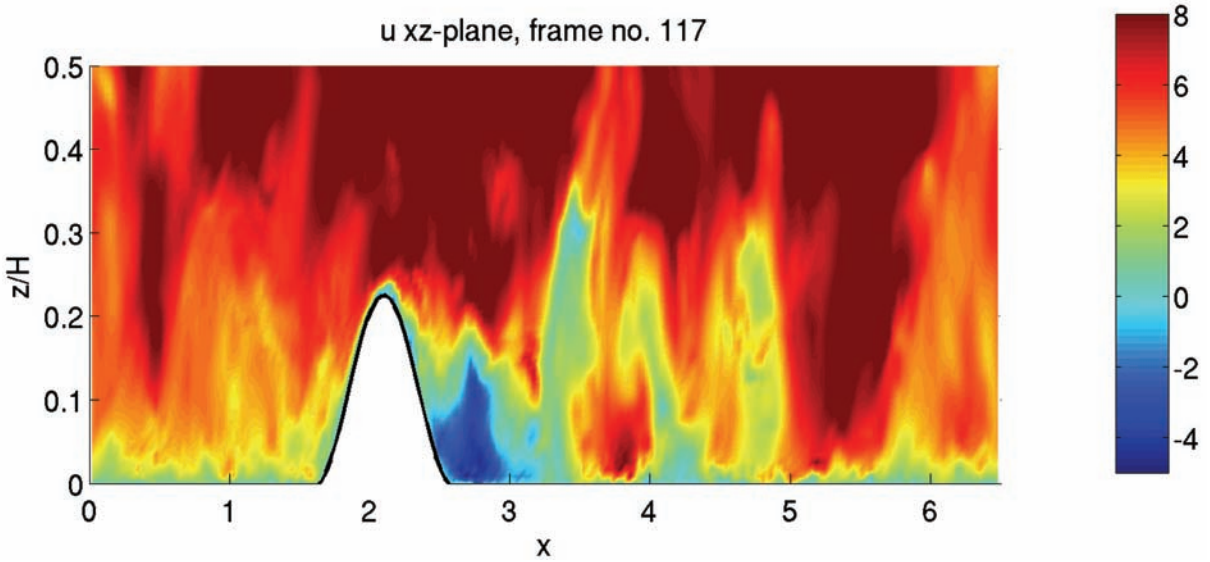

Figure 1: Snapshot of flow over a single hill: colour contours of streamwise velocity

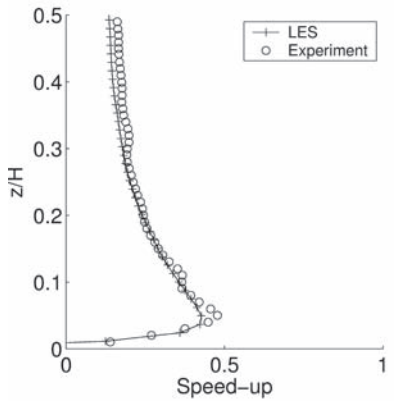

Figure 2: Speed-up of flow over a single hill

In EFLUM, we are particularly interested in the Large-Eddy Simulation (LES) to model atmospheric boundary layers over complex terrain since the method can capture the unsteady spatial variations that occur in turbulent flows around bluff bodies such as unsteady separation and vortex shedding. The current code is already validated to a variety of flow including flow over homogeneous terrain, flow over heterogeneous terrain, flow over single building, and flow in complex urban areas. As part of the development of this state-of-the-art technique, we have been applying and extending its ability to model the flow around bluff bodies, specifically flows over mountains.

Modelling Flow over complex terrains

The simulation of flow over hills has become increasingly important in recent years, especially in light of the alarmingly fast increase in glacier melt. Thus, an accurate simulation of flows over hills and mountains is essential for our understanding and ability to predict atmospheric boundary layer flows and its interaction with the ground surface. In an era of increasing concern for our environment, the ability to understand the turbulent boundary layer flow above mountain ranges such as the Alps in Europe will be critical to our ability to predict the long-term evolution of the environment.

To compare with experimental data from wind-tunnel experiments (Ross et al. 2004), we have simulated unsteady flow over a single hill. Figure 1 displays a colour contour plot for a snapshot of a 3-D 200x40x120 grid simulation of flow over hill in comparison to wind-tunnel data.

It can be seen that the flow is very unsteady with reverse flow being generated in the lee of the hill. When we compare the time-averaged numerical results with experimental data, we see that there is close agreement as shown in Figure 2 which displays the speed-up in velocity observed over the hill caused by the presence of the hill itself. We intend to now apply this model to more complex terrains such as a real mountain range such as the Gaudergraut ridge.

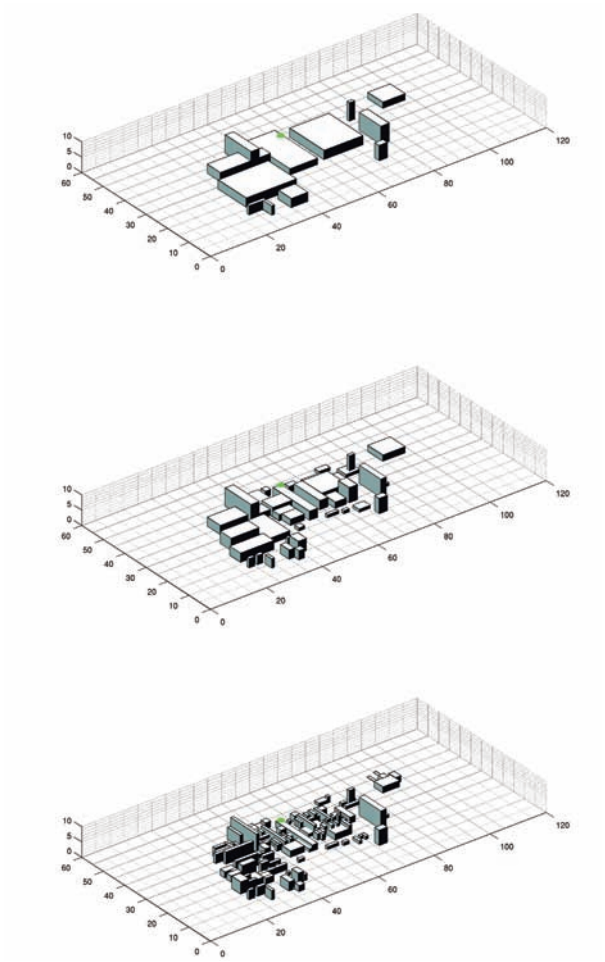

Figure 3: 3-D models of the EPFL campus increasing in detail from top to bottom

Modelling Flow over urban terrains

Also of increasing importance is the ability to model flow over urban terrains such as towns and sections of cities. In particular, the simulation of atmospheric boundary layer (ABL) flows over an urban canopy can lead to the accurate prediction of transport and dispersion of contaminants in urban environments. Pollen, dust, industrial releases and biological or radiological agents are only a few important examples of such contaminants. At EFLUM, we are using our LES model to simulate flow over the EPFL campus, looking in particular at determining the amount of building detail required of a model to yield acceptable results. Figure 3 shows three different versions of the EPFL campus that are being investigated.

Figure 4 shows the results for time-averged u-velocity in a horizontal plane we have obtained from our numerical solutions for the fine resolution description of the campus.

There is clearly recirculation behind some buildings and not behind others. Exactly how much fine detail is required to predict this is a focus of our work. We have already been able to determine that using the simplest block representation of the campus is insufficient for representing the campus and that a more detailed description is required. However, at least 6-8 grid points are required to adequately describe a structure in each co-ordinate direction.

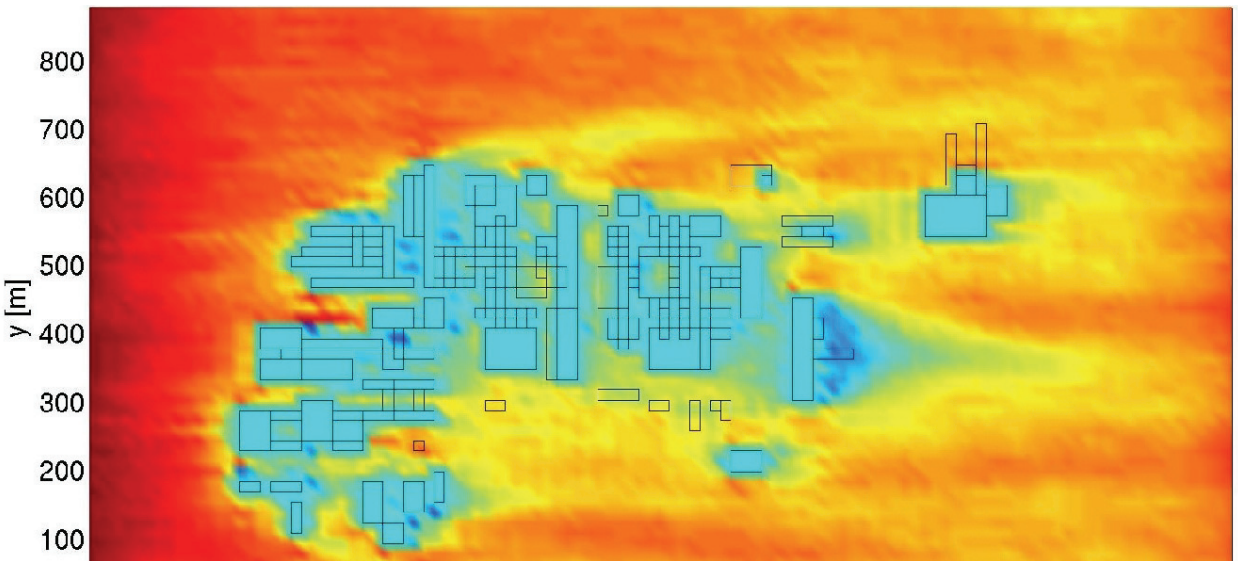

Figure 4: 3-D models of the EPFL campus increasing in detail from top to bottom

Disordered Network-Forming Materials

Prof. Alfredo Pasquarello

CSEA-ITP-SB, EPF Lausanne, Switzerland

The general goal persued within the project «Disordered Network-Forming Materials» consists in the computational study of atomic-scale phenomena in materials both from the structural and dynamical point of view. The aim is to complement experiment by providing a realistic description of the mechanisms occurring on the atomic and nanometer scale. This is achieved by accurately accounting for the interactions between atoms within a quantum mechanical description of the electronic structure, based on density functional theory. Currently, the research activity focuses on disordered network-forming materials materials and on oxide-semiconductor interfaces.

One of the research projects concerns the study of glassy materials. The main goal consists in developing methodologies for investigating the physical properties of disordered network-forming materials, such SiO_2, $GeSe_2$, B_2O_3, GeO_2, ZrO_2, etc., with the ultimate goal of unveiling their detailed atomic structure. We developed a new method to treat finite electric fields in periodic density functional calculations. The method is very promising for a series of investigations that involve electric fields. In particular, the finite field is very useful for the calculation of infrared and Raman spectra for systems of relatively large size (100 - 200 atoms). We now have a complete set of tools for studying the vibrational properties of disordered network-forming materials. Application to vitreous boron oxide illustrates the potential of the method: we were able to determine the fraction of boron atoms in boroxol rings from the experimental Raman spectrum. A similar application study to vitreous germania is currently under way. Other important results within this project concern the study of dielectric properties of Zr silicates and of the intermediate range order in chalcogenides.

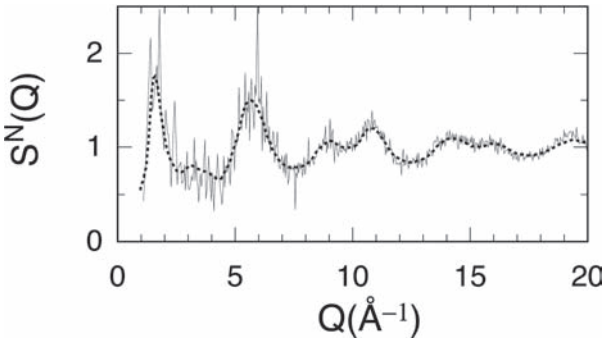

Figure 1: Calculated neutron structure factor of B_2O_3 compared to the corresponding experimental result.

The second major research project focuses on thin dielectric films on silicon. The goal of this project

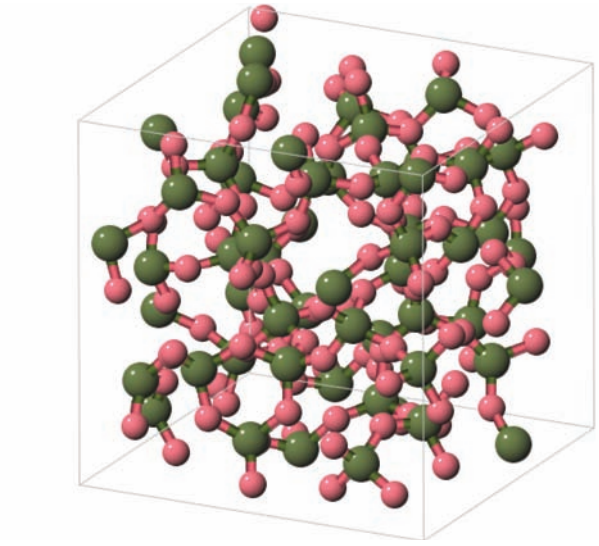

Figure 2: Atomistic model of vitreous germania.

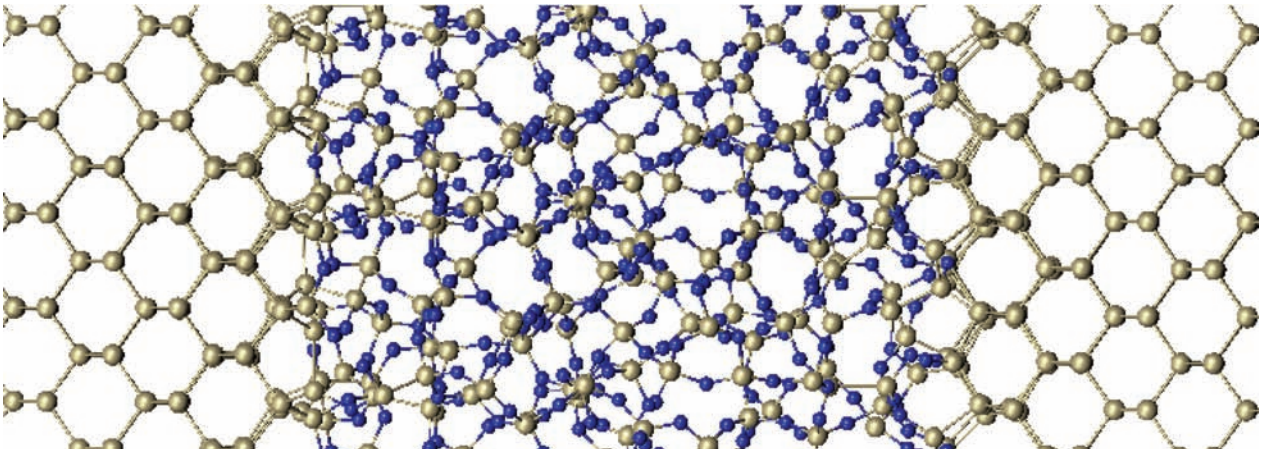

Figure 3 - Atomistic model of a Si(100)-SiO_2 superlattice.

consists in providing insight into the atomistic processes occurring at oxide-semiconductor interfaces, of relevance in nano-electronic device technology. We generated model structures of the Si(100)-SiO_2 interface which incorporate an extended list of atomic scale properties. In particular, we carried out ion scattering simulations on these models finding yields in excellent agreement with available experimental data. Using constrained ab initio molecular dynamics, we then used these model structures to investigate the reaction of the O_2 molecule at the interface. The reaction proceeds sequentially through the incorporation of the O_2 molecule in a Si-Si bond and the dissociation of the resulting network O_2 species. The oxidation reaction occurs nearly spontaneously and is exothermic, irrespective of the O_2 spin state or of the amount of excess negative charge available at the interface. Using these atomistic model structures, we also addressed the dielectric permittivity of ultrathin SiO_2 films on silicon, for oxide thicknesses up to 12 Å, finding that the permittivity significantly exceeds the bulk SiO_2 value, to the benefit of the scaling in the current nano-electronic technology. Other investigated topics concern the SiC-SiO_2 interface.

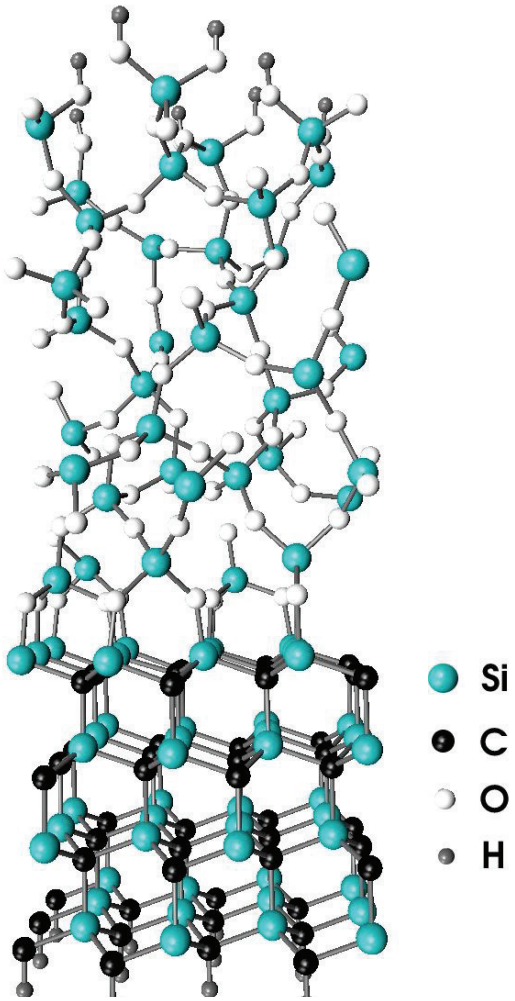

Figure 4 - Atomistic model structure of the SiC-SiO_2 interface.

Dr. Michel Posternak

with A. Läuchli, A. Gelle and Z. Sljivancanin

Institute of Theoretical Physics, SB ITP, EPF
Lausanne, Switzerland

Description

Our Large User Project is divided into the two following sub–topics: «Numerical Investigation of Strongly Correlated Systems», and «Substrate Effects on the Physical and Chemical Properties of Adsorbed Metal Clusters». Our major results during the period under consideration are:

Numerical Investigation of Strongly Correlated Systems

A. Läuchli (IRRMA–EPFL) A. Gelle (ITP–EPFL)

We are interested in the phase diagrams of spin systems with complex competing interactions: on one hand the antiferromagnetic two–body Heisenberg interation between nearest neighbor sites of a square lattice, and on the other hand four– or six–body interactions involving a square plaquette (or rectangle) of spins. Such interactions can be derived from first principles, or are introduced ad hoc in order to understand the process of vanishing antiferromagnetic order.

The first model is motivated by the recent interest in ring exchange interactions needed for an accurate modelling of LaCuO, the undoped parent compound of the high– superconductors. We determined the complete phase diagram of such a model, and novel and exciting phases have been found [1]. The most interesting one is a so called spin nematic phase, where the spin rotation symmetry is broken, but not in the conventional sense of magnetic long ranged order (<S>≠0). Here the symmetry breaking quantity is the spin current on a bond , c.f. Fig 1.

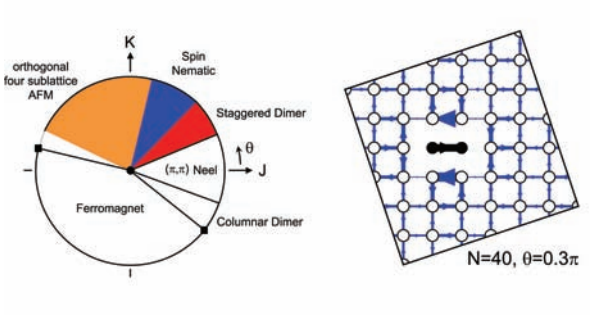

Figure 1: Left: Phase diagram of a cyclic ring exchange model on the square lattice, Ref [1]. Right: Correlation function of the spin currents on nearest neighbor bonds in the spin nematic phase.

The second model contains six–body interactions and has the very nice feature that the groundstate for a region of parameters is exactly known. The groundstate is fourfold degenerate and cristallizes in an “orthogonal” dimer state. The region between the antiferromagnetic and the exactly known states is rather complex and shows many competing instabilities. Work is in progress to characterize these phases more precisely [2].

Substrate Effects on the Physical and Chemical Properties of Adsorbed Metal Clusters

Z. Sljivananin (IRRMA–EPFL)

We apply density functional theory to study physical and chemical properties of oxide–supported metal nanoclusters. In particular we are interested in the structural and electronic properties of small

Ir clusters deposited on oxide substrates such as MgO, TiO, and γ–AlO. At the initial stage of this project, we are focused on the structural and magnetic properties of the gas–phase Ir (n≤6) clusters. Work is in progress.

Our reaserch activities in the field of oxide supported nanoclusters also include a collaboration with Prof. A. Pasquarello (ITP). We studied sequential adsorption of N molecules on Fe clusters supported by a MgO (100) surface [3]. For an increasing number of N atoms preadsorbed on the Fe nanocluster, we find that the binding energy of the molecule increases, and can become higher than that of its dissociation products. The electrostatic interaction is identified as a primary factor determining this distinct catalytic behaviour.

Catalytic properties of defected metal surfaces has been another field of research. Combining angle scanned X–ray photoelectron diffraction and first–principles calculations we studied enantiospecific adsorption of cysteine on a kinked gold surface [4]. We found different adsorption geometries and binding energies for D– and L–cysine on Au(17 11 9). This work is done in colaboration with the group of Prof. T. Greber (University of Zürich). Use of the computers at the CSCS is acknowledged in our recent work on the magnetic properties of the sodium pyroxene NaTiSiO compound [5].

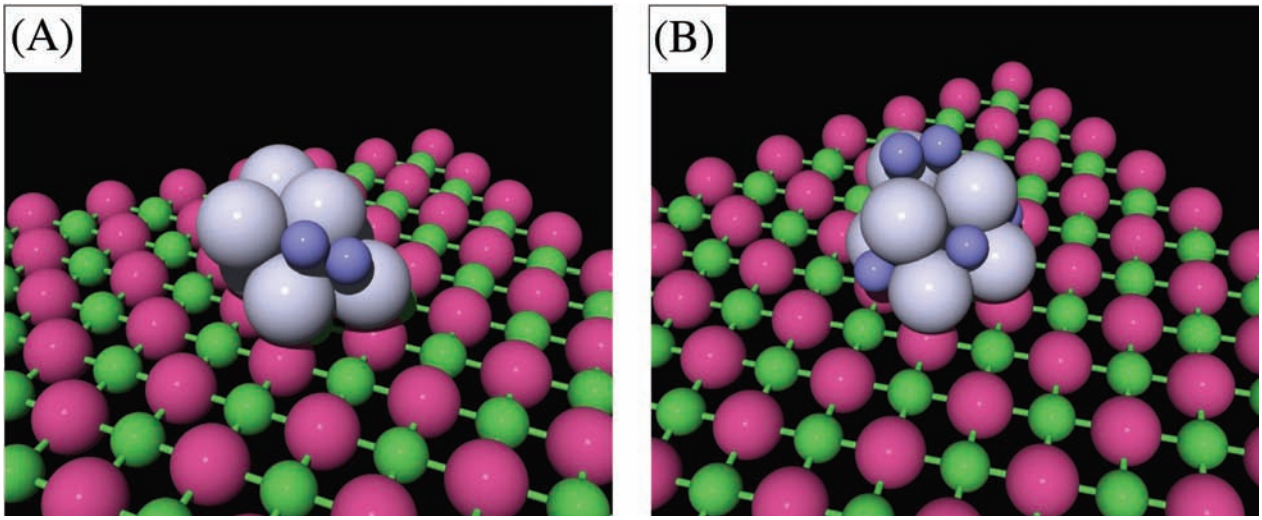

Figure 2: Side views of the adsorption geometries of the N molecule on a MgO (100) supported Fe cluster, without (A), and with four (B) preadsorbed N atoms. The adsorption energy of the molecule changes from 0.81 eV (no preadsorbed N atoms) to 1.25 eV (four preadsorbates).

References

[1] A. Läuchli, J.C. Domenge, C. Lhuillier, P. Sindzingre, and M. Troyer, Two Step Restoration of SU(2) Symmetry in a Frustrated Quantum Magnet, cond–mat/0412035, submitted to Phys. Rev. Lett.

[2] A. Gelle, A. Läuchli, B. Kumar, and F. Mila, to be submitted.

[3] Z.Sljivananin and A. Pasquarello, Phys. Rev. B 71, 081403(R) (2005).

[4] T. Greber, . ljivananin, R. Schillinger, J. Wider, and B. Hammer, submitted to Nature.

[5] Zoran S. Popovi, eljko V. ljivananin and Filip R. Vukajlovi, Phys. Rev. Lett. 93, 036401 (2004).

Modelling Weather and Climate on European and Alpine scales

Prof. Christoph Schär

with Bodo Ahrens, Erich Fischer, Christoph Frei, Olivier Fuhrer, Martin Hirschi, Cathy Hohenegger, Simon Jaun, Jan Kleinn, Michael Litschi, Daniel Lüthi, Christoph Schär, Reinhard Schiemann, Jürg Schmidli, Sonia Seneviratne, Mark Verbunt, Pier Luigi Vidale and André Walser

Institute for Atmospheric and Climate Science, ETH Zürich, Switzerland

Introduction

The research of our group concerns continental and Alpine-scale weather and climate. A broad continuum of temporal scales (from short-range weather forecasting to climate change) and horizontal resolutions (with horizontal grid spacing between 500 m to 50 km) is being considered. The integrating aspect of our research is our focus upon the water cycle and extreme events. Some of the challenges addressed are:

1. What are the key mechanisms behind natural climate variability and climate change? How does anthropogenic greenhouse gas forcing impact upon the European climate system, and how does it affect the character and frequency of extreme events such as floods and droughts?

2. What are the key dynamical and physical processes that control the generation of precipitation in regions of complex terrain? What numerical techniques should be used in the emerging high-resolution atmospheric models?

3. What is the predictability of extreme events in the Alpine region? How can we exploit numerical models to improve the short-term prediction of weather systems and their associated extreme events?

To address these issues we conduct a wide range of numerical experiments, from idealized simulations of atmospheric flow problems to realistic simulations of weather and climate. We are also investigating the numerical formulation of atmospheric prediction systems.

In our research we are using a hierarchy of numerical models: Regional climate processes are investigated with the help of two regional climate models (RCMs), namely the Climate High-Resolution Model (CHRM, running on the IBM SP4) and the Climate Lokal-Modell (CLM, running on the NEC SX-5). The dynamics of dry and moist atmospheric flows is explored using both idealized and real-case simulations integrated with non-hydrostatic high-resolution models such as LM and ARPS (both running on the NEC SX-5). The LM and CLM models share their dynamical core and many parameterizations with the aLMo model (the operational forecasting activities of MeteoSwiss). We are also exploiting a large weather and climate data archive (ERA-40) which is maintained in collaboration with other institutions at CSCS.

Regional climate studies

Research on climate aspects is dedicated to the study of natural and anthropogenic climate variations on seasonal to centennial time scales. This work involves conducting comprehensive RCM numerical simulations. The main thrust of our recent

work is dedicated towards better understanding and simulating the European summer climate, and towards assessing its sensitivity with respect to anthropogenic greenhouse gas forcing. Particular consideration is given to the role of continental-scale land-surface processes and their interactions with the water cycle. This work also includes detailed process and sensitivity studies, as well as extended validation against observational data sets.

The simulations conducted within our project are contributing towards the generation of European climate change scenarios. The generation of these scenarios is coordinated by several international projects (among them the EU PRUDENCE and ENSEMBLES) and overseen by the ntergovernmental Panel on Climate Change (IPCC). Our research is also coordinated with several other projects (among them the GCM project of Ohmura / Wild at ETH) in the framework of the Swiss NCCR Climate.

Results of our group have suggested that climate change in Europe might not merely be associated with a mean warming, but also lead to pronounced increases in interannual (year-to-year) variability (see Figure 1). Such changes would have important socio-economic consequences. Following publication of our study, our results have largely been confirmed by the work of several European modeling groups. However, there is still considerable uncertainty regarding the amplitude, geographical location and seasonal timing of the effect.

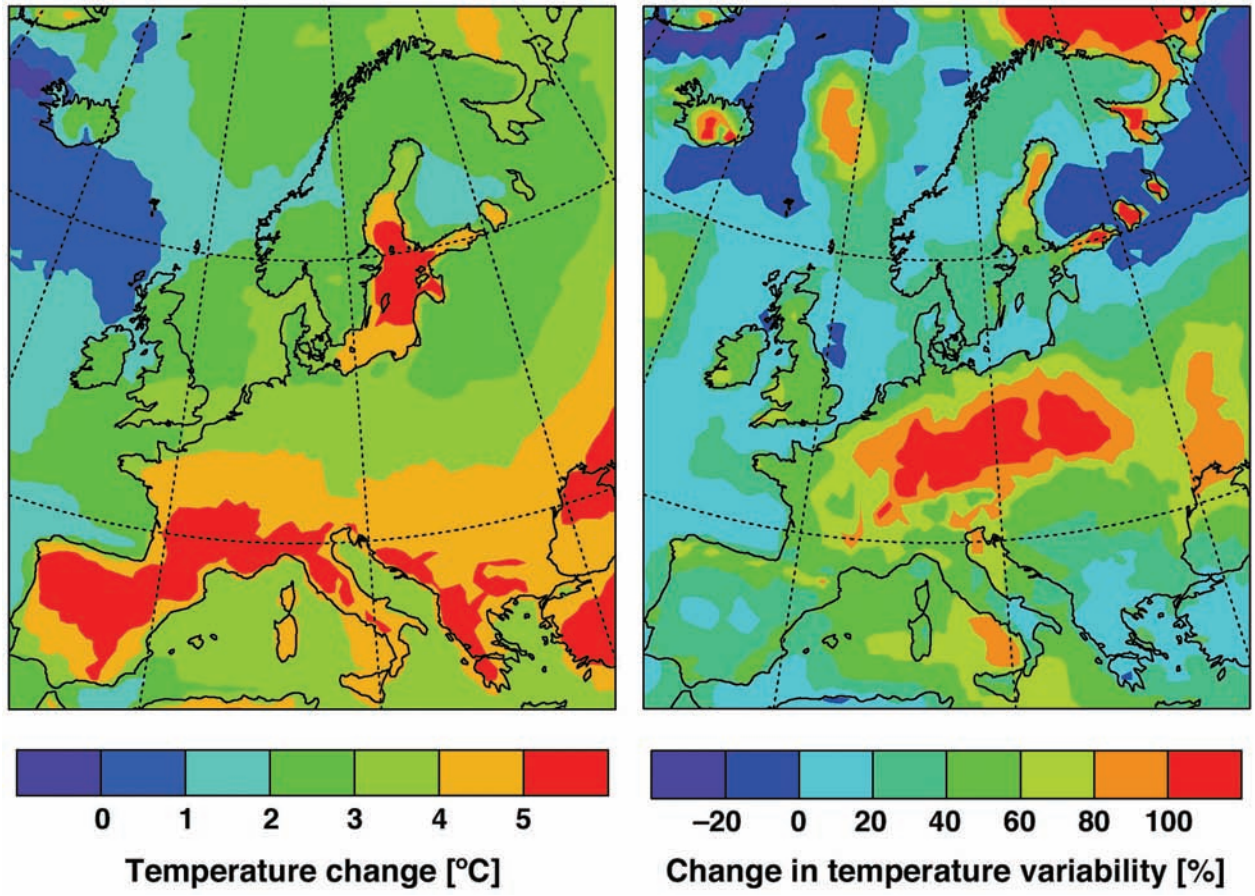

Figure1: Climate change scenarios for European summer temperatures (period 2071-2100) based on a regional climate model with a horizontal resolution of 56 km. The impact of climate change strongly depends on the region. In the Mediterranean, the changes are dominated by the mean warming (by around 5°C, see left-hand panel). In contrast, in Central and Eastern Europe there is a strong increase in year-to-year variability (by up to 100%, see right-hand panel). The combination of these two factors dramatically increases the likelihood of extreme summer heat waves. The simulations are conducted with a hydrostatic regional climate model (CHRM) and integrated over a total of 60 years with a time step of 5 minutes (Schär et al. 2004, Nature, 427, 332-336).

Idealized studies of Alpine flow systems

With the advent of atmospheric prediction models and with the rapid increase of computational power, there are promising prospects regarding research and operational applications of high-resolution atmospheric prediction systems. In particular, these models allow for the first time to explicitly resolve convective clouds and thunderstorms. These advances offer exciting avenues in quantitative precipitation and flood forecasting in regions of complex terrain. However, the formulation of high-resolution models, as well as their ability in representing convective clouds and mountain flow phenomena, is still largely unexplored.

Our group has thus started to systematically investigate some of the related key issues using idealized studies. Of particular interest to us is the flow of a conditionally unstable airstream over topography. In such a system, the release of latent heat due to the condensation of water vapor can fundamentally alter the character of the flow – from a laminar flow upstream to a moist turbulent and convective flow over the mountain. An example of an idealized study of this type is shown in Figure 2. It depicts a situation where the convection organizes such as to form streamwise oriented roles with a spacing of a few kilometers. Such role clouds are familiar from observations.

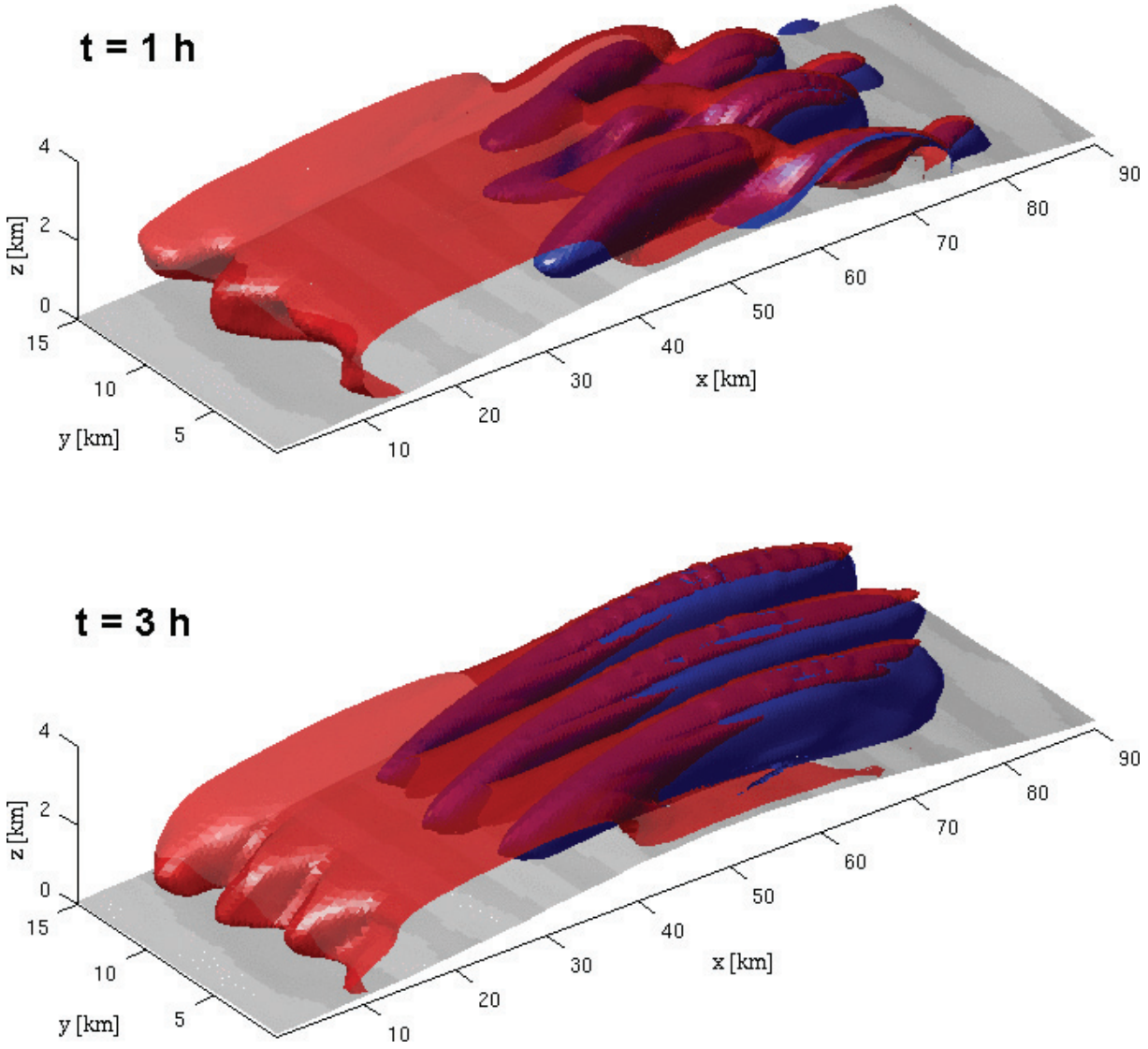

Figure 2: Two stages in the development of roll clouds in moist atmospheric flow over a two-dimensional topographic ridge. Roll clouds develop in response to moist convective activity as the flow impinges upon the ridge. The isosurfaces provide a three-dimensional view of cloud water (red isosurface at 0.1 g/kg) and rain water (blue isosurface at 0.01 g/kg). The formation of such banded structure can strongly affect the net precipitation rates associated with flow past topography. The simulations employ the non-hydrostatic ARPS model with a horizontal resolution of 500 m (Fuhrer and Schär, J. Atmos. Sci., submitted).

Our study demonstrates that these roles strongly affect the total precipitation amounts (by increasing it by up to a factor ~5) while their generation is highly sensitive to dynamical instabilities and small-amplitude perturbations.

Predictability and forecasting of extreme events

As the atmosphere is a chaotic dynamical system, there are intrinsic limits to our ability to predict its evolution. Even with a perfect numerical model, there are strict predictability limitations. It is thus essential to investigate such limitations, and to develop probabilistic (rather than deterministic) methods. The latter are derived using ensemble (or Monte Carlo) techniques, which in effect sample the possible evolution of the system. These methods have broadly been explored in medium-range synoptic-scale weather forecasting (with horizontal resolutions around 100 km), but are uncharted territory in the context of cloud-resolving models (with horizontal resolutions around 1 km). Our main objectives in this area are (i) to assess the predictability limitations associated with the moist convective dynamics in cloud-resolving

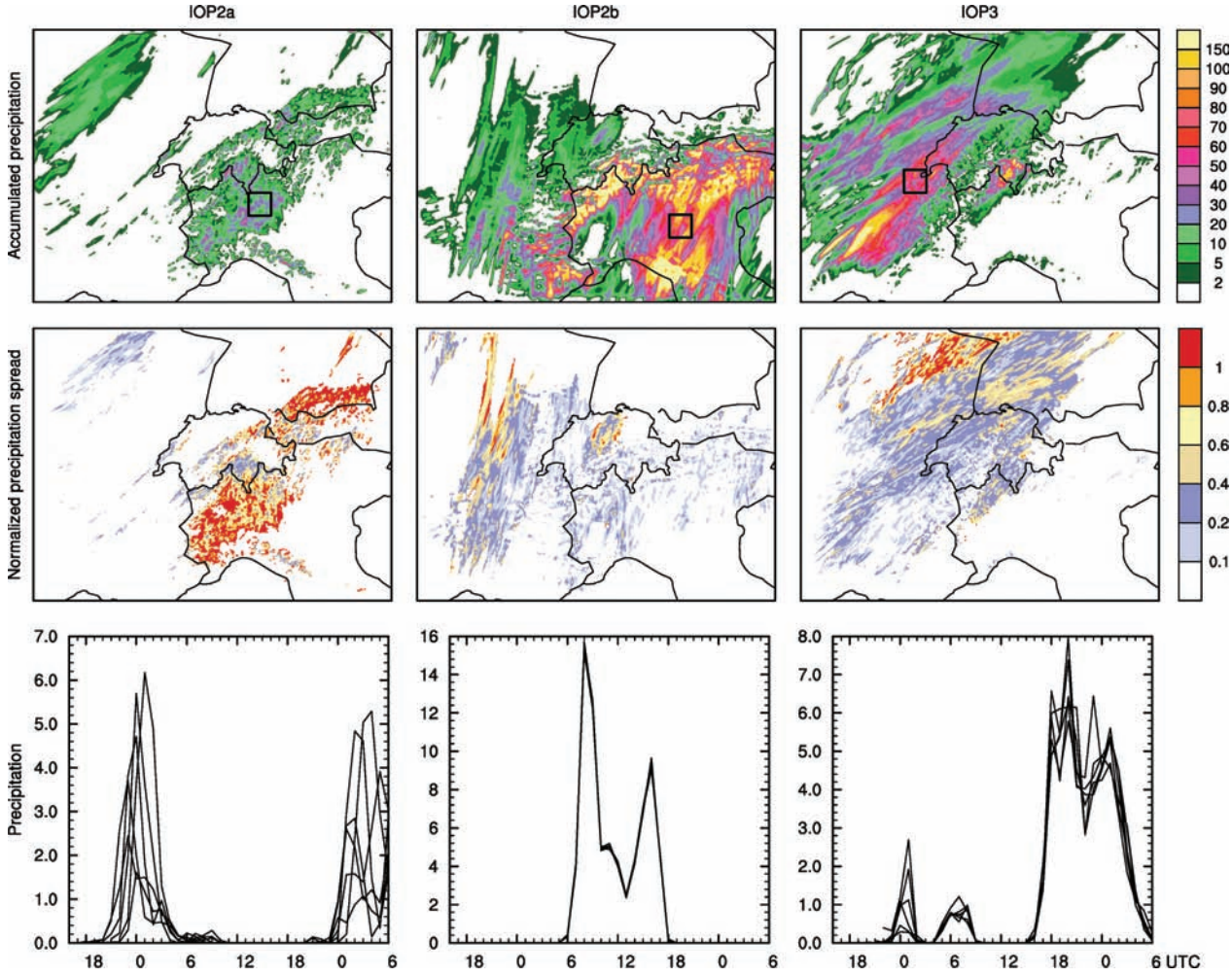

Figure 3: Predictability in three heavy precipitation events using cloud-resolving short-term forecast integrations. The cases are from the special observing period of the Mesoscale Alpine Programme which was conducted in the fall 1999: IOP2a (17-18 September 1999), IOP2b (20-21 September 1999), and IOP3 (25-26 September 1999). To assess the predictability of the events, ensemble simulations are conducted (with 6 simulations per case using slightly different initial conditions). The top panels show ensemble mean 36-h accumulated precipitation (mm, from 0 to 6 UTC). Peak precipitation amounts range from 50 to 150 mm. The middle panels show the normalized precipitation spread (standard deviation divided by mean precipitation amount). The bottom panels show time series of precipitation rates (in mm/h) for each of the simulations (averaged over the subdomains indicated on the top panels by a black rectangle). Despite similar weather patterns, the three cases show largely differing levels of predictability. The poorest predictability is seen in IOP2a, where the normalized spread is close to 1 and the different ensemble members show completely different precipitation rates. The best predictability is seen in IOP2b, where the 6 simulations essentially coincide. The simulations are conducted with a cloud-resolving version of the LM model, using a horizontal resolution of 2.2 km and a computational grid of 401x301x45 grid points. The time stepping employs a split-explicit technique using two time steps of 12 and 3s (Hohenegger et al., Mon. Wea. Rev., in press).

models, (ii) to explore ensemble methodologies that are suited for high-resolution quantitative precipitation forecasting, and (iii) to develop probabilistic methods for coupled atmospheric-hydrological flood forecasting systems.

The example in Figure 3 shows three events of heavy Alpine precipitation. Unlike classical deterministic forecasting, we try to derive not only an estimate of future precipitation (see top panels), but also an estimate of the intrinsic uncertainty (see middle panels). Such results firstly illustrate that there is apparently case-to-case variability of predictability. In some cases even convective precipitation appears well predictable, while in others there is huge uncertainty. Secondly, through a detailed analysis of the mechanisms promoting error growth and propagation in our system, it is found that there are fundamental differences between ensemble forecasting on synoptic and on cloud-resolving scales. In particular, non-linear effects become much more important at high resolution, questioning the use of singular-vector and four-dimensional variational data assimilation methods in cloud-resolving models.

Publications 2004-2005 (publications using HPC resources)

[1] Déqué M., D. Rowell, D. Lüthi, F. Giorgi, J. H. Christensen, B. Rockel, D. Jacob, E. Kjellstrom, M. de Castro and B. van den Hurk, 2006: An intercomparison of regional climate models for Europe: assessing uncertainties in model projections. Climate Dyn., submitted

[2] Déqué, M., R. G. Jones, M. Wild, F. Giorgi, J. H. Christensen, D. C. Hassell, P. L. Vidale, B. Röckel, D. Jacob, E. Kjellström, M. de Castro, F. Kucharski and B. van den Hurk, 2005a: Global high resolution versus Limited Area Model scenarios over Europe: results from the PRUDENCE project. Climate Dyn., 25, 653-670

[3] Flamant C., E. Richard, C. Schär, R. Rotunno, L. Nance, M. Sprenger, and R. Benoit 2004: The wake south of the Alps: Dynamics and structure of the lee-side flow and secondary potential vorticity banners. Quart. J. Roy. Meteorol. Soc., 130, 1275-1303

[4] Frei, C., R. Schöll, J. Schmidli, S. Fukutome and P.L. Vidale, 2006: Future change of precipitation extremes in Europe: An intercomparison of scenarios from regional climate models. J. Geophys. Res., submitted

[5] Fuhrer, O. and C. Schär, 2005: Embedded cellular convection in moist flow past topography. J. Atmos. Sci., 62, 2810-2828

[6] Fuhrer, O. and C. Schär, 2006. Triggering and Organization of Banded Convection in Moist Orographic Flows. J. Atmos. Sci., submitted

[7] Graham, L.P., S. Hagemann, S. Jaun and M. Beniston, 2006: On interpreting hydrological change from regional climate models. Clim. Change, submitted

[8] Hagemann, S., R. Jones, O.B. Christensen, M. Déqué, D. Jacob, Machenhauer, B. and P.L. Vidale, 2004: Evaluation of water and energy budgets in regional climate models applied over Europe. Climate Dyn., 23, 547-567

[9] Hirschi, M., S.I. Seneviratne and C. Schär, 2006: Seasonal variations in terrestrial water storage for major mid-latitude river basins. J. Hydrometeorol., 7, 39-60

[10] Hohenegger, C. and P.L. Vidale, 2005: Sensitivity of the European Climate to Aerosol Forcing as simulated with a Regional Climate Model, J. Geophys. Res. - Atmos., 110, D06201

[11] Hohenegger C., D. Lüthi and C. Schär, 2006: Predictability mysteries in cloud-resolving models. Mon. Wea. Rev., in press

[12] Jacob, D., L. Bärring, O.B. Christensen, J.H. Christensen, M. de Castro, M. Déqué, F. Giorgi, S. Hagemann, M. Hirschi, R. Jones, E. Kjellström, G. Lenderink, B, Rockel, E. Sánchez, C. Schär, S.I. Seneviratne, S. Somot, A. van Ulden, B. van den Hurk, 2006: An inter-comparison of regional climate models for Europe: Design of the experiments and model performance. Climatic Change, submitted

[13] Kjellström, E., L. Bärring, D. Jacob, R. Jones, G. Lenderink, and C. Schär, 2006: Modelling daily temperature extremes: Recent and future changes over Europe. Climatic Change, in press

[14] Kleinn, J. C. Frei, J. Gurtz, D. Lüthi, P.L. Vidale, and C. Schär, 2005: Hydrologic Simulations in the Rhine Basin driven by a Regional Climate Model, J. Geophys. Res. – Atmos., 110, D04102

[15] Raible, C.C., C. Casty, J. Luterbacher, A. Pauling, J. Esper, D. Frank, U. Büntgens, A. C. Roesch, M. Wild, P. Tschuck, P.-L. Vidale, C. Schär, and H. Wanner, 2006: Climate variability - observations, reconstructions and model simulations, Clim. Change, accepted for publication.

[16] Schär, C., P.L. Vidale, D. Lüthi, C. Frei, C. Häberli, M.A. Liniger and C. Appenzeller, 2004: The role of increasing temperature variability for European summer heat waves. Nature, 427, 332-336

[17] Schär, C. and G. Jendritzky, 2004: Hot news from summer 2003. Nature, 432, 559-560

[18] Schmidli J., C. Frei, and P.L. Vidale 2006: Downscaling from GCM precipitation: A benchmark for dynamical and statistical downscaling methods. Int. J. Climatol., accepted

[19] Schmidli, J., C. Goodess, C. Frei, M. Haylock, Y. Hundecha, J. Ribalaygua and T. Schmith, 2006: Statistical and dynamical downscaling of precipitation statistics: Evaluation, intercomparison and scenarios of the European Alps. J. Geophys. Res., submitted

[20] Seneviratne, S. I., P. Viterbo, D. Lüthi and C. Schär, 2004: Inferring changes in terrestrial water storage using ERA-40 reanalysis data: The Mississippi River basin. J. Climate, 17, 2039-2057

[21] Van den Hurk, B., M. Hirschi, C. Schär, G. Lenderink, E. van Meijgaard, A. van Ulden, B. Röckel, S. Hagemann, P. Graham, E. Kjellström and R. Jones, 2005: Soil control on runoff response to climate change in regional climate model simulations. J. Climate, 18(1), 3536–3551

[22] Verbunt, M., A. Walser, J. Gurtz, A. Montani and C. Schär, 2006: Probabilistic flood forecasting with a limited-area ensemble prediction system. J. Hydrometeorol., in press

[23] Vidale P.L., D. Lüthi, R. Wegmann, C. Schär, 2006: Variability of European climate in a heterogeneous multi-model ensemble. Clim. Change, in press

[24] Walser, A., and C. Schär, 2004: Convection-resolving Precipitation Forecasting and its Predictability in Alpine River Catchments. J. Hydrol, 288, 57-73

[25] Walser, A., D. Lüthi and C. Schär, 2004: Predictability of Precipitation in a Cloud-Resolving Model. Mon. Wea. Rev., 132 (2), 560-577

Reliability and degradation modelling of ultrathin dielectrics

Dr. Urs Sennhauser

with Matteo Farnesi Camellone, Joachim Reiner and Louis Schlapbach

Swiss Federal Laboratories for Materials Testing and Research (EMPA), Duebendorf, Switzerland

The essential limitations on gate insulators are related to the exponentially increasing gate current as the thickness of the oxide is reduced, and the effect of this current on both the functionality and reliability of devices and circuits. The leakage current is controlled by quantum mechanical tunneling, either by Fowler-Nordheim tunneling at high gate voltage or by direct tunneling at biases of less than about three Volts but with ultra thin (1-3 nm) gate oxides. The gate leakage current causes increased power consumption and may effect device and circuit functionality and reliability. This imposes a practical limit on oxide thickness. The rate of defect generation in the oxide is proportional to the current density flowing through it, and therefore the reliability margin for gate-oxide breakdown has been drastically reduced as a consequence of device scaling. When the concentration of defects reaches a critical value, the system is irreversibly damaged and breakdown occurs.

The idea of damage build-up to a critical value has been a key insight that led to a predictive model of oxide reliability. However this concept does not depend in any way on the physics of defect generation. Understanding the microscopic origin of gate oxide degradation may guide process modifications and lead to devices that can reliably be extended to smaller structures.

Quantum mechanical models (ab-initio calculations) can be used to simulate the formation of atomic defects of a realistic material struture. Density Functional Theory [1] has been used to model and study the properties of alpha quartz and amorphous silica. A system of alpha quartz has been relaxed using plane wave density functional theory. We used a norm conserving pseudopotential (Martin Troullier) for oxygen and a norm conserving (Goedecker type) for silicon and the Local Density Approximation to describe the exchange correlation energy. We found the optimized lattice constants and atomic positions of the silicon and oxygen atoms within the supercell. A bulk of amorphous silica has been generated using a combination of classical and ab-initio molecular dynamics starting from a cubic unit cell, matching the experimental density and following the generation procedure of [2]. The interaction

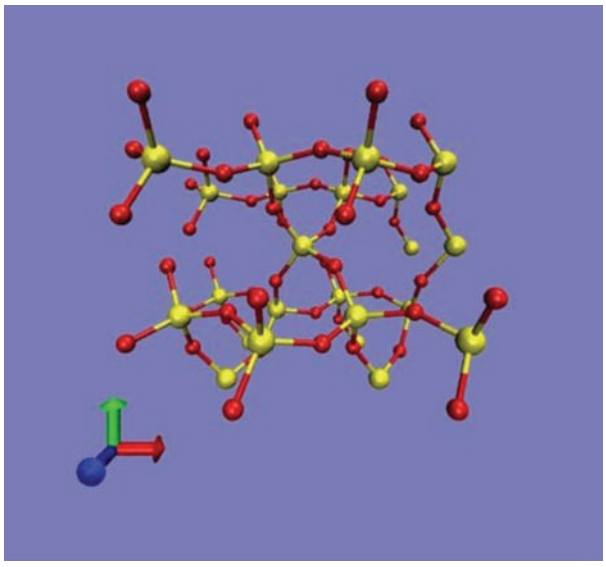

Figure 1: α-quartz supercell

between silicon and oxygen atoms has been described by a potential that has often been used recently in the study of the properties of amorphous silica. The potential energy functions are completely empirical and the same interaction is used for bonded and non-bonded terms. This is the so called BKS potential [3] that has been developed by van Beest, Kramer and van Santen by means of ab initio calculations. Although it is a simple pair potential, it has been shown to reproduce very well static and dynamic properties of amorphous silica. The system so generated has been relaxed by a Car-Parrinello quantum mechanical simulated annealing in order to reach the zero Kelvin temperature. In order to check the structure of the system so generated, we have analyzed several structural characteristics of the sample and compared them to experiments. These structural characteristics are radial distributions functions and bond angle distributions.

In both calculations we applied periodic boundary condition in space and we performed the calculations at the Gamma point only in the reciprocal space. In the presence of defects it is still possible to take advantage of the Bloch theorem. Periodic boundary conditions are applied to a supercell so that the supercell is reproduced through space.

We will investigate the nature of such defects and we are going to perform calculations on oxides in an external electric field. In particular we will investigate pre-existing defects related to hydrogen under the influence of an external electric field, because degradation of MOS structures has been attributed to hydrogen diffusing to the oxide-semiconductor interface [4], [5]. In this model, hydrogen is released from the metal oxide interface by hot electrons and diffuses to the oxide-semiconductor interface, where it depassivates hydrogenated Pb centers, i.e., silicon-dangling-bond defects.

Thus an understanding of the hydrogen chemistry in gate oxides is of great importance for the downscaling of semiconductor devices. The theoretical calculations will be compared with experimental results.

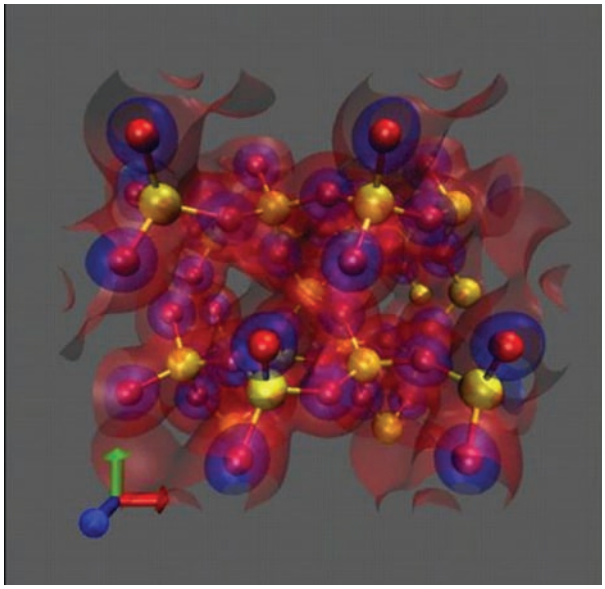

Figure 2: Electron density plot

References

[1] P. Hohenberg and W. Kohn Phys.Rev.B 136, 864-871 , 1964.

[2] M. Benoit et al. Eur.Phys.J.B 13, 631-636, 2000.

[3] B.W.H. van Beest et al. Phys.Rev.Lett. 64, 1955, 1990.

[4] D.J. Maria et al. J.Appl.Phys.73, 3367, 1993.

[5] D.L. Griscom J.Electron.Mater.21, 762, 1990.

Molecular Dynamics Computer Simulation of Nanostructured Materials

Prof. Helena Van Swygenhoven and Dr. Peter M. Derlet

ASQ/NUM-PSI, PSI-Villigen, Switzerland

Outline of 2004-2005 large user projects

Large scale atomistic simulations are used to study sizes effects in the mechanical properties of nanostructured metals. Computer simulations have revealed different possible deformation mechanisms such as grain boundary sliding and dislocations emitted and absorbed at grain boundaries – plastic deformation mechanisms that do not build up a residual dislocation network. The strength of the approach developed at PSI has been to employ such simulations as a complementary tool for interpretation of experimental results with the motivation to develop synergetic simulation tools that allow us to now simulate such experiments. This provides a context for the development of new tailor made nc structures that are more closely related to experimental obtainable structures.

By exploiting the more powerful IBM/SP5 processors, in the framework of our previous CSCS large-user-project, we have investigated the structural and mechanical properties of nanocrystalline materials using molecular dynamics simulations with up to 5 million atoms on the 32 processor queue. These CSCS simulations have contributed, in part, to our overall research program resulting in a number of publications [1-9]. This work has culminated in the publication of an article in Nature materials [5] which demonstrates that the observed slip phenomena can be understood in terms of the generalised planar defect curves in which, both the stable and unstable stacking fault energies play the crucial role in determining whether or not full or partial dislocations are seen within the simulation time. Following a Peierls model for dislocation nucleation, it is the unstable stacking fault energy which forms the energy barrier for the nucleation of the leading partial and it is the difference between the stable and unstable stacking fault energies that forms the energy barrier for the nucleation of the trailing partial. This explains why simulations spanning only very short time intervals reveal full dislocation activity for Al and extended partial activity for both Ni and Cu. Quantitatively the nucleation rates will also depend on the applied and internal stresses, GB structure, and the stress field of the already nucleated leading partial. Further aspects of this work concerning twinning and the nature of full dislocations in nc materials have also been done (see refs [3,4,7]).

During 2005 work has proceeded on three fronts: 1) studying the atomic scale mechanism of nucleation, propagation and absorption of full dislocations in Al, 2) development of numerical algorithms and associated simulations of nanocrystalline structures containing user specified missorientation interface topologies. 3) Developing synergetic simulation tools for simulation of experimental measurement procedures.

Dislocation lifetime: It is not yet entirely clear what is the role of GB structure in the process of dislocation nucleation, propagation and eventual absorption. Past work by us has demonstrated that under a constant tensile load a significant amount of discrete atomic activity occurs within the GB either via uncorrelated shuffling and stress assisted free volume migration [10] and that this acts as a pre- and post-cursor for actual nucleation [11,12]. The free volume associated with such nucleation is often emitted or absorbed in a neighboring triple junction. These observations strongly suggest that GB structure plays a crucial role.

Figure 1 displays the life time of a full dislocation in nc-Al and one can see that the full dislocation which exists as a leading and trailing partial dislo-

cation connected by a stacking fault (indicated by the red colored atoms) interacts strongly with a localized stress anomaly which subsequently is removed upon propagation of the dislocation across the entire grain. Such simulations were performed at a time resolution of 1psec with detailed structural analysis being performed for a number of interesting configurations. With the ability now to visualize local stress within the GB it now becomes possible to perform a temporal analysis in terms of local structure, energetics, and stress to observe in more detail this dislocation nucleation process. Preliminary work has already shown that stress plays a fundamentally important role in the life time of a dislocation within a nano-sized grain [3]. Recently all these local visualization algorithms have been fully integrated into our molecular dynamics code (moldyPSI) and specialized deformation simulations have been done where local structural, energy and stress analyses is performed every 250 femtoseconds of physical time. By studying the lifetime of selected dislocations we have found that the grain boundary, in terms of ledges and regions of misfit, control the nature of where and how dislocations nucleate, propagate and absorb suggesting no obvious well defined

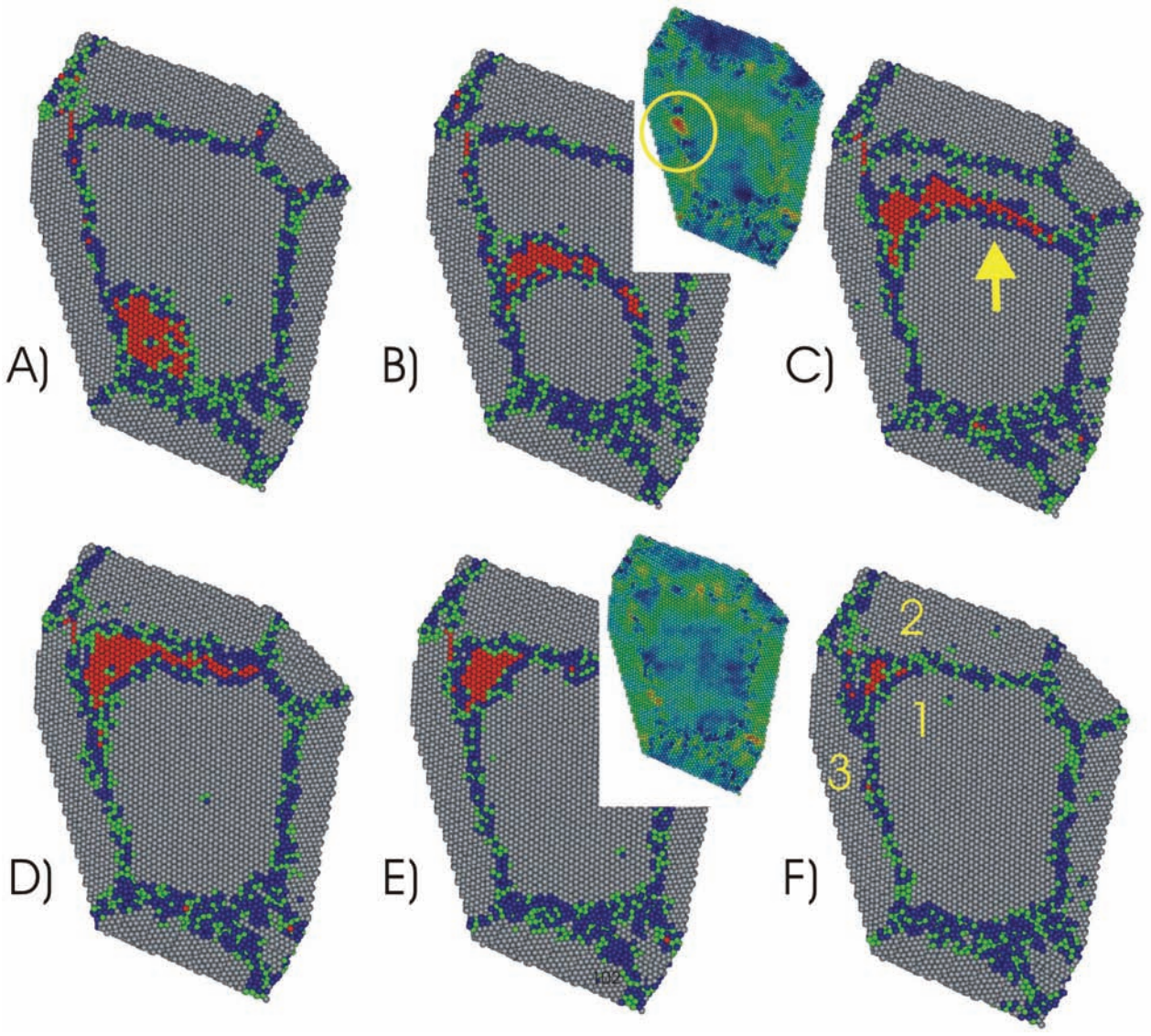

Figure 1: Full dislocation in nc-Al nucleated near a triple junction: a) The first leading partial has nucleated by 92 psecs, b) The trailing partial has nucleated forming a full dislocation by 94 psecs, c) which then propagates through the grain at 96 psecs. d) at 98 psecs, the leading partial is absorbed and e) at 100 psecs the trailing partial is then also absorbed, f) leaving a small residual stacking fault close to a triple junction that still exists at 110 psecs. In b) and e) the maximum resolved shear stress distribution is shown, indicating a shear anomaly in the GB that hinders the motion of the full dislocation through the grain, which is removed when the dislocation finally passes by (figure taken from ref [3]).

mean length scale dependence that can be associated with the activation processes associated with the lifetime of the dislocation. Moreover it becomes clear that dislocation propagation and absorption can play as an important role as dislocation nucleation and that this must be taken into account in any continuum model for the rate controlling mechanism of dislocation activity for a nanocrystalline material [13,14].

Realistic grain boundary network structures: Up until now, molecular dynamics deformation simulations of nc metals have been usually performed for a relatively small number of grains using the Voronoi construction and random grain orientations. We have developed a method using a combined Voronoi/Delaunay technique for geometrically constructing samples for atomistic simulations where the character of selected grain boundaries can be manipulated in order to produce a grain boundary network of a specific GB character distribution such as special symmetric low angle boundaries, carefully selected Coincidence Site Lattice (CSL) boundaries, and Sigma boundaries. Planar defects within grains are also known to affect strongly the experimental deformation properties of nc systems and the option of including such defect structures in the computer generated samples is now also included.

Using the Voronoi/Delaunay technique we constructed a series of samples containing clusters of grains with given configurations of CSL, low-angle tilt, and general high-angle boundaries and undertook a series large-scale MD simulations to study the influence of such GB structures on the nanocrystalline system's mechanical properties [15]. We find that the clusters in the low-angle samples accommodate deformation by rearrangement of the lattice dislocation network that constitutes the misfit of the low-angle GBs of the cluster. For the case of the random sample the clusters show high levels of atomic shuffling leading to GB sliding. However, in the CSL sample, the potential for strain accommodation is restricted by the high stability of the CSL boundaries. Consequently, the higher rate of plastic deformation in the low-angle and random sample clusters relative to the CSL sample clusters can be explained by their higher potential for strain accommodation. Although we see some dislocation activity in the samples in the form of nucleation of partials from the GBs, this does not become a major deformation mechanism due to the small grain size. Encouraged by the present results a logical next step is to perform simulations on even larger samples with larger grain sizes. This will then allow us to specifically investigate the influence of GB character on the nucleation, propagation and absorption of partial dislocations in nc 3D GB networks. These simulations are currently being performed on the IBM/SP5 system.

Synergetic simulation tools: To fully characterize the resulting GB and planar defect structures many different criteria are used. For example a medium-range-order analysis allowing the determination of a local crystallinity class and also local stress at the scale of the GB. Such atomic-scale visualization simply can not be obtained via experimental methods and this is one of the strong virtues of simulation, which can be exploited further by the simulation of experimental characterisation techniques such as the various spectroscopies involving photons, neutrons, phonons and positrons. Moreover with the combined knowledge gained from the static structural classification of the GB and GB network, the simulation of experimental probes can result in a much more fundamental understanding of how and to what extent these spectroscopies probe the nc GB structure.

We have recently developed new software that allows the simulation of a complete x-ray diffraction experiment using our multi-million atom computer generated nc samples [1]. Historically the use of x-ray diffraction techniques has played a central role in the microstructural characterization of ex-

perimental nc materials and being able to generate similar simulated x-ray spectra provides a systematic approach to directly compare simulation to experimental. Figure 2 displays simulated x-ray spectra for two computer generated nc structures, one containing perfect fcc grains and the other containing fcc grains with twin faults transecting the entire grains – see inset of figure which show twin fault atoms colored in red. In the x-ray spectra we see a clear difference in integrated peak heights (and also peak widths) between the two samples that can be explained via a Warren correction for the presence of twin faults.

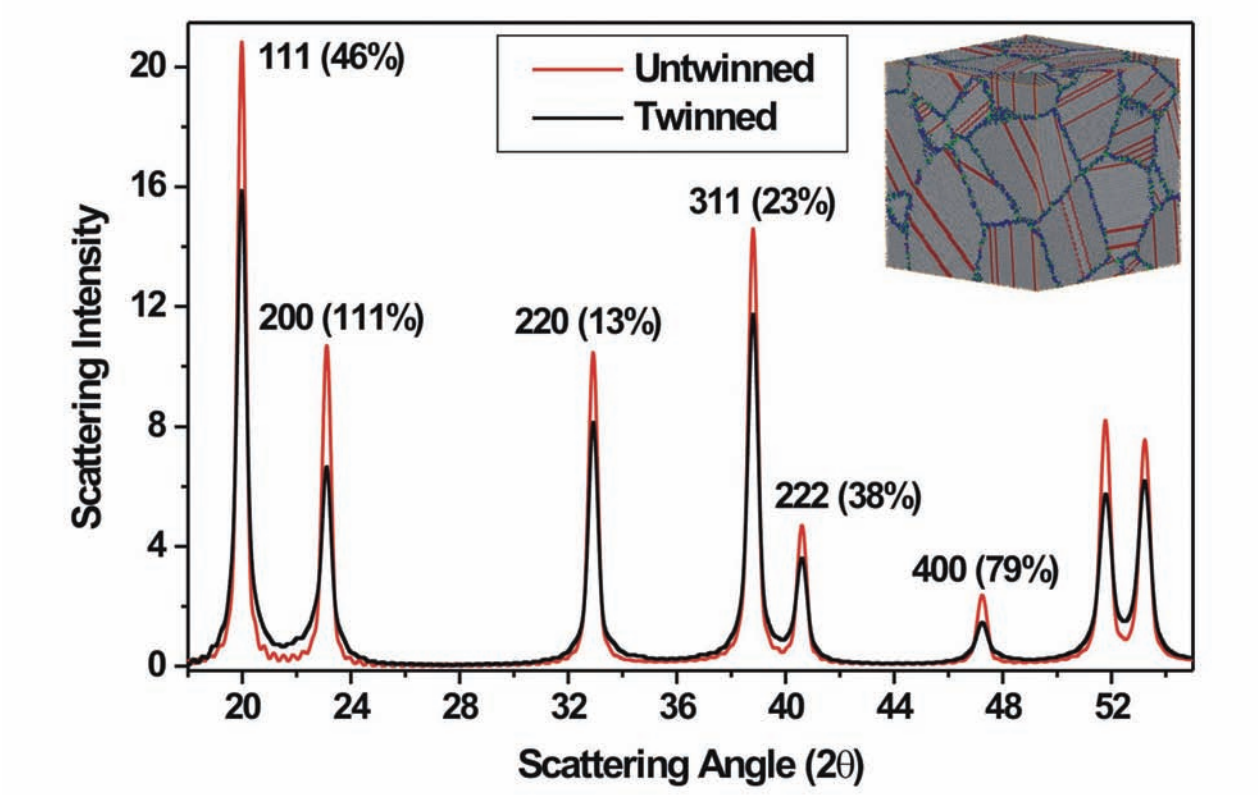

Figure 2: Simulated x-ray diffraction spectra of two computer generated samples: one containing twins and one not.The displayed percentages indicate the relative increase in peak height.

References

[1] P. M. Derlet, S. Van Petegem and H. Van Swygenhoven, “Calculation of x-ray spectra fro nanorystalline materials”, Phys. Rev. B. 71, 024114 (2005).

[2] H. Van Swygenhoven, Z. Budrovic, P. M. Derlet, A. G. Frøseth and S. Van Petegem, “In-situ diffraction profile analysis during tensile deformation motivated by molecular dynamics”, Mat. Sci. Eng. A. 400-401, 329 (2005).

[3] A. G. Frøseth, P. M. Derlet and H. Van Swygenhoven, “Dislocations emitted from nanocrystalline grain boundaries: nucleation and splitting distance”, Acta Mater. 52 5863 (2004).

[4] A. G. Frøseth, P. M. Derlet and H. Van Swygenhoven, “The Influence of grown-in twin boundaries on the dislocation mechanisms in nc- Al, Ni, and Cu”, App. Phys. Lett. 85, 5863 (2004).

[5] H. Van Swygenhoven, P. M. Derlet and A. G. Frøseth, “Nanocrystalline metals: stacking fault energies and slip”, Nature Mater. 3, 399 (2004).

[6] A. Hasnaoui, P. M. Derlet and H. Van Swygenhoven, “Interaction between dislocations and grain boundaries during nanoindentation of nanocrystalline Au – Molecular Dynamics simulations”, Acta Mater. 52, 2251 (2004).

[7] A. G. Frøseth, P. M. Derlet and H. Van Swygenhoven, “The influence of twins on the mechanical properties of nc-Al”, Acta Mater. 52, 2259 (2004)

[8] Z. Budrovic, H. Van Swygenhoven, P. M. Derlet, S. Van Petegem and B. Schmidt, “Reversible peak broadening during in-situ deformation of nanocrystalline Ni”, Science 304, 273 (2004).

[9] P. M. Derlet and H. Van Swygenhoven, “High-Frequency Vibrational Properties of Metallic Nanocrystalline Grain Boundaries”, Phys. Rev. Lett. 92, 035505 (2004).

[10] H. Van Swygenhoven and P. M. Derlet, “Grain Boundary Sliding in Nanocrystalline Fcc Metals”, Phys. Rev. B 64 224105 (2001)

[11] H. Van Swygenhoven, P.M. Derlet and A. Hasnaoui, “An atomic mechanism for dislocation emission from nanosized grain boundaries”, Phys. Rev. B. 66, 024101 (2002)

[12] P.M. Derlet, H. Van Swygenhoven and A. Hasnaoui, “Atomistic simulation of dislocation emission in nanosized grain boundaries”, Phil. Mag. 83, 3569 (2003).

[13] A. G. Frøseth, P. M. Derlet, H. Van Swygenhoven, “Non-coherent twin boundaries as dislocation sources in nanocrystalline Al”, Scripta Mater., submitted (2005).

[14] H. Van Swygenhoven, P. M. Derlet and A. G. Frøseth, “The life and death of a dislocation in an nanocrystalline fcc metal”. Acta Mater., in preparation (2005).

[15] A. G. Frøseth, H. Van Swygenhoven, P. M. Derlet, “Developing realistic grain boundary networks for use in molecular dynamics simulations”, Acta Mater., in press (2005).

Modelling and Reconstruction of North Atlantic Climate System Variability (MONALISA-2)

Prof. Thomas F. Stocker

with C.C. Raible, M. Yoshimori, and M. Renold

Climate and Environmental Physics, Physics Institute, University of Berne, Switzerland

Description

MONALISA-2 is one of the projects within the framework of National Centre of Competence in Climate Research (NCCR-Climate), which has the aim to improve our understanding in natural climate variability on decadal to centenial time scales in the past with a focus in the North Atlantic sector. Climate reconstructions with proxies, e.g. tree rings, ice cores, and historical documentary data provide estimates of the climate variability of the past millennium [1]. To investigate the underlying mechanisms relevant for the past 500 years, we have conducted an ensemble of climate simulations forced by volcanic eruptions, solar variations and greenhouse gas concentrations. These experiments have been carried out using the comprehensive climate model CCSM3 (Community Climate System Model), from NCAR (National Center of Atmospheric Research, Boulder, CO, USA). In addition, we performed sensitivity experiments which permit the investigation of associated processes between ocean, land, atmosphere and sea ice under different climate conditions and which allow us to detect thresholds and variability changes in the climate of the Atlantic region.

Achievements

One focus of the project was the investigation of the response of the climate system to an external volcanic and solar forcing during the so-called Maunder Minimum (MM, AD 1640-1715). This period is known as the time without solar spots and a significant reduction of solar activity. Regional height-resolution proxies climate reconstructions from Europe as well as other proxies from elsewhere all over the world show that the MM was a distinct cold period. An ensemble of 6 volcanic and solar forced transient runs and a control run for perpetual 1640 conditions have been carried out and compared with proxy data. The importance of external forced and internally-generated variability has been examined in order to understand the role of solar and volcanic influence to the climate. It was found that internal variability can mask the cooling signal in some region such as Greenland, Alaska and the northern part of Europe [6]. However, volcanic eruptions simulated in the ensemble runs shows a clear response of the winter NAO index (North Atlantic Oscillation). Estimating an ensemble of volcanic eruptions out of the simulated MM period a positive NAO-like pattern response was found which exhibits a warming in the northern Europe and northwestern America and a cooling in the Mediterranean and northern Africa. It has been suggested that the positive response of a volcanic eruption goes along with tropical stratospheric warming that causes a larger meridional temperature gradient, which again is probably responsible for a dynamical feedback. Due to the experimental setup the stratospheric forcing is missing and therefore this mechanisms does not work in our simulations. We found that the tropospheric forcing alone can produce a positive NAO index.

It was also demonstrated that the significant spread of ensemble members even on multi-decadal time scales is possible and therefore an important implication by comparison between modeled climate and instrumental data is given: on local scales this effect is increased due to a weaker externally-forced signal level and therefore it is an important issue by searching suitable proxies and site in order to reconstruct a solid proxy data set.

In another study we analyzed the hydrological changes between the MM ensemble experiment and a perpetual AD 1990 and AD 1640 conditions experiment to investigate the moisture transport and circulation changes between the different climate conditions [7]. The freshening of the western tropical Pacific compared with the colder condition during the MM, as indicated by proxy evidence, could be explained by an increased zonal moisture transport via trade winds. This effect is mainly a result of increase atmospheric water vapor content in the warmer present climate. The meridional vapor transport is generally weaker than the zonal vapor transport, particularly in the tropics during the MM period.

Another focus of our project was directed to a artificial freshwater discharge experiment. There is strong evidence in proxy records that so-called Dansgaard-Oeschger (D-O) events are associated with a substantial change in the meridional heat transport to higher latitudes in the Atlantic sector. Weakening of the heat transport has not only a strong impact on the climate in high latitudes, but also in the tropics. In a sensitivity study, we applied an artificial freshwater pulse of 3 different strengths into Northern Atlantic, which causes a strong reduction of the North Atlantic meridional

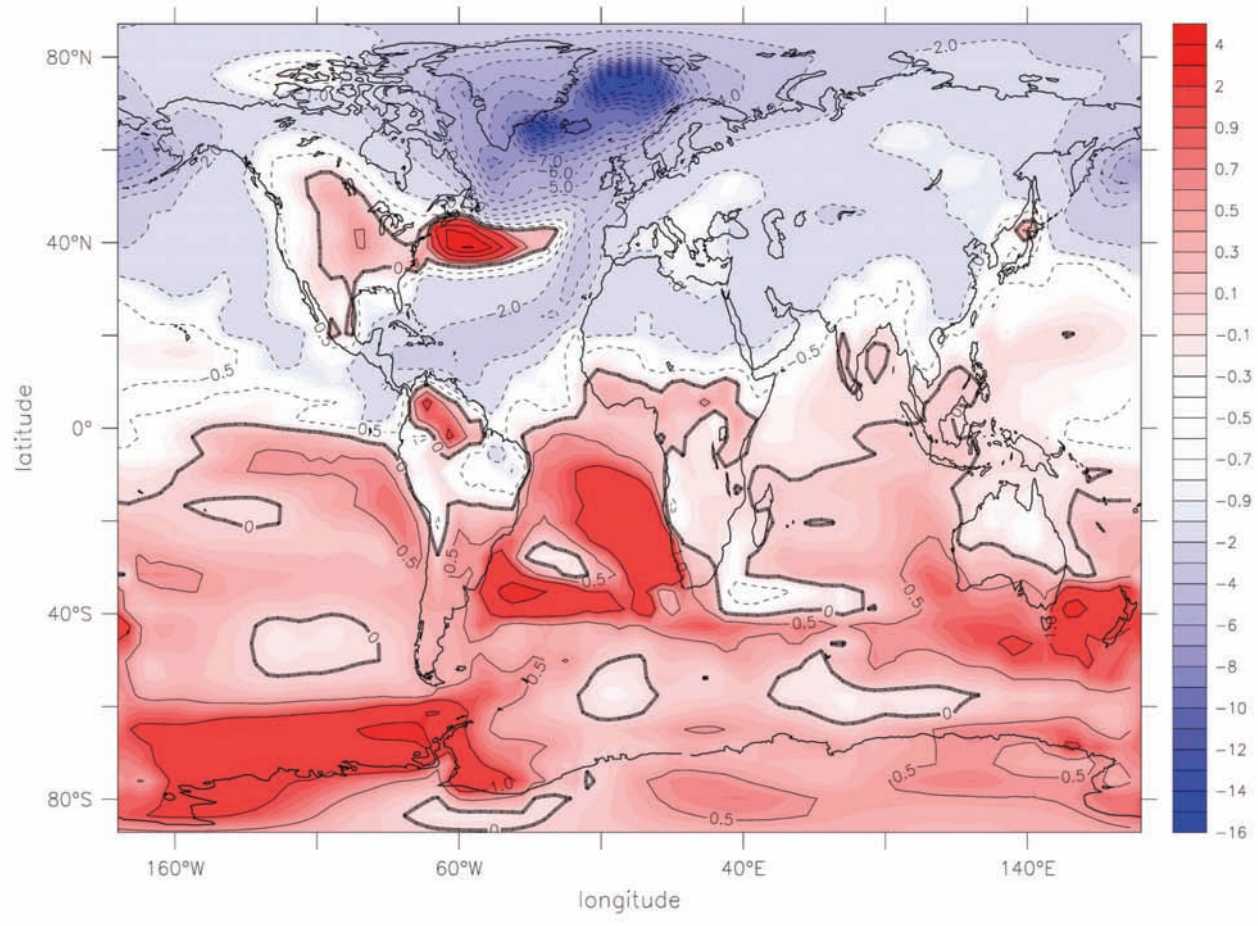

Figure 1: Surface air temperature anomalies averaged from the period of the collapsed meridional overturning circulation in comparison with the control run with perpetual 1990 conditions. The Northern Hemisphere shows a significant cooling, due to a reduced heat transport from the tropics, whereas the Southern Hemisphere warms up by a maximum of 2°C.

overturning circulation by 10Sv. As a consequence of the reduction of the meridional heat transport, a strong decrease of the surface air temperature with a minimum of -14°C was found (Figure 1). Whereas the Northern Hemisphere shows as significant cooling, the Southern Hemisphere warms uniformly by approximately +2°C [2]. As found in earlier studies the Intertropical Convergence Zone (ITCZ) and the Hadley circulation moves southward, due to a stronger meridional temperature gradient which is the result of a higher requirement of heat to be transported northwards. The increased rainfall in southern Africa and South America during the freshwater experiments results from a combination of southward shift of the ITCZ and an increase in the tropical temperature gradient. In addition, by comparing a control run with perpetual 1990 conditions, an increased variability of sea surface temperature in the late boreal spring took place. We could show that a climate change in the North Atlantic has a clear impact on the climate in the tropics. Whereas the strongest response in temperature was in the Northern Hemisphere high latitudes the hydrological signal was most pronounced in the tropical regions.

A further research focus by our group has been devoted on the atmospheric trends in the Northern Hemisphere. The aim of this investigation was to explain to what extent the Northern Hemispheric atmospheric trends can be explain by internal variability versus external forcing in the Atlantic and Pacific region and whether a possible connection exists. The dominant atmospheric mode in the North Atlantic region is the North Atlantic Oscillation (NAO). During the last 50 years a strong positive trend of the NAO index has been detected, whereas during the investigated time the Aleutian Low showed a strong negative trend in its variability. The comparison of two different control simulations for perpetual present day conditions, carried out with the CCSM3 and the ECHAM4 model, led to the conclusion that the observed trend of NAO could caused by internal variability of the climate system, but the negative trend of the Aleutian Low is probably influenced by external forcing, e.g., the anthropogenic greenhouse effect [3,4].

In spring 2004, we migrated to version 3, the latest development stage of the CCSM-NCAR model, which eliminated some important physical shortcomings and improved the computational performance of the model code. In addition we made load balancing tests and comparisons with other architectures to optimize our computational output [5].

Reference

[1] Casty, C., D. Handorf, C.C. Raible, J. Luterbacher, A. Weisheimer, E. Xoplaki, J. F. Gonzalez-Rouco, K. Dethloff, and H. Wanner (2005), Recurrent climate winter regimes in reconstructed and modeled 500 hPa geopotential height over the North Atlantic-European sector 1649-1990. Climate Dynamics., 24, 809-822.

[2] Knutti R., Flueckiger J. T. F. Stocker, and A. Timmermann, Strong hemispheric coupling of glacial climate through freshwater discharge and ocean circulation, Nature, 430, 851-856 (2004).

[3] Raible, C. C., T. F. Stocker, M. Yoshimori, M. Renold, U. Beyerle, C. Casty, and J. Luterbacher (2005) Northern Hemispheric trends of pressure indices and atmospheric circulation patterns in observational, reconstructions, and coupled GCM simulations. Journal of Climate, 18, 3968-3982, 2005.

[4] Raible, C.C., C. Casty, J. Luterbacher, A. Pauling, J. Esper, D. C. Frank, U. Büntgens, A. C. Roesch, M. Wild, P. Tschuck, P.-L. Vidale, C. Schär and H. Wanner, 2005: Climate Variability - Observations, Reconstructions and Model Simulations, Climate Change, in press.

[5] Renold M., U. Beyerle, C. C. Raible, R.Knutti, T.F. Stocker, T. Craig, Climate modeling with a Linux cluster, EOS, 85/31, 290 (2004).

[6] Yoshimori M., T.F. Stocker, C.C. Raible, and M. Renold (2005a), Externally-forced and Internal Variability in Ensemble Climate Simulations of the Maunder Minimum. Journal of Climate, in press.

[7] Yoshimori M., T.F. Stocker, C.C. Raible, and M. Renold (2005b), On the Interpretation for Low-latitude Hydrological Proxy Records Based on Maunder Minimum Simulations, American Meteorological Society, 4253-4270, 2005.

Websites related to the MONALISA-2 project:

NCCR-Climate: http://www.nccr-climate.unibe.ch/index.html
NCCR-Climate (MONALISA): http://www.climate.unibe.ch/~raible/nccr/start_p11_intro.html

New Organic Chemistry with Sulfur Dioxide

Prof. Pierre Vogel

Laboratoire de glycochimie et de synthèse asymétrique (LGSA), EPF Lausanne, Switzerland

Prof. José Àngel Sordo

Departamento de química física y analítica, Universidad de Oviedo, Spain.

Summary

Although sulfur dioxide (SO_2) is one of the major natural and man-made air pollutant and that burning of sulfur, which generates SO_2, has been used for more than 8000 years to sanitize containers of food and beverages, the organic chemistry of SO_2 is today quite limited. Applying high level quantum calculations, we intend to understand newly discovered reactions and reaction cascades involving SO_2. These studies have led us to invent new synthetic procedures of high potential for material sciences and medicinal chemistry. Our studies are also pertinent to acid rain and smog formation. They help in the interpretation of experimental data (thermodynamics, kinetics, isotope effects) in connection with the ene-reaction, the cheletropic and the hetero-Diels-Alder additions of SO_2. We are studying also the catalysis of these reactions and of others involving polysulfone polymers. The project establishes a fruitfull synergy between experience (EPFL) and theory (Oviedo).

Results

A new reaction cascade (Scheme 1) has been discovered which condenses electron-rich dienes **1** and alkenes **2** with SO_2 in the presence of an acid catalyst at low temperature [1]. The silyl sulfinates **3** so-obtained can be converted into libraries of sulfones **4** [2], sulfonamides **5** [3] and sulfonic esters **6** [3] of biological interest (one-pot, four com-

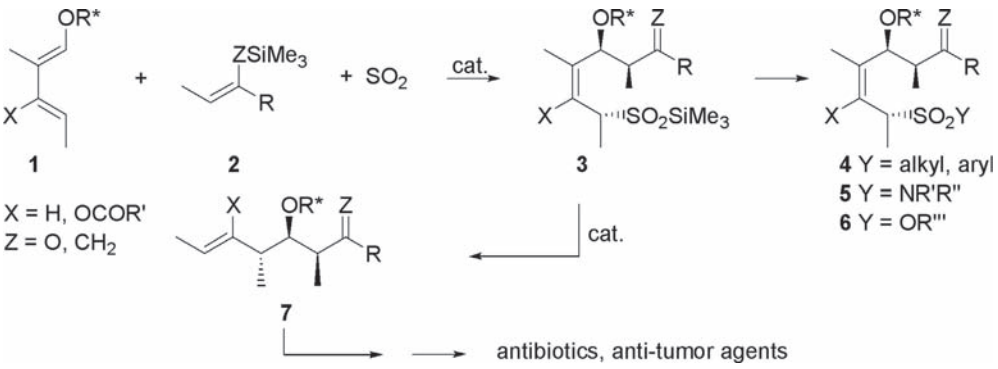

Scheme 1

ponent syntheses), or be transformed into polyketide and polypropionate fragments **7** containing up to three contigous stereogenic centers in one-pot operations [4]. The latter reactions have allowed the efficient construction of important antibiotics and anti-tumor agents including Rifamycin S [5] and apoptolidinone [6].

Quantum calculations and experimental studies have established that transformations **1** +**2** + SO_2 → **3** involve first the hetero-Diels-Alder addition of SO_2 to dienes **1** generating instable sultines **8** that are ionized into electrophilic intermediates **9**. The latter react with alkenes **2** with good stereoselectivity (asymmetric formation of C-C bond) giving **3** (Scheme 2). Predictions based on quantum calculations [7] about the ground state properties of the sultines and their reactivity [8] have led us to tune up the experimental conditions for high yielded and stereoselective reactions.

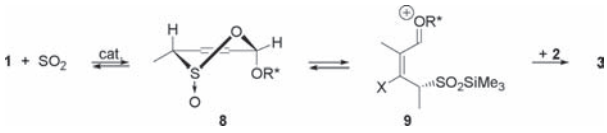

Scheme 2

The conversion of silyl sulfinate intermediates **3** into polypropionates **7** imply retro-ene eliminations of SO_2 form β,γ-unsaturated sulfinic acids [9]. Quantum calculations have been carried out recently to define better reaction conditions for this transformation. During these studies we discovered that the admitted mechanism (ene-reaction/ sigmatropic rearrangement/retro-ene elimination) for SO_2-induced alkene isomerizations is not always followed. Alkenes and SO_2 generate polysulfone polymers that are responsible for the alkene isomerization. Experiments and calculations are consistent with a mechanism involving alkanesulfonyl radicals that abstract a hydrogen atom from the alkenes to generate allyl radical intermediates[10]. Details of the mechanism of the subsequent alkene isomerization are under exploration now (calculations and experiments). The rate of this hydrogen transfer depends on the nature of the alkenes. This has led us to invent a new strategy for polyol (carbohydrates, polyketides) semi-protection by methyl substituted allyl ethers. The latter can be cleaved under neutral conditions in the presence of a neutral solid polysulfone as catalyst [11].

The reactivity sequence methylisoprenylOR > isoprenylOR > methallylOR >>allylOR has been found for the liberation of the corresponding alcohols ROH (Scheme 3). Detailed quantum cal

Scheme 3

culations on the reactions of $MeSO_2$• + propene

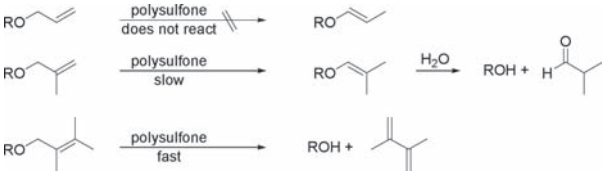

and isobutylene led us to establish the mechanism of the allyl radical formation and to explain the origin of the chemoselectivity (Bell-Evans-Polanyi polarisability effect, special hydrogen-bridging, see Figure 1) [12].

Conclusion

This project has led to the invention of new organic chemistry of sulfur dioxide and to the devel-

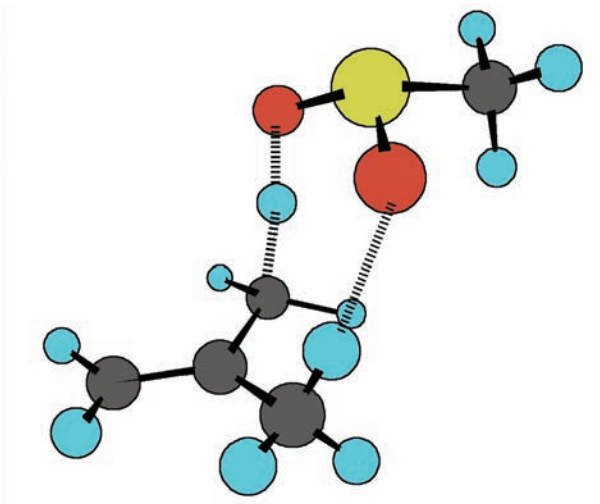

Figure 1: Transition structure of the hydrogen abstraction $MeSO_2$• + isobutylene.

opment of new synthetic tools useful for material sciences and medicinal chemistry. Our discoveries raise several fundamental questions for which quantum calculations give us extremely precious answers. The calculations guide us and suggest new experiments.

Acknowledgements

The continous support by the Centro Svizzero di Calculo Scientifico (Manno) and the Socrates (Oviedo/EPFL) program is greatly appreciated. Financial support under projects BQU-3660-CO2-01, BQU-0705-CO2-02 (Madrid) and 200020-108103, 108105 (Swiss NSF) is greatfully acknowledged.

References

[1] Narkevitch, V.; Schenk, K.; Vogel, P. Angew. Chem. Int. Ed. 2000, 39, 1806; Narkevitch, V.; Megevand, S.; Schenk, K.; Vogel, P. J. Org. Chem. 2001, 66, 5080.

[2] Huang, X.; Vogel, P. Synthesis, 2002, 232; Deguin, B.; Roulet, J.-M.; Vogel, P. Tetrahedron Lett. 1997, 38, 6197.

[3] Bouchez, L. C.; Dubbaka, S. R.; Turks, M.; Vogel, P. J. Org. Chem. 2004, 69, 6413.

[4] Turks, M.; Fonquerne, F.; Vogel, P. Org. Lett. 2004, 6, 1053.

[5] Turks, M.; Huang, X.; Vogel, P. Chem. Eur. J. 2005, 11, 465.

[6] Bouchez, L. C.; Craita, C.; Vogel, P. Org. Lett. 2005, 7, 897; Bouchez, L. C.; Vogel, P. Chem. Eur. J. 2005, 11, 4609.

[7] Markovic, D.; Roversi, E.; Scoppelliti, R.; Vogel, P.; Meana, R.; Sordo, J. A. Chem. Eur. J. 2003, 9, 4911; Monnat, F.; Vogel, P.; Rayón, V. M.; Sordo, J. A. J. Org. Chem. 2002, 67, 1882.

[8] Vogel, P.; Sordo, J. A. Curr. Org. Chem. 2005, in press.

[9] Huang, X.; Craita, C.; Vogel, P. J. Org. Chem. 2004, 69, 4272.

[10] Markovic, D.; Vogel, P. Angew. Chem. Int. Ed. 2004, 43, 2928.

[11] Markovic, D.; Vogel, P. Org. Lett. 2004, 6, 2693; Markovic, D.; Steunenberg, P.; Ekstrand, M.; Vogel, P. J. Chem. Soc., Chem. Commun. 2004, 2444.

[12] Sordo, J. A.; Meana, R.; Markovic, D.; Vogel, P. In preparation

Computational Quantum Chemistry of Increasingly Complex Systems

Prof. Jacques Weber

with Pierre-Yves Morgantini, Tomasz Adam Wesolowski, Delphine Bas, Clémence Corminboeuf, Marcin Dulak, Fabien Tran

Department of Physical Chemistry, University of Geneva, Switzerland

Description

The computer resources at CSCS in Manno increased significantly the pool of computers available to our group. As a result, some of the subprojects studied in our lab could be totally or partially achieved. They are listed below.

Achievements

A) We have been studying gaseous adsorption in zeolites. This work has been carried out in collaboration with A. Goursot, using a formalism recently developed in our group by T. Wesolowski and coworkers. Two commonly used probe molecules (CO and CO_2) have been employed as adsorbates on the basis of experimental results performed by Garrone and coworkers. This work has been motivated by the industrial interest of a better understanding of host-guest interactions and therefore a helpful contribution to the development of advanced materials where zeolites act as hosts for encapsulating and activing small molecules. The results (Figure 1) are presented in refs. [1,2].

B) A new analysis tool for stability and aromaticity of rings has been recently developed in our group. It is based on the calculation of NMR Nucleus Independent Chemical Shifts (NICS) of molecular orbitals, MO-NICS. The method has been applied to study n-annulenes [3], Diels-Alder reaction or stability of all-metal clusters and further calculations will be devoted to a new family of tetracoordinate planar carbon compounds and other unexpectedly stable organic compounds.

C) An elaborate Density Functional Theory (DFT) investigation has been performed of the potential energy surface and related properties of large chiral ligands of Ru(II) [4]. The calculations lead to a coherent description of the mechanism of inversion of the pyramidal geometry of the ligand at the metal center and provide an energy diagram for this process.

D) Further DFT calculations have shown that spiro diarylazepinium cations possess a high chemical stability in basic media, making them robust phase-transfer catalysts [5]. Their treatment with strong phosphazene bases leads to a [1,2]-Stevens rearrangement in favour of a ring-expanded amine.

E) In collaboration with the group of J. Lacour, theoretical investigations have been performed on chiral phosphate anions [6]. In addition, the absolute configuration of a dinitrogen cations (Figure 2), experimentally used as catalyst to enhance the efficiency of various reactions via a phase transfer process has been determined using a joint theoretical and experimental study of the vibrational circular dicroïsm (VCD) (Figure 3) properties [1].

F) Volume and energy profiles for two distinct water exchange mechanisms (D and I_a) have been computed using quantum chemical calculations in-

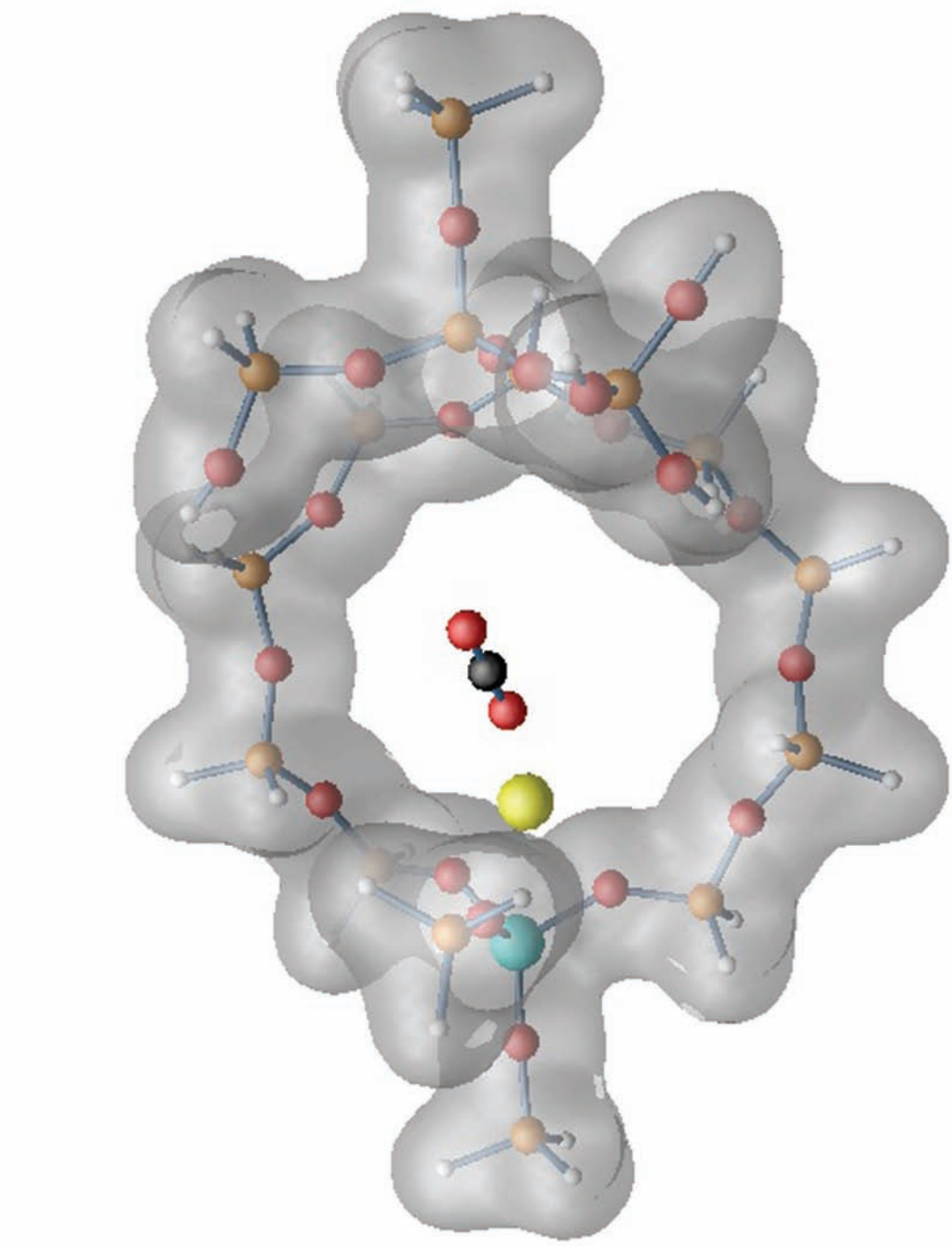

Figure 1: Structure and isoelectronic density surface (in grey) of a cluster model zeolite with CO_2, adsorbed on a lithium cation.

cluding hydration effects for rhodium(III) and iridium(III) hexaaquo complexes [7]. The calculations show that the activation energies for the water exchange on $Rh(OH_2)_6^{3+}$ via the I_a and D pathways is 21kJ mol^{-1} in favour of the former. The activation energy for $Ir(OH_2)_6^{3+}$ was found 32.2. kJ mol^{-1} in favour of the I_a mechanism (127.9 kJ mol^{-1}) in opposition to a D pathway, the value for the I_a mechanism being close to ΔH^+ and ΔG^+ experimental values for both aquaions. Volumes of activation, computed using Connolly surfaces, for the Ia pathway ($\Delta V^{\#}$+calc = -3.9 and -3.5 cm^3 mol^{-1}, respectively for Rh^{3+} and Ir^{3+}) were also found to be in agreement with the experimental values. Further, it has been demonstrated for both mechanisms that the contribution to the volume of activation due to the changes in bond lengths between Ir(III) and the spectator water molecules is negligible : -1.8 for the D, and -0.9 cm^3 mol^{-1} for I_a mechanism, as for the Rh(III). This finding has helped to defini-

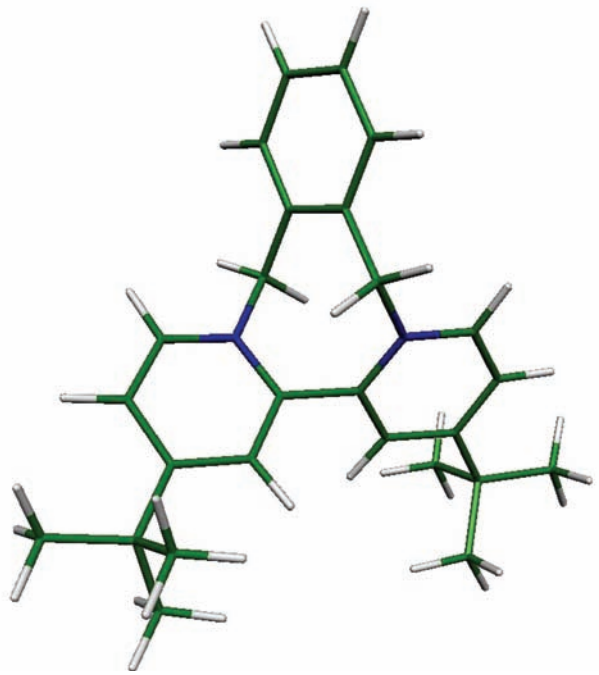

*Figure 2: Optimized structure of the S-enantiomer of a dinitrogen system of C2 symmetry at the B3LYP/6-311G** level.*

tively solve the debate about the interpretation of $\Delta V^{\#}$, unequivocally confirming the occurrence of an I_a mechanism with retention of configuration and a small A character for both Rh(III) and Ir(III) hexaquaions [7].

G) The dibenzo-18-crown-6 (DB18C6) crown crystallizes forming channel-like structures of the diameter large enough to host a water molecule. Such solids are synthesized and studied by K. Fromm and collaborators at University of Basel. X-ray diffraction data show a chain-like arrangement of oxygen atoms in the centre of the channel which could be attributed to such species as H_2O, H_3O^+ or even larger chain-like structures. In order to characterise the interior of the channel, the vibrations spectroscopy (IR and Raman – H.R. Hagemann-University of Geneva) and computer modelling (Kohn-Sham calculations) were applied. The calculations were performed for a simplified model comprising isolated DB18C6 unit and its complexes with either H_2O or H_3O^+ guests, which are the simplest model ingredients of a one-dimensional diluted acid chain, to get structural and energetic data concerning the formation of the complex and to assign the characteristic spectroscopic bands [8]. The oxygen centres in the previously reported crystallographic structure were assigned to either H_2O or protonated species.

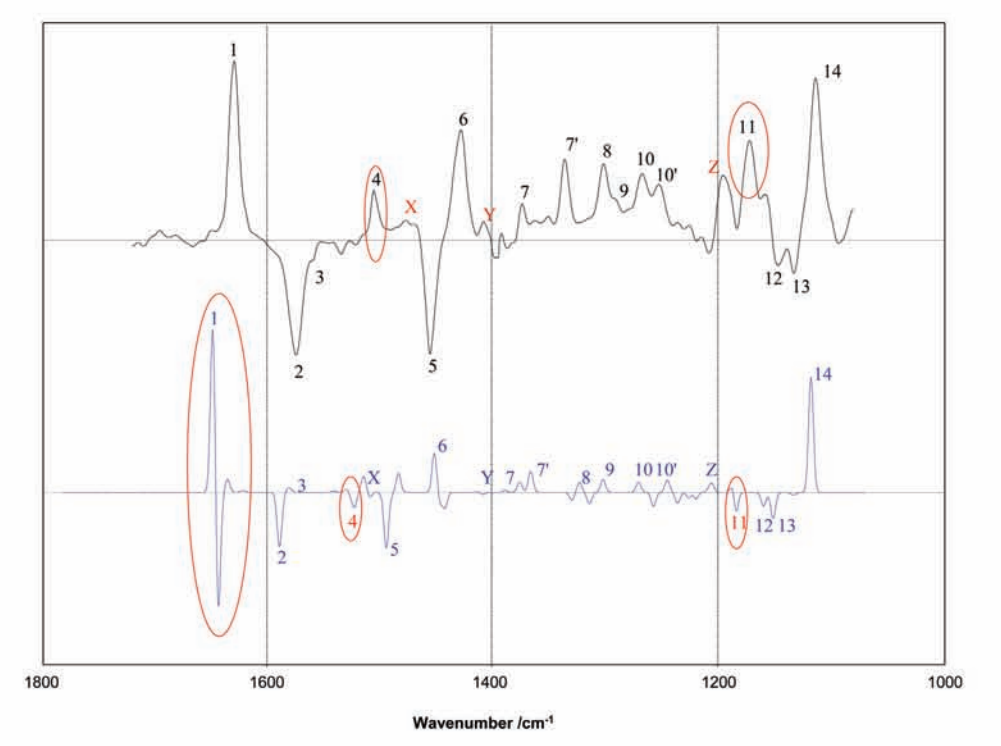

Figure 3: Calculated (down) and experimental (up) VCD spectra of the dinitrogen cation of Fig. 2.

References

[1] D. Bas, Ph.D. thesis, University of Geneva, 2005

[2] D. Bas, J. Weber, T.A. Wesolowski and A. Goursot, Theoretical study of the adsorption of carbon dioxide on the alkali-metal-exchanged ZSM-5 zeolite, J. Chem. Phys., submitted for publication

[3] C. Corminboeuf, T. Heine, G. Seifert, P.v.R. Schleyer and J. Weber, Induced magnetic fields in aromatic [n]-annulenes-interpretation of NICS tensor components, Phys. Chem. Chem. Phys. 6, 273 (2004)

[4] V. Alezra, G. Bernardinelli, C. Corminboeuf, U. Frey, E.P. Kündig, A.E. Merbach, C.M. Saudan, F. Viton and J. Weber, $[C_pRu((R)\text{-BINOP-F})(H_2O)][SbS_6]$, a new fluxional chiral Lewis acid catalyst : synthesis, dynamic NMR, asymmetric catalysis and theoretical studies, J. Am. Chem. Soc. 126, 4843 (2004)

[5] L. Vial, M.H. Gonçalves, P.Y. Morgantini, J. Weber, G. Bernardinelli and J. Lacour, Unusual regio- and enantioselective [1,2]-Stevens rearrangement of a spirobi[dibenzazepinium] cation, Synlett 1565 (2004)

[6] D. Bas, T. Bürgi, J. Lacour, J. Vachon and J. Weber, Vibrational and electronic circular dichroism of Δ-TRISPHAT [Tris(tetrachlorobenzenediolato)-phosphate(V)] anion, Chirality, 17, S143 (2005)

[7] D. De Vito, J. Weber and A.E. Merbach, Calculated volume and energy profiles for water exchange on t_{2g}^6 rhodium(III) and iridium(III) hexaaquaions : conclusive evidence for an I_a mechanism, Inorg. Chem. 43, 858 (2004)

[8] M. Dulak, R. Bergougnant, K.M. Fromm, H.R. Hagemann, A.Y. Robin, T.A. Wesolowski. Water trapped in dibenzo-18-Crown-6: theoretical and spectroscopic (IR, Raman) studies, Spectrochimica Acta, submitted for publication

List of Large User Projects 2004

Name	Organiszation	Project Title
Arbenz P.	ETH Zürich	Large scale eigenvalue problems in opto-electronic semico ductor lasers and accelerator cavities
Avellan F.	EPF Lausanne	Unsteady flow analysis in hydraulic turbomachinery
Baiker A.	ETH Zürich	Hydrogenation reactions in heterogeneous enatioselective catalysis and homogeneous catalysis in supercritical CO2
Baldereschi A.	EPF Lausanne	Structural and electronic properties of solids and surfaces
Beniston M.	Uni Fribourg	Global and regional climate modelling
Bey I.	EPF Lausanne	Coupling tropospheric chemistry and aerosols in the general circulation model ECHAM
Böckmann R.	Uni Zürich	Nanodynamics of MHC/peptide complexes and its dependnce on MHC polymorphism
Bürgi Th.	Uni Neuchâtel	Structure and enantiospecificity of chiral nanoparticles and interfaces
Cooper W.A.	EPF Lausanne	Computation of stellarator coils, equilibrium and Sstability
Davies H.C.	ETH Zürich	ERA40 for NCCR-Climate
Fäh D.	ETH Zürich	Site effects assessment using earthquake and seismic ambient vibration simulation
Fichtner W.	ETH Zürich	Computational science and engineering in microelectronics and optoelectronics
Folini D.	EMPA	Inverse modeling to monitor source regions of air pollutants in Europe
Gödecker St.	Uni Basel	Structure of large clusters, surfaces and biomolecules
Hasenfratz P.	Uni Berm	Hadron spectroscopy in QCD with 2+1 light flavours
Hauser A.	Uni Genève	Photophysics and photochemistry of transition metal compounds: Theoretical Approaches
Hutter J.	Uni Zürich	Development and application of ab-initio molecular dynamics methods
Keller J.	PSI	Air quality modeling in Switzerland
Kleiser L.	ETH Zürich	Numerical simulation of transitional, turbulent and multiphase flows
Koumoutsakos P.	ETH Zürich	Simulations using particle methods. Optimization of real world problems using evolutionary algorithms Multiscale modeling, simulation and optimization of complex systems
Leriche E.	EPF Lausanne	Direct numerical simulation ot the buoyancy-driven turbulence in a cavity: The DNSBDTC project
Leutwyler S.	Uni Bern	Proton transfer and hydrogen bonding in microsolvent clusters and nucleic acid base pairs: theroy and dynamics

Name	Organization	Project Title
Leyland P.	EPF Lausanne	Aerothermodynamic simulations in aerospace and aeronautic applications
Lüthi H.P.	ETH Zürich	Computational quantum chemistry of large molecules
Mareda J.	Uni Genève	Studies of uncatalyzed and antibody catalyzed reactions: modeling of cation-olefin cyclizations
Meuwly M.	Uni Basel	Electronic structure calculations for molecular dynamics simulations of iron-containing, reactive centers of biomolecules Theoretical investigations of iridium-catalyzed reactions
Moore B.	Uni Zürich	Computational cosmology
Ohmura A.	ETH Zürich	Global climate change: modelling atmosphere/ocean variability on decadel time scales
Parrinello/Deubel	ETH Zürich	Quantum chemical studies on the interaction of anticancer drugs with biological targets
Pasquarello A.	EPF Lausanne	Disordered network-forming materials
Quack M.	ETH Zürich	Quantum mechanical simulation of molecules and molecular clusters
Röthlisberger U.	EPF Lausanne	Mixed quantum mechanics / molecular mechanics study of systems of biological interest
Samland M.	Uni Basel	The Milky way and its satellite dwarf galaxies
Schär Ch.	ETH Zürich	Modelling weather and climate on european and alpine scales
Sennhauser U.	EMPA	Nanoxid
Steurer W.	ETH Zürich	Minerals and planetary materials
Stocker Th.	Uni Bern	Monalisa: modelling and reconstruction of north Atlantic climate system variability
Troyer M.	ETH Zürich	Simulation of quantum phase transitions
Van Swygenhoven H.	PSI	Modelling of nanostructured materials
Vogel P.	EPF Lausanne	New organic chemistry with sulfur dioxide Electron releasing homoconjugated carbonyl group
Weber J.	Uni Genève	Computational quantum chemistry of increasingly complex systems
Yadigaroglu G.	ETH Zürich	DNS and LES of multiphase flows

List of Large User Projects 2005

Name	Organiszation	Project Title
Arbenz P.	ETH Zürich	Large scale eigenvalue problems in opto-electronic semiconductor lasers and accelerator cavities
Baiker A.	ETH Zürich	Hydrogenation reactions in heterogeneous enatioselective catalysis and homogeneous catalysis in supercritical CO_2
Bakowies D.	ETH Zürich	Atomizations energies from ab-inition calculations without empirical corrections
Beniston M.	Uni Fribourg	Global and regional climate modelling
Besson O.	Uni Neuchâtel	Numerical solution of Navier Stokes equation in shallow domains
Bey I.	EPF Lausanne	Coupling tropospheric chemistry and aerosols in the general circulation model ECHAM
Bürgi Th.	Uni Neuchâtel	Structure and enantiospecificity of chiral nanoparticles and interfaces
Cooper W.A.	EPF Lausanne	Computation of stellarator coils, equilibrium and stability
Deubel D.	ETH Zürich	Quantum chemical studies on the interaction of anticancer drugs with biological targets
Fäh D.	ETH Zürich	Numerical modelling of seismic local effect estimation on complex sites
Fichtner W.	ETH Zürich	Computational science and engineering in microelectronics and optoelectronics
Folini D.	EMPA	Inverse modeling to monitor source regions of air pollutants in Europe
Hasenfratz P.	Uni Bern	Chiral symmetric dirac oparator in lattice QCD
Hauser A.	Uni Genève	Photophysics and photochemistry of transition metal compounds: Theoretical Approaches
Helm L.	EPF Lausanne	Iperfine interaction anysotropy on first and second coordination sphere water molecules, in paramagnetic metal ion solutions
Hutter J.	Uni Zürich	Development and application of ab-initio molecular dynamics methods
Jakob A.	PSI	Molecular modelling of radionuclide mobility and retardation in clay minerals
Joos F.	Uni Bern	Carboclime: modelling carbon cycle climate feedbacks
Keller J.	PSI	Air quality modeling in Switzerland
Kleiser L.	ETH Zürich	Numerical simulation of transitional, turbulent and multiphase flows
Koumoutsakos P.	ETH Zürich	Simulations using particle methods optimization of real world problems using evolutionary algorithms multiscale modelling, simulations and optimization of complex systems

Name	Organiszation	Project Title
Leriche E.	EPF Lausanne	Direct numerical simulation ot the buoyancy-driven turbulence in a cavity: the DNSBDTC project
Leutwyler S.	Uni Bern	Proton and hydrogen atom transfer in solvent clusters and nucleic acid base pairs: theory and dynamics
Leyland P.	EPF Lausanne	Large scale simulation for aerospace applications
Lohmann U.	ETH Zürich	Effect of aerosols on clouds and climate
Lüthi H.P.	ETH Zürich	Computational quantum chemistry of large molecules
Meuwly M.	Uni Basel	Electronic structure calculations for molecular dynamics simulations of iron-containing, reactive centers of biomolecules. Theoretical investigations of iridium-catalyzed reactions.
Oganov A.	ETH Zürich	Computational mineral physics and cristallography
Ohmura A.	ETH Zürich	Global climate change: modelling climate variability on decadel time scales
Parlange M.B.	EPF Lausanne	Large eddy simulation of atmospheric boundary layer flow over complex terrain
Parinello M.	ETH Zürich	Simulating chemical reactions with Car-Parrinello metadynamics
Pasquarello A.	EPF Lausanne	Disordered network-forming materials
Posternak M.	EPF Lausanne	Computational physic in condesed matter
Poulikakos D.	ETH Zürich	Biothermofluidics for Cerebrospinal fluid diagnostic and control-development of a knowledge base Explosive vaporization phenomena in microenclosures
Röthlisberger U.	EPF Lausanne	Mixed quantum mechanics / molecular mechanics study of systems of biological interest
Samland M.	Uni Basel	The Milky way and its satellite warf galaxies
Schär Ch.	ETH Zürich	Modelling weather and climate on european and alpine scales
Sennhauser U.	EMPA	Nanoxid
Stocker Th.	Uni Bern	Monalisa: modelling and reconstruction of north Atlantic climate system variability
Van Lenthe H.	ETH Zürich	Identifying genetic determinats of bone strengh - a high troughput phenomics approach in mice
Van Swygenhoven H.	PSI	Molecular dynamics computer simulation of nanostructured materials
Vogel P.	EPF Lausanne	New organic chemistry with sulfur dioxide. Electron releasing homoconjugated carbonyl group

Impressum

CSCS Swiss National Supercomputing Centre
Autonomous unit of ETH Zurich
Via Canotnale
CH-6928 Manno
Switzerland
Tel +41 (0) 91 610 82 11
Fax +41 (0) 91 610 82 09
http://www.cscs.ch

Design, Production:
Dorothea Gerhardt, CSCS

Printing:
Hürzeler AG, Regensdorf

Print-run:
350